

SYNTHESIS AND UTILIZATION OF Si_6H_{12} AND Si_6X_{12} ($\text{X} = \text{Cl}, \text{Br}$) FOR THE
GENERATION OF NOVEL SILICON MATERIALS

A Thesis
Submitted to the Graduate Faculty
of the
North Dakota State University
of Agriculture and Applied Science

By

Matthew Todd Frohlich

In Partial Fulfillment of the Requirements
for the Degree of
MASTER OF SCIENCE

Major Program:
Materials and Nanotechnology

May 2017

Fargo, North Dakota

North Dakota State University
Graduate School

Title

SYNTHESIS AND UTILIZATION OF Si_6H_{12} AND Si_6X_{12} (X=Cl, Br) FOR
THE GENERATION OF NOVEL SILICON MATERIALS

By

Matthew Todd Frohlich

The Supervisory Committee certifies that this *disquisition* complies with North Dakota State
University's regulations and meets the accepted standards for the degree of

MASTER OF SCIENCE

SUPERVISORY COMMITTEE:

Philip Boudjouk

Chair

Erik Hobbie

Konstantin Pokhodnya

Xinnan Wang

Xiangfa Wu

Approved:

5/3/17

Date

Erik Hobbie

Department Chair

ABSTRACT

Cyclohexasilane (Si_6H_{12}) and its derivatives, Si_6X_{12} ($\text{X} = \text{Cl}, \text{Br}$), have chemical and physical properties different from linear and branched polysilanes, thus creating interest in their use as starting materials for a variety of applications. The liquid nature and lower activation energy of Si_6H_{12} give it advantages as a starting material for silicon based materials including quantum dots (SiQDs), nanorods (SiNRs) and nanowires (SiNWs), as well as novel processing methods such as roll to roll deposition of silicon thin films. The electronegative elements on Si_6X_{12} create Lewis acid sites above and below the ring, giving it the ability to form novel salts and 1-dimensional stacked polymers.

This work developed a new route toward Si_6H_{12} and $\text{Si}_6\text{Cl}_{12}$ by focusing on the production of the precursor $[\text{Si}_6\text{Cl}_{14}]^{2-}$ dianion salts and studying their physical and chemical properties. This thesis also describes the preparation of novel Si_6X_{12} based materials.

ACKNOWLEDGEMENTS

There are many people I credit for providing me with the guidance necessary to complete this thesis.

I am thankful for my advisor Dr. Phil Boudjouk. In addition to serving as my supervisor and mentor throughout this process, his work in creating NDSU's Research and Technology Park laid the groundwork years in advance for the research that made this thesis possible.

I am indebted to my first supervisor, Dr. Samy Elangovan. Despite my lack of formal experience, his dedication to my personal development quickly transformed me into someone who is capable of working independently in a research environment.

My colleague Kenny Anderson has not only been a source of daily guidance for me over the past 6 years, but he has also provided me an example for how one can dedicate their life to the pursuit of science.

The guidance provided by my committee members, Erik Hobbie, Xinnan Wang and Xiang Wu, has been invaluable.

I appreciate my colleagues Konstantin Pokhodnya, Guruvenket Srinivasan and Justin Hoey for helping to create a work environment where research can thrive.

And finally, I am thankful for the friends I made along the way, including Ahmed Elbaradei, Sam Brown and Matt Semmler.

TABLE OF CONTENTS

ABSTRACT.....	iii
ACKNOWLEDGEMENTS.....	iv
LIST OF TABLES.....	viii
LIST OF FIGURES.....	ix
LIST OF ABBREVIATIONS.....	xi
LIST OF APPENDIX TABLES.....	xiii
LIST OF APPENDIX FIGURES.....	xiv
1. INTRODUCTION AND APPLICATIONS.....	1
1.1. Abstract.....	1
1.2. Goals of this Thesis.....	1
1.3. Cyclohexasilane's Unique Properties.....	2
1.4. Synthesis of Si_6H_{12} , Si_6X_{12} and Si_6X_{12} Diadducts.....	5
1.4.1. Hengge's Synthesis.....	7
1.4.2. Boudjouk's Synthesis.....	8
1.4.3. Tillman's Synthesis.....	10
1.4.4. Frohlich's Synthesis.....	12
1.4.5. Synthesis of Si_6X_{12} Diadducts.....	14
2. SYNTHESIS, OPTIMIZATION AND ISOLATION OF CRUDE RR' AND R2 SALTS.....	15
2.1. Abstract.....	15
2.2. Background.....	15
2.3. Results and Discussion.....	17
2.4. Experimental Methods.....	27
2.4.1. Preparation of Starting Materials.....	27

2.4.2.	Characterization of Materials.....	28
2.4.3.	Experimental Procedures	28
3.	CRUDE R2 AND R2 SALTS AS PRECURSORS TO $\text{Si}_6\text{Cl}_{12}$	40
3.1.	Abstract.....	40
3.2.	Background.....	40
3.3.	Results and Discussion	41
3.4.	Experimental Methods.....	45
3.4.1.	Preparation of Starting Materials.....	45
3.4.2.	Characterization of Materials.....	46
3.4.3.	$[\text{Ph}_3\text{BnP}^+]_2[\text{Si}_6\text{Cl}_{14}^{2-}] + 2.5 \text{ AlCl}_3 \rightarrow \text{Si}_6\text{Cl}_{12}$ with Hexane Extraction	46
3.4.4.	$[\text{Ph}_3\text{BnP}^+]_2[\text{Si}_6\text{H}_n\text{Cl}_{14-n}^{2-}] + 2.5 \text{ AlCl}_3 \rightarrow \text{Si}_6\text{H}_n\text{Cl}_{12-n}$ with Hexane Extraction.....	47
3.4.5.	$[\text{Ph}_3\text{BnP}^+]_2[\text{Si}_6\text{Cl}_{14}^{2-}] + 2.5 \text{ AlCl}_3 \rightarrow \text{Si}_6\text{Cl}_{12}$ with n-Heptane Extraction.....	48
3.4.6.	Scale Up $[\text{Ph}_3\text{BnP}^+]_2[\text{Si}_6\text{Cl}_{14}^{2-}] + 2.5 \text{ AlCl}_3 \rightarrow \text{Si}_6\text{Cl}_{12}$ with n-Heptane Extraction.....	49
4.	GENERATING NOVEL MATERIALS FROM Si_6X_{12}	51
4.1.	Abstract.....	51
4.2.	Background.....	51
4.3.	Results and Discussion	52
4.3.1.	Diadducts of Si_6X_{12} (X = Cl, Br) and $\text{Ph}_4\text{PX}'$ (X' = Cl, Br)/p-Tolunitrile	52
4.3.2.	Synthesis and Characterization of $[\text{Tr}^+]_2[\text{Si}_6\text{X}_{12}\text{X}'_2^{2-}]$ (X = X' = Cl, Br).....	53
4.4.	Experimental Methods.....	63
4.4.1.	Preparation of Starting Materials.....	63
4.4.2.	Characterization of Materials.....	64

4.4.3. Experimental Procedures	65
5. FUTURE WORK.....	70
REFERENCES	71
APPENDIX: CRYSTALLOGRAPHIC INFORMATION.....	75

LIST OF TABLES

<u>Table</u>	<u>Page</u>
1. Comparison of yields for routes to Si_6H_{12} and $\text{Si}_6\text{Cl}_{12}$	5
2. Summary of crude RR' syntheses.	26
3. Solubility of the following $[\text{Si}_6\text{Cl}_{14}^{2-}]$ salts in CH_2Cl_2 : R2 salt, $[\text{PEDETA}\cdot\text{H}_2\text{SiCl}^+]_2[\text{Si}_6\text{Cl}_{14}^{2-}]$ (synthesized in lab), and $[\text{PEDETA}\cdot\text{H}_2\text{SiCl}^+]_2[\text{Si}_6\text{Cl}_{14}^{2-}]$ (purchased from vendor).	27
4. Summary of reactions $[\text{Ph}_3\text{BnP}^+]_2[\text{Si}_6\text{Cl}_{14}^{2-}] + 2.5 \text{ AlCl}_3 \rightarrow \text{Si}_6\text{Cl}_{12}$	41
5. Summary of characterization methods used on Si_6X_{12} diadducts.	52
6. Summary of reactions between Si_6X_{12} and trityl·X'	54
7. Theoretical/experimental Raman shifts for totally symmetric Si-Si stretching frequency mode in $[\text{Si}_6\text{X}_{12}\text{X}'_2^{2-}]$	54
8. Observed and calculated FTIR frequencies with corresponding assignments for trityl chloride, $[\text{Tr}^+][\text{AlCl}_4^-]$, and $[\text{Tr}^+]_2[\text{Si}_6\text{X}_{12}\text{X}'_2^{2-}]$	59
9. Summary of $[\text{Tr}^+]_2[\text{Si}_6\text{Cl}_{14}^{2-}]$ syntheses.	62
10. Theoretical/experimental elemental analysis results for synthesis of $[\text{Tr}^+]_2[\text{Si}_6\text{Cl}_{14}^{2-}]$	62
11. Theoretical/experimental elemental analysis results for dichloromethylphenylsilane.	63
12. Comparison of elemental compositions for pure dichloromethylphenylsilane and $[\text{Tr}^+]_2[\text{Si}_6\text{Cl}_{14}^{2-}]$	63

LIST OF FIGURES

<u>Figure</u>	<u>Page</u>
1.	Formation of inverse sandwich complexes upon having the Lewis acid wells in Si_6X_{12} accept nitriles (top) or halogen anions (bottom)..... 4
2.	Pathways towards Si_6H_{12} , Si_6X_{12} and Si_6X_{12} diadducts..... 6
3.	Thermal ellipsoid plot of reaction mixture precipitate. Thermal ellipsoids set at 50% probability. Hydrogen atoms omitted for clarity. Formula conforms to that of $[\text{Ph}_3\text{BnP}^+]_2[\text{EDIPA}\cdot\text{H}^+]_2[\text{Si}_6\text{Cl}_{14}^{2-}][\text{Cl}^-]_2[\text{CH}_2\text{Cl}_2]_4$: 4(Cl), 2($\text{C}_{25}\text{H}_{22}\text{P}$), $\text{Si}_6\text{Cl}_{12}$, 2($\text{C}_8\text{H}_{20}\text{N}$), 4 (CH_2Cl_2)..... 18
4.	^1H -NMR spectrum for reaction mixture precipitate (crude RR') washed with CH_2Cl_2 in CD_2Cl_2 . δ (Ph_3BnP^+): 7.81 (t, 6H, p-Ph), 7.66 (m, 12H, m-Ph), 7.53 (m, 12H, o-Ph), 7.29 (t, 2H, p-Bn), 7.17 (t, 4H, m-Bn), 6.94 (d, 4H, o-Bn), 4.71 (d, 4H, PCH_2Bn). δ ($\text{EDIPA}\cdot\text{H}^+$): 10.99 (s, 2H, $\text{EDIPA}\cdot\text{H}^+$), 3.58 (sep, 8H, $(\text{CH}_3)_2\text{CHN}$), 3.04 (q, 8H, $\text{CH}_3\text{CH}_2\text{N}$), 1.38-1.46 (m, 60H, $(\text{CH}_3)_2\text{CHN}$ and $\text{CH}_3\text{CH}_2\text{N}$). δ [$\text{Si}_6\text{Cl}_{12-n}\text{H}_n\text{Cl}_2^{2-}$]: 4.99..... 19
5.	^{29}Si -NMR spectrum for reaction mixture precipitate (crude RR') washed with CH_2Cl_2 in CD_2Cl_2 . δ [$\text{Si}_6\text{Cl}_{14}^{2-}$]: -21.25. ⁶³ δ [$\text{Si}_6\text{Cl}_{12-n}\text{H}_n\text{Cl}_2^{2-}$]: -17.44, -22.19, -36.33. ⁶⁴ 20
6.	^1H -NMR spectrum for $\text{Ph}_3\text{BnP}^+\text{Cl}^-$ in CD_2Cl_2 . δ ($\text{Ph}_3\text{BnP}^+\text{Cl}^-$): 7.62-7.80 (m, 15H, $\text{Ph}_3\text{BnP}^+\text{Cl}^-$), 7.09-7.28 (m, 5H, $\text{Ph}_3(\text{Ph})\text{CH}_2\text{P}^+\text{Cl}^-$), 5.44 (d, 2H, $\text{Ph}_3(\text{PH})\text{CH}_2\text{P}^+\text{Cl}^-$). Note that peak shifting differs from that seen for $[\text{Ph}_3\text{BnP}^+]_2[\text{EDIPA}\cdot\text{H}^+]_2[\text{Si}_6\text{Cl}_{14}^{2-}][\text{Cl}^-]_2[\text{CH}_2\text{Cl}_2]_4$ in figure 4..... 21
7.	^1H -NMR spectrum for EDIPA in CD_2Cl_2 . δ (EDIPA): 3.00 (sep, 2H, $(\text{CH}_3)_2\text{CHN}$), 2.45 (q, 2H, $\text{CH}_3\text{CH}_2\text{N}$), 0.97 (m, 15H, $(\text{CH}_3)_2\text{CHN}$ and $\text{CH}_3\text{CH}_2\text{N}$). Note that peak shifting differs from that seen for $[\text{Ph}_3\text{BnP}^+]_2[\text{EDIPA}\cdot\text{H}^+]_2[\text{Si}_6\text{Cl}_{14}^{2-}][\text{Cl}^-]_2[\text{CH}_2\text{Cl}_2]_4$ in figure 4..... 22
8.	^1H -NMR spectrum for the resulting precipitate of crude RR' in CHCl_3 (crude R2 salt) in CD_2Cl_2 . δ (Ph_3BnP^+): 7.83 (t, 6H, p-Ph), 7.68 (m, 12H, m-Ph), 7.52 (m, 12H, o-Ph), 7.29 (t, 2H, p-Bn), 7.19 (t, 4H, m-Bn), 6.91 (d, 4H, o-Bn), 4.62 (d, 4H, PCH_2Bn). δ [$\text{Si}_6\text{Cl}_{12-n}\text{H}_n\text{Cl}_2^{2-}$]: 4.98..... 23
9.	FTIR spectrum for crude RR' in a KBr pellet. 24
10.	FTIR data for crude R2 salt (top) and trityl chloride treated R2 salt (bottom)..... 25
11.	Raman data for product of R2 salt + 2.5 AlCl_3 (reaction A). Note the characteristic peak for the $\text{Si}_6\text{Cl}_{12}$ ring breathing mode at 278 cm^{-1} 42

12.	Raman data for product of crude R2 salt + 2.5 AlCl ₃ (reaction B). Note the characteristic peak for the Si ₆ Cl ₁₂ ring breathing mode at 276 cm ⁻¹ along with Si-H bonding at 2143 cm ⁻¹	43
13.	Raman data for product of R2 salt + 2.5 AlCl ₃ with a heptane extraction of the product (reaction C). Note the characteristic peak for the Si ₆ Cl ₁₂ ring breathing mode at 276 cm ⁻¹ along with Si-H bonding at 2146 cm ⁻¹	44
14.	Raman data for product of scale up reaction R2 salt + 2.5 AlCl ₃ with a heptane extraction of the product (reaction D). Note the characteristic peak for the Si ₆ Cl ₁₂ ring breathing mode at 277 cm ⁻¹	45
15.	Chemical structure of [Ph ₄ P ⁺] ₂ [Si ₆ Cl ₁₂ Br ₂ ²⁻].	53
16.	Chemical structure of [Ph ₄ P ⁺] ₂ [Si ₆ Br ₁₄ ²⁻].	53
17.	Comparison Raman spectra for Si ₆ Cl ₁₂ (black) and [Tr ⁺] ₂ [Si ₆ Cl ₁₄ ²⁻] (red) with the totally symmetric Si-Si stretching frequency mode relaxing from 278 to 257 cm ⁻¹ upon complexation of Si ₆ Cl ₁₂ with trityl chloride.	55
18.	Comparison Raman spectra for Si ₆ Br ₁₂ (black) and [Tr ⁺] ₂ [Si ₆ Br ₁₂ Cl ₂ ²⁻] (red) with the totally symmetric Si-Si stretching frequency mode relaxing from 185 to 172 cm ⁻¹ upon complexation of Si ₆ Br ₁₂ with trityl chloride.	56
19.	Comparison Raman spectra for Si ₆ Br ₁₂ (black) and [Tr ⁺] ₂ [Si ₆ Br ₁₄ ²⁻] (red) with the totally symmetric Si-Si stretching frequency mode relaxing from 185 to 173 cm ⁻¹ upon complexation of Si ₆ Br ₁₂ with trityl bromide.	57
20.	Diffusion crystallization method used for Si ₆ X ₁₂ /Ph ₄ PX' product. Inner vial contains saturated solution of product in DMF while outer vial contains toluene. Diffusion of toluene over several days causes toluene to accumulate in inner vial, resulting in precipitation.	66

LIST OF ABBREVIATIONS

$^1\text{H-NMR}$	^1H nuclear magnetic resonance spectroscopy
$^{29}\text{Si-NMR}$	^{29}Si nuclear magnetic resonance spectroscopy
4-MeTrCl	4,4',4''-(chloromethanetryl)tris(methylbenzene)
AA-APCVD	Aerosol assisted atmospheric pressure chemical vapor deposition
Bn	Benzyl
Crude R2 Salt	$[\text{Ph}_3\text{BnP}^+]_2[\text{Si}_6\text{Cl}_{14-n}\text{H}_n^{2-}]$
Crude RR' Salt	$[\text{Ph}_3\text{BnP}^+]_2[\text{EDIPA}\cdot\text{H}^+]_2[\text{Si}_6\text{Cl}_{14-n}\text{H}_n^{2-}][\text{Cl}^-]_2[\text{CH}_2\text{Cl}_2]_4$
DFT	Density functional theory
Diglyme	Diethylene glycol dimethyl ether
E_a	Activation energy
EA	Elemental Analysis
EDIPA	N,N-diisopropylethylamine
FTIR	Fourier transform infrared spectroscopy
GC-MS	Gas chromatography-mass spectroscopy
Glyme	1,2-dimethoxyethane
LAH	Lithium aluminum hydride, LiAlH_4
NDSU	North Dakota State University
PEDETA	N,N,N',N'',N'''-pentaethylethylenediamine
Ph	Phenyl
PJT	Pseudo-Jahn-Teller
PTFE	Polytetrafluoroethylene
R2 Salt	$[\text{Ph}_3\text{BnP}^+]_2[\text{Si}_6\text{Cl}_{14}^{2-}]$

Si ₆ H ₁₂	Cyclohexasilane
SiNRs	Silicon nanorods
SiNWs	Silicon nanowires
SiQDs	Silicon quantum dots
SLS	Solid-liquid-solid
TEEDA	N,N,N',N'-tetraethylethylenediamine
TMEDA	N,N,N',N'-tetramethylethylenediamine
Tr ⁺	Trityl ⁺ cation
UV-Vis	Ultraviolet-visible spectroscopy
VLS	Vapor-liquid-solid
XRD	X-ray diffraction

LIST OF APPENDIX TABLES

<u>Table</u>	<u>Page</u>
A1. Crystallographic data for $[\text{Ph}_4\text{P}^+]_2[\text{Si}_6\text{Cl}_{12}\text{Br}_2^{2-}]$ and $[\text{Ph}_4\text{P}^+]_2[\text{Si}_6\text{Br}_{14}^{2-}]$	75

LIST OF APPENDIX FIGURES

<u>Figure</u>	<u>Page</u>
A1. Thermal ellipsoid plot of $[\text{Ph}_4\text{P}^+]_2[\text{Si}_6\text{Cl}_{12}\text{Br}_2^{2-}]$. Thermal ellipsoids set at 50% probability. Hydrogen atoms omitted for clarity.	75
A2. Thermal ellipsoid plot of $[\text{Ph}_4\text{P}^+]_2[\text{Si}_6\text{Br}_{14}^{2-}]$. Thermal ellipsoids set at 50% probability. Hydrogen atoms omitted for clarity.	76

1. INTRODUCTION AND APPLICATIONS

1.1. Abstract

This chapter summarizes the existing research on cyclohexasilane and its derivatives, with particular emphasis on the syntheses of Si_6H_{12} and $\text{Si}_6\text{Cl}_{12}$. That emphasis is merited because this work focused on the development of alternative routes for synthesizing these materials. This chapter provides a comparison of this work with routes reported in literature. A more thorough analysis and justification of the work that went into developing this route is provided elsewhere, with chapter 2 summarizing the research on developing $[\text{Ph}_3\text{BnP}^+]_2[\text{Si}_6\text{Cl}_{14}^{2-}]$, a precursor to $\text{Si}_6\text{Cl}_{12}$ and Si_6H_{12} (Ph = phenyl, Bn = benzyl). Chapter 3 summarizes the synthesis of $\text{Si}_6\text{Cl}_{12}$ from $[\text{Ph}_3\text{BnP}^+]_2[\text{Si}_6\text{Cl}_{14}^{2-}]$.

Past studies have revealed that the Lewis acid wells on Si_6X_{12} (X = Cl, Br) can be utilized to produce diadducts with nitriles or ionic salts. In the case of nitriles, the lone electron pairs function as the Lewis base. In the case of ionic salts, the halogen anion functions as the Lewis base, forming an $[\text{Si}_6\text{X}_{12}\text{X}'_2]^{2-}$ dianion salt. The 2^- charge is offset by the two cations.

The results reported in chapter 4 expand upon this work by discussing the synthesis and characterization of the novel $[\text{Si}_6\text{X}_{12}\text{X}'_2]^{2-}$ dianion salts offset by two trityl carbenium cations. In addition, the chapter discusses the attempts to complete the characterization of the reported Si_6X_{12} diadducts.

1.2. Goals of this Thesis

- Develop a route toward synthesizing a salt containing the dianion $[\text{Si}_6\text{Cl}_{14}^{2-}]$ which is both soluble in organic solvents and offset by a simple cation.
- Develop a route towards synthesizing both Si_6H_{12} and $\text{Si}_6\text{Cl}_{12}$ using that salt as the starting material.

- Do a comparative analysis of the pros and cons of said route in comparison to the known ones reported in literature.
- Use the known salt [PEDETA·H₂SiCl⁺]₂[Si₆Cl₁₄²⁻] as a starting material for Si₆Cl₁₂.
- Complete the following characterization of the known Si₆X₁₂ diadducts: x-ray diffraction (XRD), elemental analysis (EA), ²⁹Si-nuclear magnetic resonance spectroscopy (²⁹Si-NMR) and ultraviolet-visible spectroscopy (UV-Vis).
- Synthesize and characterize Si₆I₁₂ along with its corresponding nitrile and ionic salt diadducts.
- Synthesize and characterize the novel [Si₆X₁₂X'₂²⁻] dianion salts offset by carbenium cations.

1.3. Cyclohexasilane's Unique Properties

Cyclohexasilane (Si₆H₁₂) has two properties that make it unique in comparison to the other commonly used linear and branched polysilanes: it is a liquid at room temperature and it has a lower activation energy.¹ In addition, its halogenated counterparts (Si₆X₁₂, X = Cl, Br) contain Lewis acid sites both above and below the center of the ring.²

The liquid nature and lower activation energy of Si₆H₁₂ gives it potential advantages over the commonly used acyclicsilanes as a starting material for silicon based materials. Such materials include silicon quantum dots (SiQDs),³⁻⁴ silicon nanorods (SiNRs)⁵ and silicon nanowires (SiNWs).⁶

For comparison, the traditional methods of producing SiQDs has been discussed in several review articles,⁷⁻⁸ however some notable methods include: fragmenting bulk Si into SiQDs using laser ablation⁹⁻¹¹ or ultrasonic dispersion,¹² reduction of gaseous silanes/organosilanes using thermal,¹³⁻¹⁴ laser¹⁵ or plasma treatment,¹⁶⁻¹⁸ and reduction of silanes

in supercritical fluid.¹⁹ In the case of Si_6H_{12} , SiQDs are produced from the gas-phase pyrolysis of Si_6H_{12} .

There is overlapping literature on the production of SiNRs and SiNWs, which has been previously outlined in a review article.²⁰ The production of SiNWs from Si_6H_{12} involves the novel method of electrospinning solutions of Si_6H_{12} . A common method is the metal-seeded growth of SiNRs in solutions of silane; typically trisilane with gold or tin nanoparticles. This method is known as solution-liquid-solid (SLS) growth.²¹⁻²⁵ The vapor-liquid-solid (VLS) method is based on a similar principle, however it uses gaseous silanes (i.e. SiCl_4 or SiH_4) as the source of silicon.²⁶⁻²⁷

This is particularly true for silicon thin film deposition. In the case of silicon thin film deposition, activation energy (E_a) refers to the slope of the film growth rate vs. substrate temperature (typical temperature range is 350-950°C).¹ The activation energy of Si_6H_{12} and its five membered ring counterpart, Si_5H_{10} , are 0.30 and 0.34 eV, respectively. This is significantly lower than the other commonly used linear silanes: SiH_4 (1.62-2.5 eV),²⁸ Si_2H_6 (2.38-3.0 eV),²⁹⁻³⁰ Si_3H_8 (1.63 eV)³¹ and Si_4H_{10} (1.38 eV).³²

Researchers at North Dakota State University (NDSU) have successfully developed a method of depositing silicon thin films from Si_6H_{12} known as aerosol assisted atmospheric pressure chemical vapor deposition (AA-APCVD). Utilizing Si_6H_{12} 's unique properties gives AA-APCVD potential advantages over the current state-of-the-art industrial silicon thin film deposition process known as plasma-enhanced chemical vapor deposition (PECVD). The potential advantages include: an increased deposition rate,²⁸ higher deposition efficiency,³³⁻³⁴ and the ability to function at atmospheric pressure.¹

The electron withdrawing nature of the halogens in Si_6X_{12} causes Lewis acid sites to appear both above and below the center of the ring. The Lewis acid sites have the capability of accepting Lewis bases such as the lone electron pairs in a nitrile species³⁵ or a halogen anion.³⁶ The formation of these adducts causes the traditionally puckered structure of Si_6X_{12} to be flattened, creating what is known as an “inverse sandwich complex.” In the instances where Si_6X_{12} accepts halogen anions, a dianion complex is formed with an overall charge of 2^- . These species are offset by two cations forming an $[\text{Si}_6\text{X}_{12}\text{X}'_2]^{2-}$ dianion salt (figure 1). In addition to constituting novel materials, dianion salts such as these are utilized by some syntheses as starting materials to Si_6H_{12} and $\text{Si}_6\text{Cl}_{12}$.³⁷⁻⁴⁰

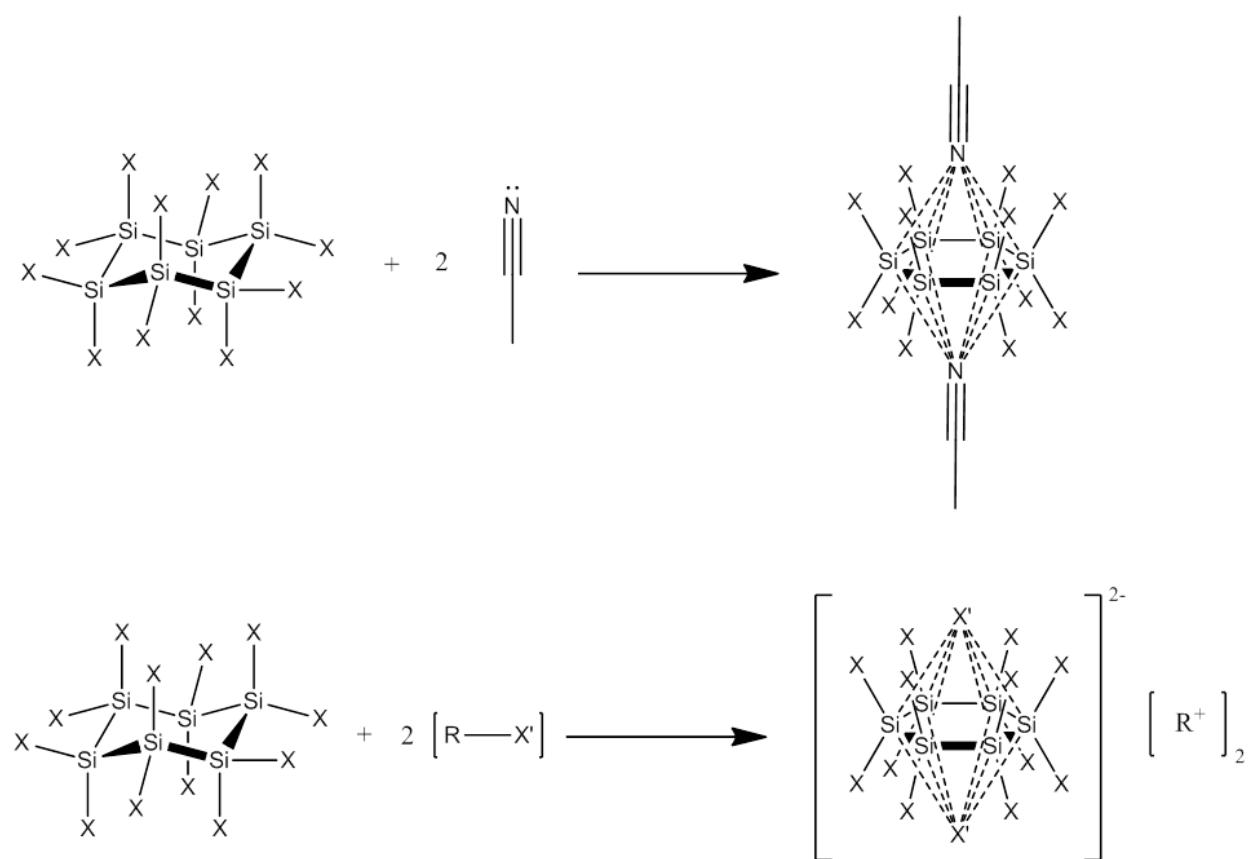


Figure 1. Formation of inverse sandwich complexes upon having the Lewis acid wells in Si_6X_{12} accept nitriles (top) or halogen anions (bottom).

$[\text{Si}_6\text{Cl}_{14}^{2-}]$ dianion salts can serve as an alternative starting material^{38,41} for previously synthesized derivatives such Si_6R_{12} (R = methyl, ethyl, propyl, tert-butyl and phenyl).⁴²⁻⁴⁴

1.4. Synthesis of Si_6H_{12} , Si_6X_{12} and Si_6X_{12} Diadducts

The work in this thesis developed syntheses for Si_6H_{12} , Si_6X_{12} and Si_6X_{12} diadducts. These syntheses are shown in comparison to other syntheses which have been previously reported in literature (figure 2). Of particular interest is the pathway towards producing $\text{Si}_6\text{Cl}_{12}$, of which there are four, with Frohlich's synthesis being based on the research described in this thesis. Table 1 provides a comparison of the yields for these 4 routes.

Table 1. Comparison of yields for routes to Si_6H_{12} and $\text{Si}_6\text{Cl}_{12}$.

Silane	Hengge	Boudjouk	Tillman	Frohlich
$\text{Si}_6\text{Cl}_{12}$	2.3%	39%	11.1%	58.3%
Si_6H_{12}	3.4%	55.4%	----	----

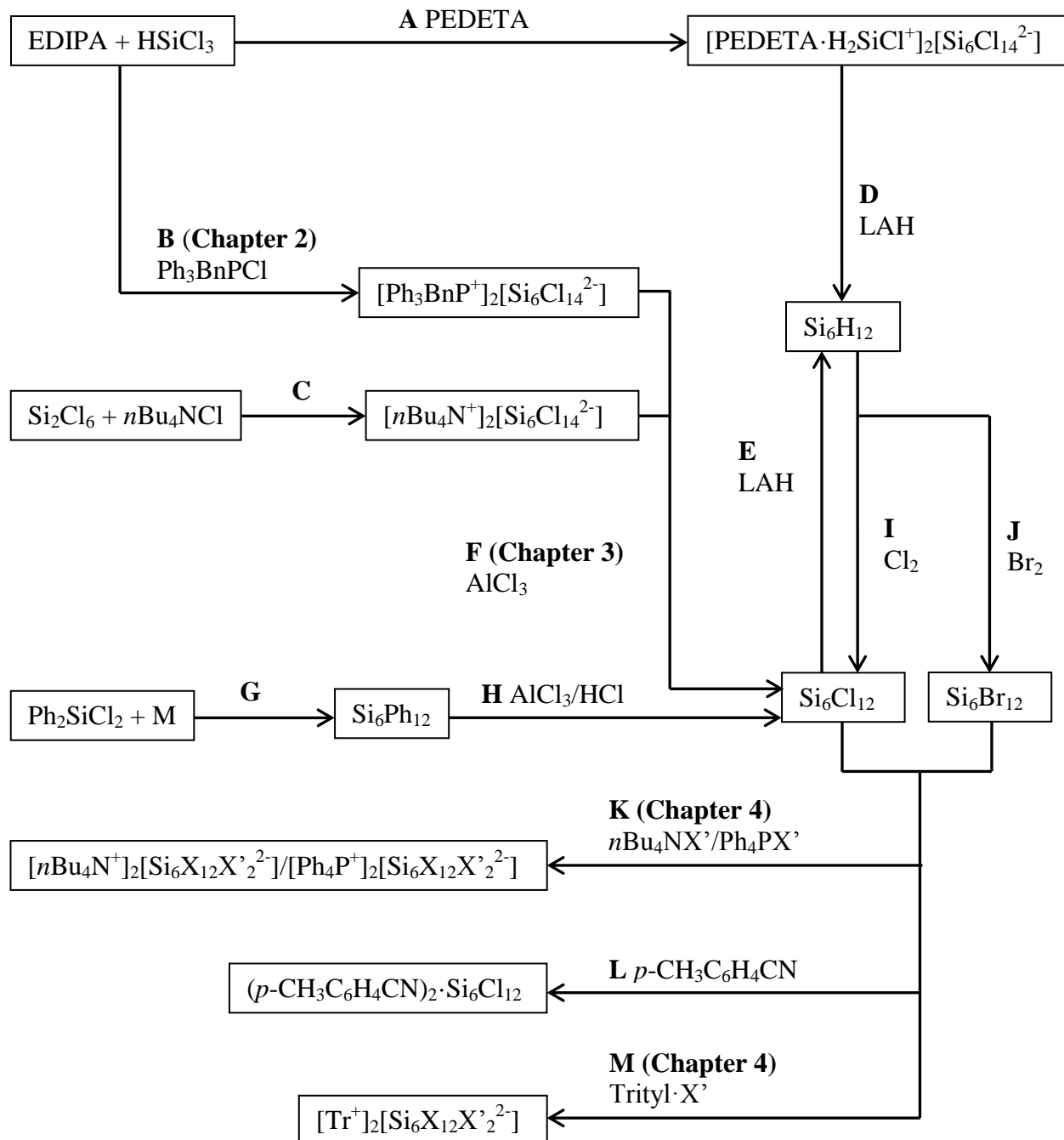


Figure 2. Pathways towards Si₆H₁₂, Si₆X₁₂ and Si₆X₁₂ diadducts.

1.4.1. Hengge's Synthesis

Though the original synthesis of $\text{Si}_6\text{Ph}_{12}$ can be traced back to 1921,⁴⁵ it was not until 1960 that it was officially characterized by *Gilman et al* (reaction **G**).⁴⁶ In 1977 *Hengge et al* used $\text{Si}_6\text{Ph}_{12}$ as a precursor for producing $\text{Si}_6\text{Cl}_{12}$ which was in turn used as a precursor for Si_6H_{12} (reactions **H** and **E**).⁴⁷⁻⁴⁸ Collectively, this series of reactions will be referred to as “Hengge's synthesis.”

$\text{Si}_6\text{Ph}_{12}$ arises from the reaction of Ph_2SiCl_2 with an alkali metal.^{46,49-51} A mixture of 35.6 g finely cut Na (1.55 mol) in 700 mL toluene is heated until the Na melts. The heat is removed and the subsequent addition of 180 g Ph_2SiCl_2 (0.71 mol) is accompanied by an exotherm and the formation of blue insoluble solid. The addition rate of Ph_2SiCl_2 is controlled to maintain a gentle reflux.

The reaction mixture is returned to room temperature and the excess Na quenched by adding the reaction mixture to ethanol. The solids are filtered via filtration and washed thoroughly with water. $\text{Si}_6\text{Ph}_{12}$ is recrystallized from the filtrate's organic layer following drying over Na_2SO_4 . A second recrystallization is performed in a mixture of benzene and petroleum ether, giving 7.5 g $\text{Si}_6\text{Ph}_{12}$ (6.9 mmol), for a yield of 5.8%. Additional fractions of $\text{Si}_6\text{Ph}_{12}$ cannot be isolated from the organic phase due to the large amount of diphenylsilylene polymers.

$\text{Si}_6\text{Ph}_{12}$ is mixed with a catalytic amount of AlCl_3 in dry benzene. The reaction mixture is boiled for 1 h while adding dry HCl gas. The AlCl_3 is removed via filtration and the benzene removed via distillation. The resulting product is sublimed (145°C, 0.1 Torr). 0.22 g $\text{Si}_6\text{Cl}_{12}$ (0.37 mmol) is produced for every 1.0 g $\text{Si}_6\text{Ph}_{12}$ (0.91 mmol), giving a yield of 41%. This brings the overall yield of $\text{Si}_6\text{Cl}_{12}$ for Hengge's synthesis to 2.3%.

In lieu of removing the benzene from the filtrate, an ethereal solution of lithium aluminum hydride can be added while under ice cooling to convert the $\text{Si}_6\text{Cl}_{12}$ to Si_6H_{12} . After stirring for 1 h, the ether is removed via vacuum, and the resulting precipitate removed via filtration. The benzene is removed at 1 Torr and the remaining Si_6H_{12} distilled at 0.01 Torr/80°C to give a clear colorless liquid. 0.39 g Si_6H_{12} (2.2 mmol) is isolated for every 4.0 g $\text{Si}_6\text{Ph}_{12}$ (3.7 mmol) used as starting material, giving a yield of 59%. This brings the overall yield of Si_6H_{12} for Hengge's synthesis to 3.4%.

1.4.2. Boudjouk's Synthesis

Boudjouk's synthesis is based upon the demonstrated ability of H_2SiCl_2 and HSiCl_3 to form hexacoordinate complexes with alkylated polyamines such as N,N,N',N'-tetramethylethylenediamine (TMEDA), N,N,N',N'-tetraethylethylenediamine (TEEDA) or N,N,N',N'',N''-pentaethyldiaminetriamine (PEDETA).⁵²⁻⁵⁴ One notable reaction is that of HSiCl_3 with TEEDA in the presence of a quaternary salt, such as Ph_4PCl , which produces $[\text{Ph}_4\text{P}^+]_2[\text{Si}_6\text{Cl}_{14}^{2-}]$ (reaction **B**). In this case, the hexacoordinate species formed between HSiCl_3 and TEEDA is an intermediate to the final product. Another notable reaction is that of HSiCl_3 with PEDETA in CH_2Cl_2 to produce $[\text{PEDETA}\cdot\text{H}_2\text{SiCl}^+]_2[\text{Si}_6\text{Cl}_{14}^{2-}]$, wherein the hexacoordinate species $[\text{PEDETA}\cdot\text{H}_2\text{SiCl}^+]$ serves as a reaction intermediate and forms the counterion to the $[\text{Si}_6\text{Cl}_{14}^{2-}]$ dianion (reaction **A**). $[\text{Si}_6\text{Cl}_{14}^{2-}]$ dianion salts can be converted to Si_6H_{12} via reduction with lithium aluminum hydride (LAH) in diethyl ether (reaction **E**).^{41,55} Reacting Si_6H_{12} with Cl_2 or Br_2 in CH_2Cl_2 at -89°C produces $\text{Si}_6\text{Cl}_{12}$ and $\text{Si}_6\text{Br}_{12}$, respectively (reactions **I** and **J**).³⁵ This series of reactions will be collectively referred to as "Boudjouk's synthesis."

The original reaction was improved by introducing a deprotonating reagent, such as a tertiary amine with a pKa greater than 10.5, the most useful of which has been determined to be

N,N-diisopropylethylamine (EDIPA).⁵⁶ EDIPA abstracts both a H and Cl atom during the reaction, producing the quaternary salt EDIPA·HCl as a byproduct.

Suitable reaction conditions vary based primarily on reagents, stoichiometry, solvent and reaction time. The optimized laboratory-scale conditions for producing the $[\text{Si}_6\text{Cl}_{14}^{2-}]$ precursor to Si_6H_{12} use a 1:3:5 ratio of PEDETA:EDIPA:HSiCl₃ in CH₂Cl₂ to produce $[\text{PEDETA}\cdot\text{H}_2\text{SiCl}^+]_2[\text{Si}_6\text{Cl}_{14}^{2-}]$.⁵⁷ The reaction is performed under a dry N₂ atmosphere and all starting materials are dried and deoxygenated. The reaction vessel is fitted with a condenser set to -10°C. The reaction vessel is charged with 400 mL CH₂Cl₂, 81.5 g PEDETA (0.335 mol) and 129.9 g EDIPA (1.005 mol). 226.9 g HSiCl₃ (1.675 mol) is added via an addition funnel over 1 h while stirring the reaction mixture. The reaction vessel is subsequently heated at 55°C for 72 h, after which time the heating and stirring are removed to facilitate precipitation of the product.

The product is filtered and washed 3x with 100 mL CH₂Cl₂. It is dried for 30 min using an N₂ stream. Typical yields are 140. g (109 mmol), for a yield of 65.1% (reaction uses excess HSiCl₃, so yields treat PEDETA/EDIPA as the limiting reagent).

$[\text{PEDETA}\cdot\text{H}_2\text{SiCl}^+]_2[\text{Si}_6\text{Cl}_{14}^{2-}]$ is reduced to Si_6H_{12} by reacting with LAH in diethyl ether. The reaction vessel is a jacketed reactor cooled to 10°C and stirred via overhead mixer. 116.95 g $[\text{PEDETA}\cdot\text{H}_2\text{SiCl}^+]_2[\text{Si}_6\text{Cl}_{14}^{2-}]$ (91.166 mmol) is added to 450 mL diethyl ether. 442.5 mL 1.03 M LAH/diethyl ether solution (456 mmol) is slowly added to the reaction mixture via cannula transfer. The reaction mixture is stirred at 20°C for 16 h. Solids are removed by filtration and washed with 200 mL diethyl ether. The filtrate is concentrated by removing diethyl ether via vacuum. The resulting solution is extracted with 100 mL pentane. The pentane extract is washed with 3x50 mL 9 N H₂SO₄ washes. The H₂SO₄ is added slowly via dropwise addition to control the resulting gas formation. The pentane layer is decanted, dried over Na₂SO₄, filtered and

fractionally distilled under reduced pressure to give 14.0 g Si_6H_{12} (77.5 mmol), for a yield of 85.0%. This brings the overall yield of Boudjouk's synthesis to 55.4%.⁵

The original literature cites producing $\text{Si}_6\text{Cl}_{12}$ in 89% yield by reacting Si_6H_{12} with Cl_2 in -89°C CH_2Cl_2 . However, subsequent laboratory experiments showed that this product contained a mixture of chlorosilanes impurities. The crude product was purified by dissolving in hexane and removing the insoluble impurities via filtration. The $\text{Si}_6\text{Cl}_{12}$ was crystallized from the resulting filtrate, lowering the yield to 70%, giving an overall yield of 39% for Boudjouk's synthesis.⁵⁸

Alternatively, $\text{Si}_6\text{Br}_{12}$ can be synthesized by reacting Si_6H_{12} with Br_2 in CH_2Cl_2 . 0.300 g Si_6H_{12} (1.67 mmol) is added to 10 mL CH_2Cl_2 and cooled to -89°C . A solution of 1.1 mL Br_2 (3.43 g, 2.14 mmol) in 10 mL CH_2Cl_2 is added to the reaction mixture over 1 h. Excess Br_2 is removed via vacuum while holding the reaction mixture at -89°C . Following this, solvent is removed, revealing 1.76 g of pale orange solid (1.56 mmol), for a yield of 94.0%. This brings the overall yield for Boudjouk's synthesis to 52.1%.

1.4.3. Tillman's Synthesis

Tillman's synthesis is based on the 2012 observation that the reaction of TMEDA with Si_2Cl_6 in pentane produced the species $\text{Si}_2\text{Cl}_6\cdot\text{TMEDA}$. Isolation of this species and subsequent dissolution in CH_2Cl_2 produced a mixture of the oligochlorosilanes $\text{Si}_n\text{Cl}_{2n}$ ($n = 4, 6, 8, 10$) and the dianion salts $[\text{Si}_n\text{Cl}_{2n+2}]^{2-}$. Of particular interest was the product $[\text{Me}_3\text{NCH}_2\text{CH}_2\text{NMe}_2^+]_2[\text{Si}_6\text{Cl}_{14}^{2-}]$, which was successfully isolated and characterized via XRD.⁵⁹

This synthesis was modified in 2014 using $n\text{Bu}_4\text{NCl}$ with Si_2Cl_6 in CH_2Cl_2 . A variety of $[n\text{Bu}_4\text{N}^+]_2[\text{Si}_6\text{Cl}_{14}^{2-}]$ based salts were produced, including those with chlorosilyl groups protruding from the ring, such as $[n\text{Bu}_4\text{N}^+]_2[(\text{SiCl}_3)\text{Si}_6\text{Cl}_{13}^{2-}]$ and $[n\text{Bu}_4\text{N}^+]_2[(1,1-$

$(\text{SiCl}_3)_2\text{Si}_6\text{Cl}_{12}]^{2-}$. Despite the mixture of products, pure $[\text{nBu}_4\text{N}^+]_2[\text{Si}_6\text{Cl}_{14}]^{2-}$ was successfully isolated by altering the stoichiometry, reaction time and crystallization conditions (reaction C).⁶⁰ $[\text{nBu}_4\text{N}^+]_2[\text{Si}_6\text{Cl}_{14}]^{2-}$ was successfully reacted with AlCl_3 to produce $\text{Si}_6\text{Cl}_{12}$ (reaction F).³⁷ Conceivably, $[\text{nBu}_4\text{N}^+]_2[\text{Si}_6\text{Cl}_{14}]^{2-}$ could be reacted with LAH to produce Si_6H_{12} as in Boudjouk's synthesis, however this synthesis has not yet been reported in literature.

The reaction proceeds by combining 14.5 g Si_2Cl_6 (53.9 mmol), 5.0 g nBu_4NCl (18 mmol) and 20 mL CH_2Cl_2 , producing a clear pale yellow solution, whose color faded overnight upon storage at room temperature. Crystalline material began precipitating after several days' storage at room temperature, but was not collected until 20 days. 2.96 g of a 4:1 mixture of $[\text{nBu}_4\text{N}^+]_2[(1,1-(\text{SiCl}_3)_2\text{Si}_6\text{Cl}_{12})^{2-}]:[\text{nBu}_4\text{N}^+]_2[\text{Si}_8\text{Cl}_{18}]^{2-}$ isomers was isolated. Storage for an additional 60 days at room temperature resulted in the precipitation of 3.50 g $[\text{nBu}_4\text{N}^+]_2[\text{Si}_6\text{Cl}_{14}]^{2-}$ (3.04 mmol), giving a yield of 16.9%.

145 mg AlCl_3 (1.09 mmol) is combined with 5 mL C_6H_6 in a Schlenk tube. 500 mg $[\text{nBu}_4\text{N}^+]_2[\text{Si}_6\text{Cl}_{14}]^{2-}$ (43.5 mmol) is added to the mixture while stirring in quarter increments every 30 min. The reaction mixture is stirred an additional h to produce a clear colorless solution. The solvent is removed under reduced pressure and 5 mL *n*-hexane added to the resulting colorless solid residue. The reaction vessel is immersed in liquid nitrogen until the *n*-hexane solidifies. The reaction vessel is evacuated via vacuum and sealed shut. It is then heated to 85°C for 30 min and subsequently cooled to room temperature. The mixture is filtered via a 0.2 μm polytetrafluoroethylene (PTFE) syringe filter, producing a clear colorless liquid. The solvent is removed from the filtrate via vacuum, producing colorless product which is dried an additional 2 h under reduced pressure. 169 mg $\text{Si}_6\text{Cl}_{12}$ (28.5 mmol) is isolated for a yield of 65.5%, thus giving Tillman's synthesis an overall yield of 11.1%.

1.4.4. Frohlich's Synthesis

This synthesis is a modified version of Boudjouk's synthesis and is based on the work performed for this thesis. It includes the synthesis of $[\text{Ph}_3\text{BnP}^+]_2[\text{Si}_6\text{Cl}_{14}^{2-}]$ (R2 salt, reaction **B**) and its subsequent conversion to $\text{Si}_6\text{Cl}_{12}$ with AlCl_3 (reaction **F**). The synthesis of R2 salt is discussed in greater detail in chapter 2 and that of $\text{Si}_6\text{Cl}_{12}$ in chapter 3.

Suitable reaction conditions for the synthesis of R2 salt vary based primarily on reagents, stoichiometry, solvent and reaction time. The optimized laboratory-scale conditions for producing R2 salt use a 1:0.1:3:5 mole ratio of $\text{Ph}_3\text{BnP}^+:\text{glyme}:\text{EDIPA}:\text{HSiCl}_3$ and 72 h reaction time (glyme = 1,2-dimethoxyethane). The reaction is performed under a dry N_2 atmosphere and all starting materials are dried and deoxygenated. The reaction vessel is fitted with a condenser set to -10°C . The reaction vessel is charged with 51.19 g Ph_3BnP^+ (131.6 mmol), 1.19 g glyme (13.2 mmol), 51.2 g EDIPA (396 mmol), and 150. mL CH_2Cl_2 . 67.0 mL HSiCl_3 (664 mmol) was added via addition funnel over 30 min while stirring. Heat was applied and refluxing controlled at ≤ 1 drop/second ($\sim 50^\circ\text{C}$). Heating ceased after 72 h. Storage at -28°C for 21 h resulted in precipitation of white crystals (crude RR'). The ratio of $\text{Ph}_3\text{BnP}^+:\text{EDIPA}\cdot\text{H}^+$ varies between reactions, however an isolated crystal of crude RR' characterized via XRD had the chemical structure $[\text{Ph}_3\text{BnP}^+]_2[\text{EDIPA}\cdot\text{H}^+]_2[\text{Si}_6\text{Cl}_{14}^{2-}][\text{Cl}^-]_2[\text{CH}_2\text{Cl}_2]_4$ (yields assume CH_2Cl_2 was removed during vacuum drying). Note that ^1H -nuclear magnetic resonance spectroscopy (^1H -NMR) showed the presence of Si-H bonds in crude RR', which would give the dianion a chemical formula of $[\text{Si}_6\text{Cl}_{14-2}\text{H}_n^{2-}]$. 59.72 g crystals (35.07 mmol) were filtered via frit and dried under vacuum for 1 h.

The crude RR' is converted to crude R2 salt by dissolving in CHCl_3 . A cation exchange occurs, causing the newly formed $[\text{Ph}_3\text{BnP}^+]_2[\text{Si}_6\text{Cl}_{14-n}\text{H}_n^{2-}]$ to precipitate.⁶¹ 124.9 g crude RR'

(73.34 mmol) was added to 625 mL CHCl_3 , forming a clear colorless solution in <2 min. Following this, white solids began precipitating within 5 min. The mixture was stirred 1 h and subsequently allowed to settle for 15 min. The precipitate was filtered via frit and washed 3x with 80. mL -9°C CHCl_3 (CHCl_3 was kept cold to minimize dissolution of crude R2 salt). 45.6 g crude R2 (33.2 mmol) was collected. 36.5% of the original crude RR' was converted to crude R2 salt. Hypothetically, this would have converted the 59.72 g crude RR' from the initial reaction to 21.8 g crude R2 salt, giving a yield of 65.9% (reaction uses excess HSiCl_3 , so yields treat $\text{Ph}_3\text{BnPCl/EDIPA}$ as the limiting reagent).

The Si_6 ring in the crude R2 salt contains some remaining Si-H bonds that are converted to Si-Cl upon reaction with trityl chloride.⁵⁸ 4.990 g crude R2 salt (3.638 mmol) was reacted with 3.048 g trityl chloride (10.93 mmol) in 160. mL CH_2Cl_2 . The reaction mixture was stirred for 24 h. 160. mL hexanes were added to the reaction mixture to facilitate precipitation of the R2 salt dissolved in CH_2Cl_2 . It was stirred an additional 5 min and subsequently allowed to sit undisturbed for 2 h. The reaction mixture was filtered via frit and washed 3x with 20. mL -28°C CHCl_3 . 4.905 g R2 salt (3.576 mmol) was isolated following 1.5 h drying under vacuum (98.3% yield). This lowers the overall yield to 64.8%.

R2 salt was reacted with AlCl_3 in benzene to produce $\text{Si}_6\text{Cl}_{12}$. The reaction vessel was charged with 5.86 g AlCl_3 (43.9 mmol) in 200.0 mL benzene. 24.1 g R2 salt (17.6 mmol) was added to the reaction mixture in quarter increments every 15 min. The solvent was removed via vacuum, revealing green/yellow solids. The solids were dried an additional 30 min following complete solvent removal. The $\text{Si}_6\text{Cl}_{12}$ was extracted from the solids by adding 200.0 mL n-heptane and extracting for 30 min at 95°C while under stirring. The mother liquor was decanted and filtered via 0.2 μm PTFE filter upon returning to room temperature. The solvent was

removed from the filtrate via vacuum, revealing 9.38 g $\text{Si}_6\text{Cl}_{12}$ (15.8 mmol, 89.9% yield), bringing the overall yield in Frohlich's synthesis to 58.3%.

Note that Frohlich's synthesis could provide a potential pathway towards Si_6H_{12} by reducing either the crude RR' or crude R2 salt via LAH, however as of yet no definitive conclusions have been drawn on the feasibility of this route. If Frohlich's synthesis were to be utilized for this purpose, the chlorination of the crude R2 salt with trityl chloride would not necessarily be required as the presence of Si-H bonds would not affect the quality of the final product.

1.4.5. Synthesis of Si_6X_{12} Diadducts

1.4.5.1. Synthesis of $[\text{nBu}_4\text{N}^+]_2[\text{Si}_6\text{Cl}_{14}^{2-}]$

0.278 g nBu_4NCl (1.00 mmol) is added to a solution of 0.300 g $\text{Si}_6\text{Cl}_{12}$ (0.500 mmol) in 3.0 mL CH_2Cl_2 . The reaction mixture is stirred 2 h to produce a cloudy mixture. Product is precipitated by adding 0.5 mL hexane and stirring for 2 min. The reaction mixture is subsequently filtered to give 0.357 g crude product (0.310 mmol, 62.1% yield).

1.4.5.2. Synthesis of $(\text{p-CH}_3\text{C}_6\text{H}_4\text{CN})_2(\text{Si}_6\text{Cl}_{12})$

0.120 g $\text{p-CH}_3\text{C}_6\text{H}_4\text{CN}$ (1.02 mmol) is added to a solution of 0.235 g $\text{Si}_6\text{Cl}_{12}$ (0.396 mmol) in 2 mL CH_2Cl_2 , resulting in the immediate precipitation of white solids. The solids are collected by filtration and washed with CH_2Cl_2 to give 0.294 g product (0.355 mmol, 89.6% yield).

2. SYNTHESIS, OPTIMIZATION AND ISOLATION OF CRUDE RR' AND R2 SALTS

2.1. Abstract

The reaction of HSiCl_3 with EDIPA and a chelating ligand (TEEDA, glyme or diglyme) in CH_2Cl_2 proved to be a viable route towards producing working quantities of crude RR' (diglyme = diethylene glycol dimethyl ether). A series of crude RR' syntheses were conducted wherein the reaction conditions were altered by starting material ratio, chelating ligand, scale and time. The exact composition of crude RR' remains unknown as the ratio of $\text{Ph}_3\text{BnP}^+:\text{EDIPA}\cdot\text{H}^+$ appears to vary between reactions, however an isolated crystal of crude RR' had the chemical structure $[\text{Ph}_3\text{BnP}^+]_2[\text{EDIPA}\cdot\text{H}^+]_2[\text{Si}_6\text{Cl}_{14}^{2-}][\text{Cl}^-]_2[\text{CH}_2\text{Cl}_2]_4$.

Subsequent treatment of crude RR' with CHCl_3 caused a cation exchange to occur, wherein the newly formed $[\text{Ph}_3\text{BnP}^+]_2[\text{Si}_6\text{Cl}_{14-n}\text{H}_n^{2-}]$ (crude R2 salt) precipitated. The remaining compounds stayed in solution, allowing for the easy separation of crude R2 salt. Crude R2 salt contained Si-H bonds on the Si_6 ring which were chlorinated using trityl chloride, producing R2 salt. The solubility of R2 salt in CH_2Cl_2 proved to be higher than that of $[\text{PEDETA}\cdot\text{H}_2\text{SiCl}^+]_2[\text{Si}_6\text{Cl}_{14}^{2-}]$ produced in house (5.97 g/mL versus 0.830 g/mL), however it was lower than that for $[\text{PEDETA}\cdot\text{H}_2\text{SiCl}^+]_2[\text{Si}_6\text{Cl}_{14}^{2-}]$ which was purchased from a vendor (9.59 g/mL).

2.2. Background

There were two primary motivations for synthesizing $[\text{Ph}_3\text{BnP}^+]_2[\text{Si}_6\text{Cl}_{14}^{2-}]$ (R2 salt). The first is that it would provide a viable route towards producing working quantities of soluble $[\text{Si}_6\text{Cl}_{14}^{2-}]$, which have been previously limited due to either the insoluble nature of $[\text{Si}_6\text{Cl}_{14}^{2-}]$ salts or the difficulty in producing soluble varieties. Soluble $[\text{Si}_6\text{Cl}_{14}^{2-}]$ could be used as a starting material for $\text{Si}_6\text{Cl}_{12}$, potentially conferring an advantage over existing routes towards $\text{Si}_6\text{Cl}_{12}$.

The second motivation is that R2 salt could serve as a starting material for Si_6H_{12} via LAH reduction, with potential advantages over the traditionally used $[\text{PEDETA}\cdot\text{H}_2\text{SiCl}^+]_2[\text{Si}_6\text{Cl}_{14}^{2-}]$.

While Boudjouk's synthesis had an advantage over Hengge's and Tillman's syntheses in terms of producing Si_6H_{12} , there was room for improvement in the synthesis of $\text{Si}_6\text{Cl}_{12}$. Boudjouk's synthesis involved reducing $[\text{PEDETA}\cdot\text{H}_2\text{SiCl}^+]_2[\text{Si}_6\text{Cl}_{14}^{2-}]$, which contains an intact $\text{Si}_6\text{Cl}_{12}$ ring, to Si_6H_{12} via LAH. The Si_6H_{12} is subsequently converted back to $\text{Si}_6\text{Cl}_{12}$ by reacting with Cl_2 .

This introduced an extra step (the reduction of $[\text{PEDETA}\cdot\text{H}_2\text{SiCl}^+]_2[\text{Si}_6\text{Cl}_{14}^{2-}]$ via LAH) which could potentially be bypassed by converting $[\text{PEDETA}\cdot\text{H}_2\text{SiCl}^+]_2[\text{Si}_6\text{Cl}_{14}^{2-}]$ directly to $\text{Si}_6\text{Cl}_{12}$ by reacting with AlCl_3 as in Tillman's synthesis. It also involved using Cl_2 , which is a highly toxic gas.

R2 salt was partially developed on the pretense that the notoriously insoluble $[\text{PEDETA}\cdot\text{H}_2\text{SiCl}^+]_2[\text{Si}_6\text{Cl}_{14}^{2-}]$ would have potential difficulties in this reaction as Tillman's synthesis used $[n\text{Bu}_4\text{N}^+]_2[\text{Si}_6\text{Cl}_{14}^{2-}]$, which is soluble in common solvents. This hypothesis is untested, meaning $[\text{PEDETA}\cdot\text{H}_2\text{SiCl}^+]_2[\text{Si}_6\text{Cl}_{14}^{2-}]$ could still be a viable starting material for $\text{Si}_6\text{Cl}_{12}$. R2 salt, however, has a demonstrated solubility in CH_2Cl_2 , thus it was used as a starting material for $\text{Si}_6\text{Cl}_{12}$ (see chapter 3).

Conceivably, $[n\text{Bu}_4\text{N}^+]_2[\text{Si}_6\text{Cl}_{14}^{2-}]$ could be synthesized by Boudjouk's synthesis, however product isolation would be an issue as it would be in solution with the byproducts SiCl_4 and $\text{EDIPA}\cdot\text{HCl}$, along with any unreacted starting materials. An ideal quaternary salt would be one that produces an $[\text{Si}_6\text{Cl}_{14}^{2-}]$ salt that precipitates from solution, but is soluble in organic solvents when separated from the reaction mixture. Ph_3BnPCl was selected for this reason as the similar quaternary salt Ph_4PCl was successfully used to synthesize $[\text{Ph}_4\text{P}^+]_2[\text{Si}_6\text{Cl}_{14}^{2-}]$, which

subsequently precipitated from the reaction mixture. However, the isolated $[\text{Ph}_4\text{P}^+]_2[\text{Si}_6\text{Cl}_{14}^{2-}]$ was not soluble in organic solvents. The replacement of one phenyl group with a benzyl group introduces dissymmetry that could potentially make $[\text{Ph}_3\text{BnP}^+]_2[\text{Si}_6\text{Cl}_{14}^{2-}]$ more soluble than $[\text{Ph}_4\text{P}^+]_2[\text{Si}_6\text{Cl}_{14}^{2-}]$. Another advantage of using R2 salt is that it takes 12-72 h to synthesize, versus the $[\text{nBu}_4\text{N}^+]_2[\text{Si}_6\text{Cl}_{14}^{2-}]$ approach by Tillman which takes 80 days.

The disadvantage of $[\text{PEDETA}\cdot\text{H}_2\text{SiCl}^+]_2[\text{Si}_6\text{Cl}_{14}^{2-}]$ in LAH reduction is that the H_2SiCl^+ species are reduced to SiH_4 . This increases the danger of the reduction due to the fact that SiH_4 is not only pyrophoric, but a gas, and thus difficult to safely contain. This is in comparison to R2 salt which would not generate unwanted SiH_4 byproduct, because there is no silicon in the cation. Instead, the Ph_3BnP^+ cations would be reduced to a combination of Ph_3PH_2 , Ph_3P and toluene.⁶² No experiments have been conducted yet where R2 salt was reduced via LAH in this manner, so it remains unknown whether the advantages of reducing R2 salt would outweigh the disadvantages of reducing $[\text{PEDETA}\cdot\text{H}_2\text{SiCl}^+]_2[\text{Si}_6\text{Cl}_{14}^{2-}]$.

2.3. Results and Discussion

This reaction of HSiCl_3 with EDIPA and a chelating ligand in CH_2Cl_2 resulted in the formation of a clear colorless reaction mixture (slightly offset with yellow color due to EDIPA and TEEDA) which precipitated white crystalline solids upon freezing at -28°C . Characterization of the white solids via XRD revealed them to have the crystal structure $[\text{Ph}_3\text{BnP}^+]_2[\text{EDIPA}\cdot\text{H}^+]_2[\text{Si}_6\text{Cl}_{14}^{2-}][\text{Cl}^-]_2[\text{CH}_2\text{Cl}_2]_4$ (figure 3). $^1\text{H-NMR}$ and $^{29}\text{Si-NMR}$ corroborated this by showing the presence of Ph_3BnP^+ , $\text{EDIPA}\cdot\text{H}^+$ and $[\text{Si}_6\text{Cl}_{14}^{2-}]$ (figures 4 and 5). Note that there is shifting between the peaks for free Ph_3BnP^+ and $[\text{Ph}_3\text{BnP}^+]_2[\text{Si}_6\text{Cl}_{14}^{2-}]$ as shown in the $^1\text{H-NMR}$ spectrum for Ph_3BnP^+ in CD_2Cl_2 (figure 6). Likewise, free EDIPA can be differentiated from $\text{EDIPA}\cdot\text{H}^+$ by observing the spectrum for EDIPA in CD_2Cl_2 (figure 7).

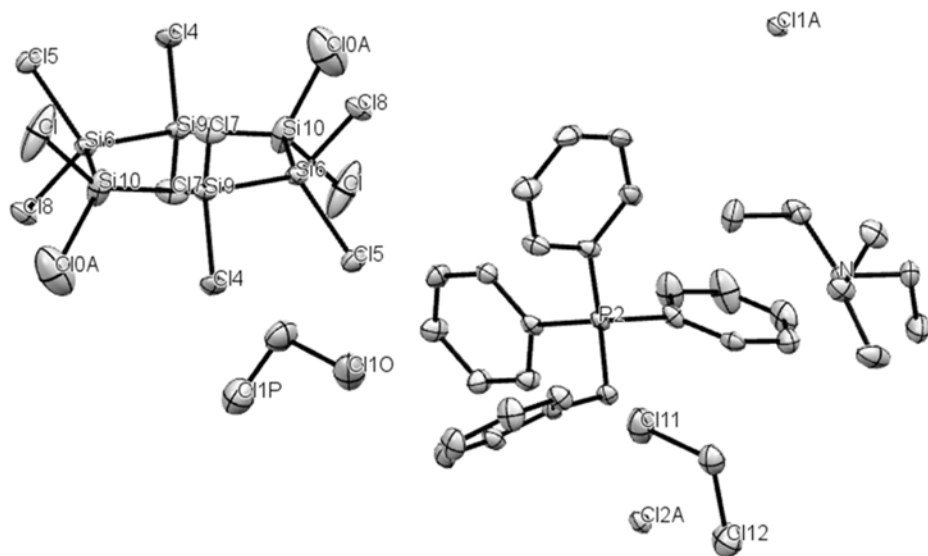


Figure 3. Thermal ellipsoid plot of reaction mixture precipitate. Thermal ellipsoids set at 50% probability. Hydrogen atoms omitted for clarity. Formula conforms to that of $[\text{Ph}_3\text{BnP}^+]_2[\text{EDIPA}\cdot\text{H}^+]_2[\text{Si}_6\text{Cl}_{14}^{2-}][\text{Cl}]_2[\text{CH}_2\text{Cl}_2]_4$: 4(Cl), 2($\text{C}_{25}\text{H}_{22}\text{P}$), $\text{Si}_6\text{Cl}_{12}$, 2 ($\text{C}_8\text{H}_{20}\text{N}$), 4 (CH_2Cl_2).

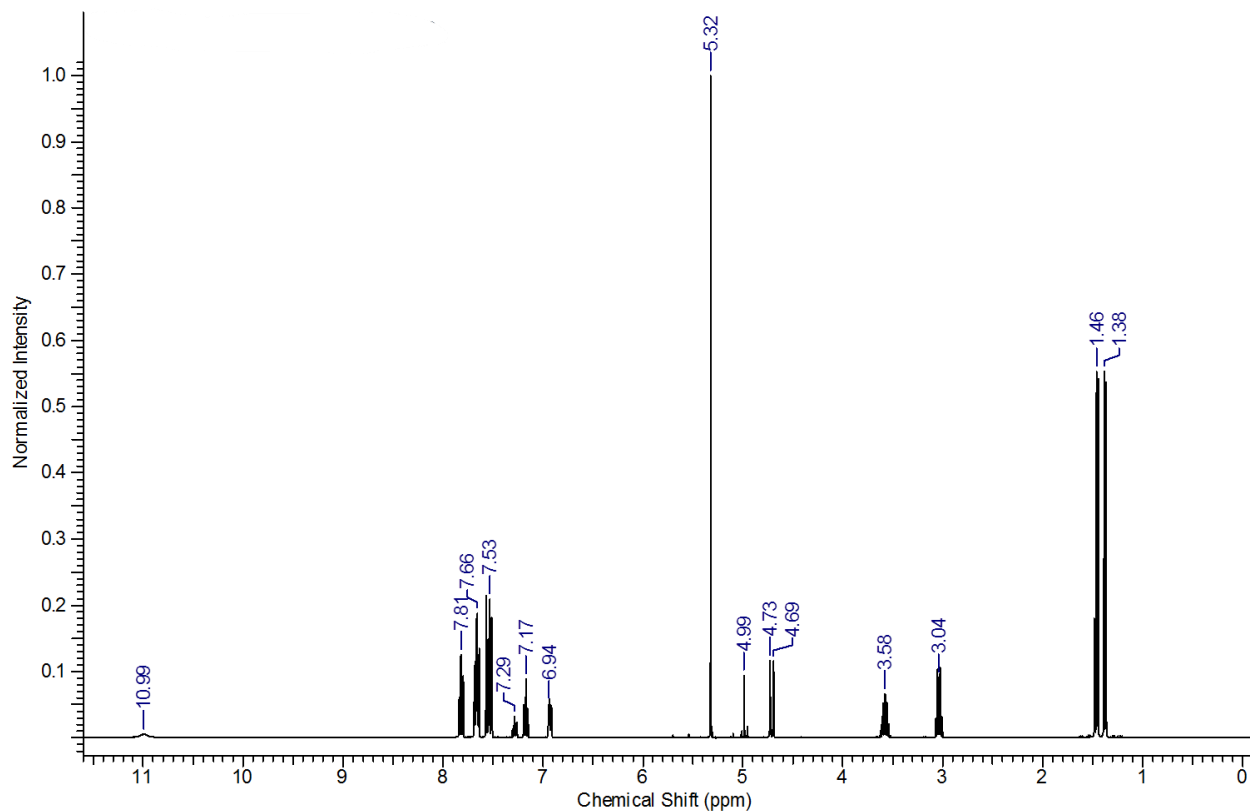


Figure 4. ¹H-NMR spectrum for reaction mixture precipitate (crude RR') washed with CH₂Cl₂ in CD₂Cl₂. δ (Ph₃BnP⁺): 7.81 (t, 6H, p-Ph), 7.66 (m, 12H, m-Ph), 7.53 (m, 12H, o-Ph), 7.29 (t, 2H, p-Bn), 7.17 (t, 4H, m-Bn), 6.94 (d, 4H, o-Bn), 4.71 (d, 4H, PCH₂Bn). δ (EDIPA·H⁺): 10.99 (s, 2H, EDIPA·H⁺), 3.58 (sep, 8H, (CH₃)₂CHN), 3.04 (q, 8H, CH₃CH₂N), 1.38-1.46 (m, 60H, (CH₃)₂CHN and CH₃CH₂N). δ [Si₆Cl_{12-n}H_nCl₂²⁻]: 4.99.

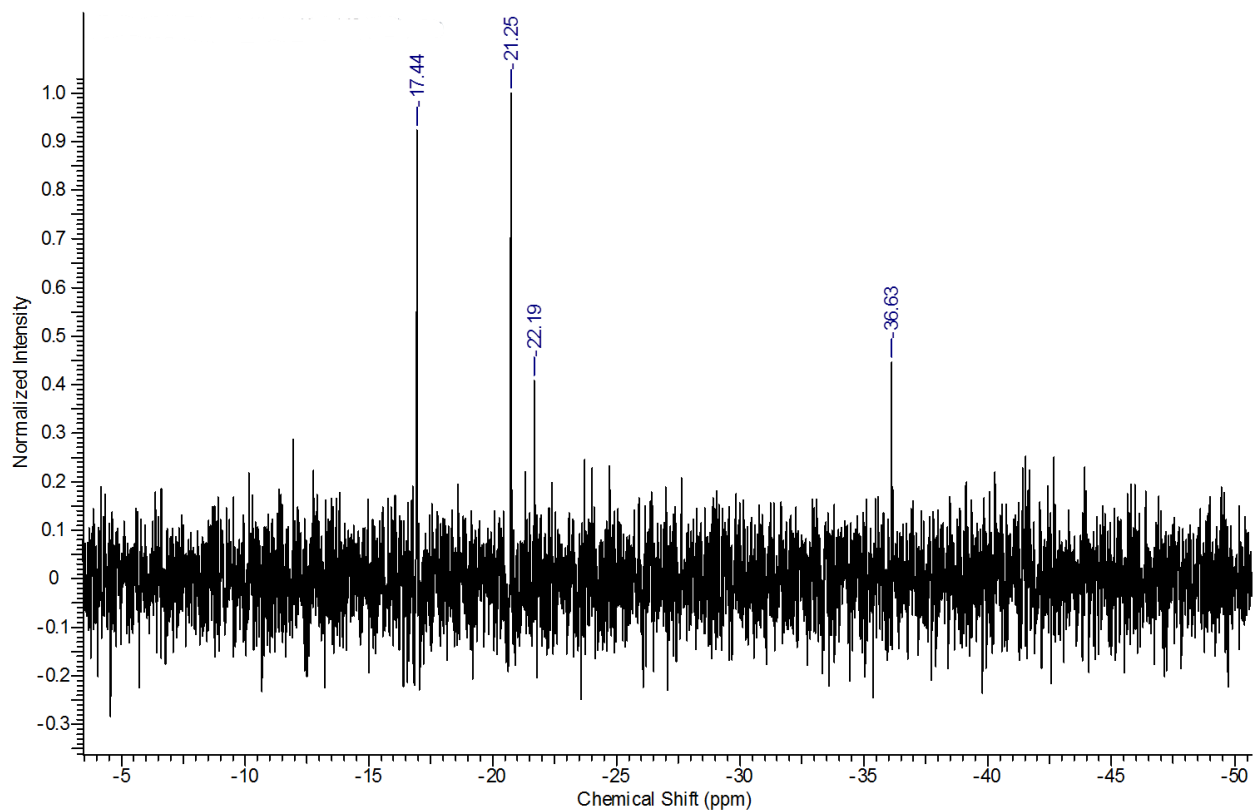


Figure 5. ^{29}Si -NMR spectrum for reaction mixture precipitate (crude RR') washed with CH_2Cl_2 in CD_2Cl_2 . δ [$\text{Si}_6\text{Cl}_{14}^{2-}$]: -21.25.⁶³ δ [$\text{Si}_6\text{Cl}_{12-n}\text{H}_n\text{Cl}_2^{2-}$]: -17.44, -22.19, -36.33.⁶⁴

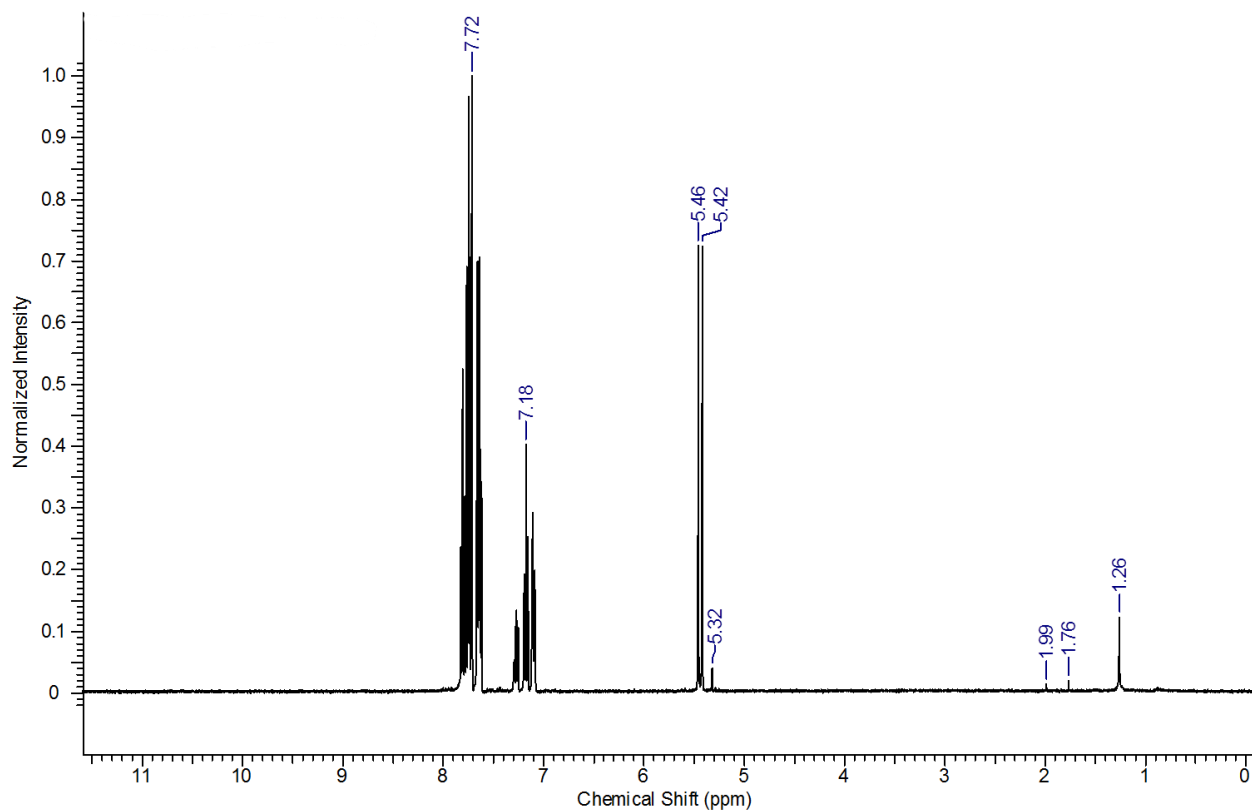


Figure 6. ¹H-NMR spectrum for Ph₃BnPCl in CD₂Cl₂. δ (Ph₃BnPCl): 7.62-7.80 (m, 15H, Ph₃BnPCl), 7.09-7.28 (m, 5H, Ph₃(Ph)CH₂PCl), 5.44 (d, 2H, Ph₃(PH)CH₂PCl). Note that peak shifting differs from that seen for [Ph₃BnP⁺]₂[EDIPA·H⁺]₂[Si₆Cl₁₄²⁻][Cl⁻]₂[CH₂Cl₂]₄ in figure 4.

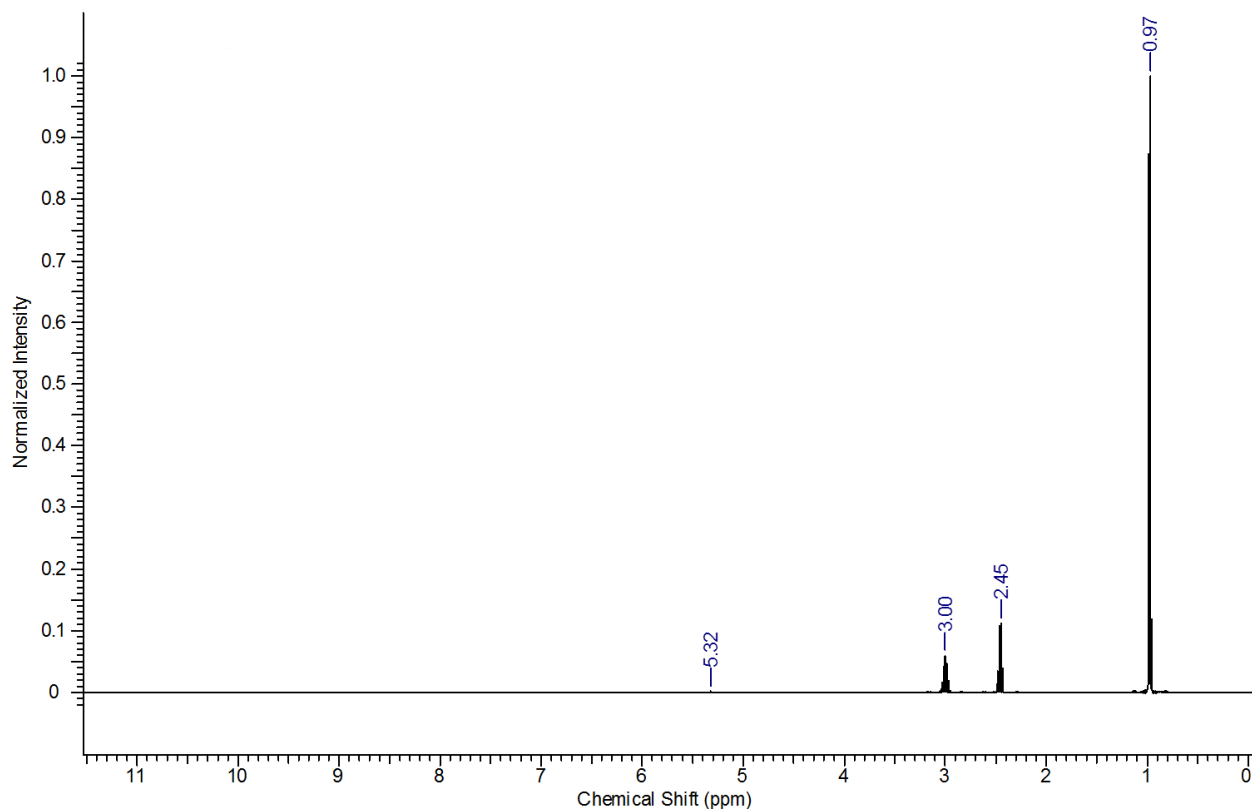


Figure 7. $^1\text{H-NMR}$ spectrum for EDIPA in CD_2Cl_2 . δ (EDIPA): 3.00 (sep, 2H, $(\text{CH}_3)_2\text{CHN}$), 2.45 (q, 2H, $\text{CH}_3\text{CH}_2\text{N}$), 0.97 (m, 15H, $(\text{CH}_3)_2\text{CHN}$ and $\text{CH}_3\text{CH}_2\text{N}$). Note that peak shifting differs from that seen for $[\text{Ph}_3\text{BnP}^+]_2[\text{EDIPA}\cdot\text{H}^+]_2[\text{Si}_6\text{Cl}_{14}^{2-}][\text{Cl}^-]_2[\text{CH}_2\text{Cl}_2]_4$ in figure 4.

Crude RR' initially dissolved in CHCl_3 , producing a clear colorless solution, however white solids began precipitating within 5 min. Subsequent filtration and washing of the solids following 1 h stirring revealed the solids to be R2 salt as evidenced by the characteristic peak shifting for Ph_3BnP^+ and lack of $\text{EDIPA}\cdot\text{H}^+$ in the $^1\text{H-NMR}$ (figure 8).

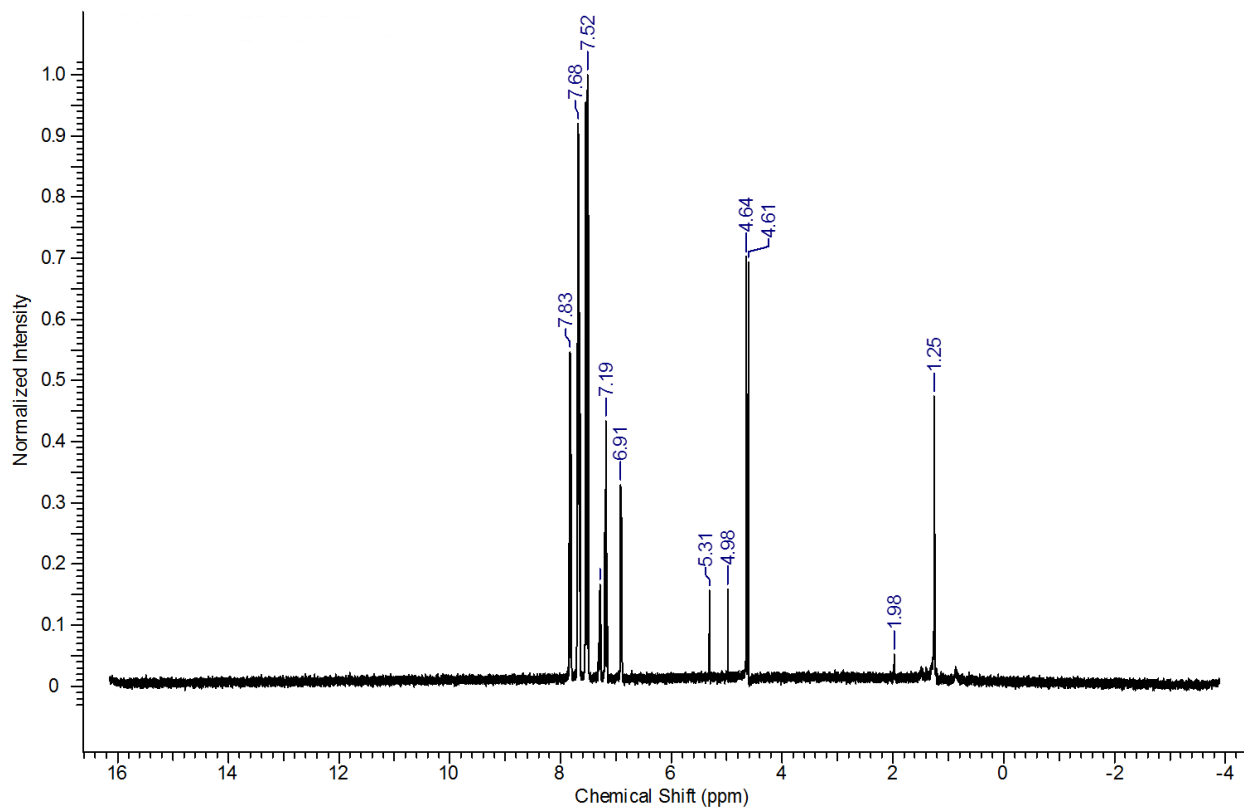


Figure 8. $^1\text{H-NMR}$ spectrum for the resulting precipitate of crude RR' in CHCl_3 (crude R2 salt) in CD_2Cl_2 . δ (Ph_3BnP^+): 7.83 (t, 6H, p-Ph), 7.68 (m, 12H, m-Ph), 7.52 (m, 12H, o-Ph), 7.29 (t, 2H, p-Bn), 7.19 (t, 4H, m-Bn), 6.91 (d, 4H, o-Bn), 4.62 (d, 4H, PCH_2Bn). δ [$\text{Si}_6\text{Cl}_{12-n}\text{H}_n\text{Cl}_2^{2-}$]: 4.98.

The presence of [$\text{Si}_6\text{Cl}_{12-n}\text{H}_n\text{Cl}_2^{2-}$] in crude RR' was detected by $^1\text{H-NMR}$ and $^{29}\text{Si-NMR}$ as shown in figures 4 and 5, with Si-H peaks in the $^1\text{H-NMR}$ spectrum and extra silicon peaks in $^{29}\text{Si-NMR}$. The silicons in [$\text{Si}_6\text{Cl}_{14}^{2-}$] should all be equivalent, meaning a $^{29}\text{Si-NMR}$ spectrum should have a single peak. The addition of Si-H bonds would create dissymmetry, thus producing more peaks. Another [$\text{Si}_6\text{Cl}_{14}^{2-}$] synthesis cited in literature using HSiCl_3 , chelating ligand, proton abstracting agent and quaternary salt have reported similar results.⁶⁴

Fourier transform infrared spectroscopy (FTIR) spectra for crude RR' and crude R2 salt consistently show a Si-H peak around 2100 cm^{-1} that is attributed to a non-fully chlorinated Si_6 ring (figure 9).⁶⁵⁻⁶⁷ This could potentially be detrimental to subsequent reactions that utilize $\text{Si}_6\text{Cl}_{12}$ generated from crude R2 salt as the resulting $\text{Si}_6\text{Cl}_{12}$ may not be fully chlorinated.

Reacting crude R2 salt with t in CH_2Cl_2 for 24 h effectively chlorinated the remaining Si-H bonds on the Si_6 ring, as seen by the lack of Si-H in its FTIR spectrum (figure 10).

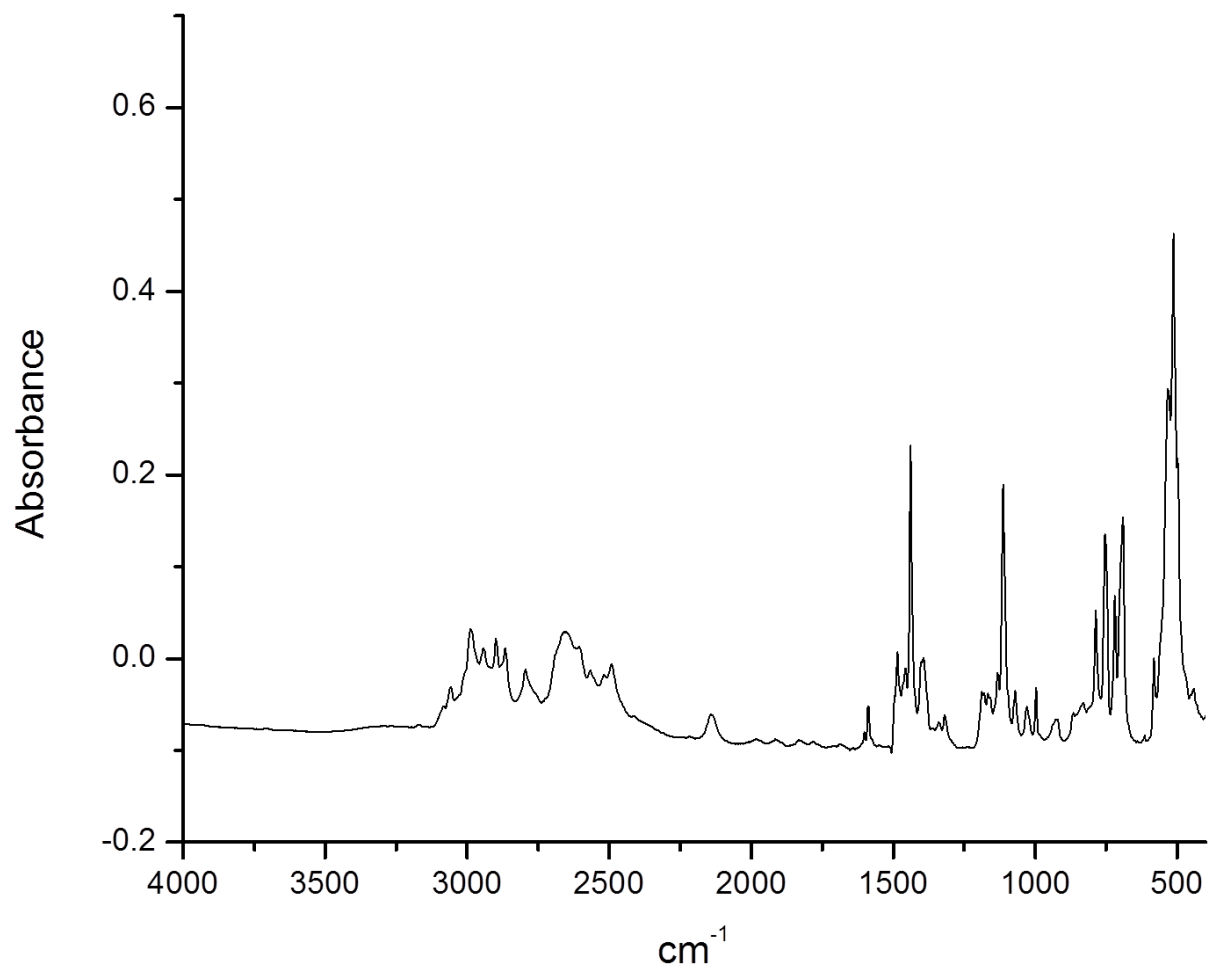


Figure 9. FTIR spectrum for crude RR' in a KBr pellet.

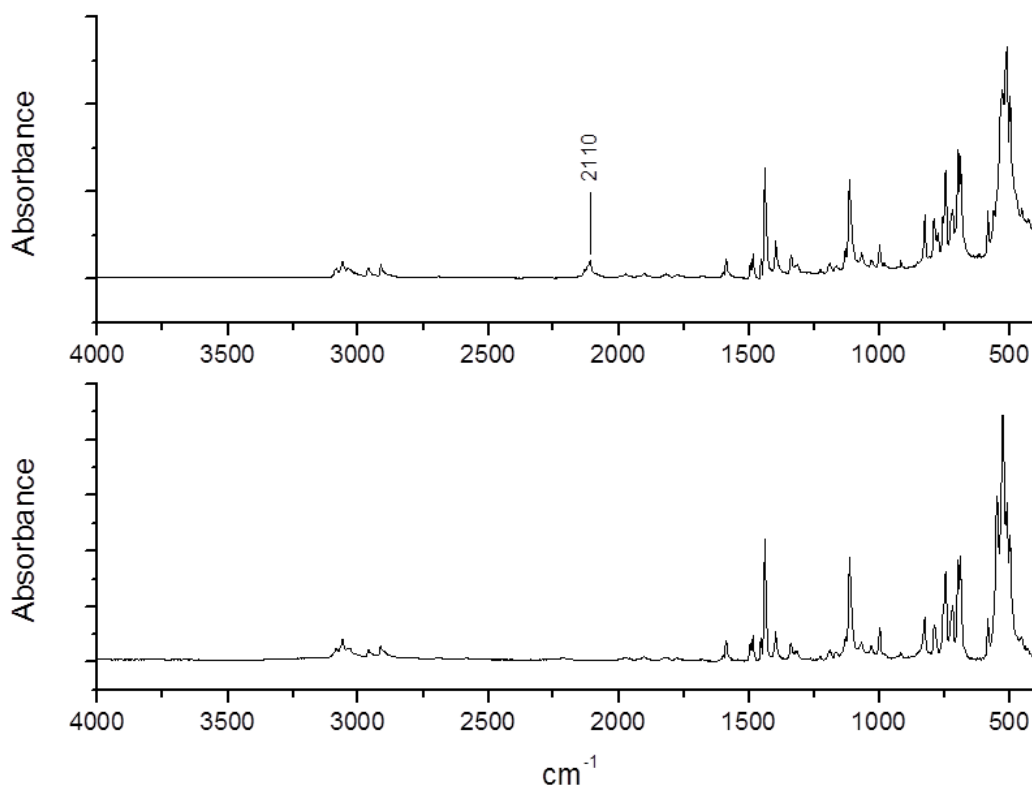


Figure 10. FTIR data for crude R2 salt (top) and trityl chloride treated R2 salt (bottom).

The synthesis of crude RR' was optimized for yield by altering the type of chelating ligand, starting material ratios, reaction time and reaction scale (table 2). Crude yields use $\text{Ph}_3\text{BnPCl}/\text{EDIPA}$ as the limiting reagents and are based on the product characterized via XRD: $[\text{Ph}_3\text{BnP}^+]_2[\text{EDIPA}\cdot\text{H}^+]_2[\text{Si}_6\text{Cl}_{14}^{2-}][\text{Cl}^-]_2$ (MW = 1703.10). CH_2Cl_2 is assumed to have been removed from the crystalline lattice during drying of crude product under vacuum.

Table 2. Summary of crude RR' syntheses.

Reaction	Mole Ratios				Time (h)	Yield
	Ph ₃ BnPCl	Chelating Ligand	EDIPA	HSiCl ₃		
A (TEEDA)	1	1	3	3	72	2.65 g (64.8%)
B (TEEDA)	1	1	3	5	72	2.96 g (72.4%)
C (TEEDA)	1	0.1	3	5	72	2.03 g (49.7%)
D (Diglyme)	1	1	3	3	72	1.19 g (29.1%)
E (Diglyme)	1	1	3	5	72	1.35 g (33.0%)
F (Diglyme)	1	0.1	3	5	72	1.50 g (36.7%)
G (Glyme)	1	1	3	3	72	1.80 g (44.0%)
H (Glyme)	1	1	3	5	72	1.88 g (46.0%)
I (Glyme)	1	0.1	3	5	72	2.09 g (51.1%)
J (TEEDA)	1	1	3	5	24	2.80 g (68.5%)
K (TEEDA)	1	1	3	5	24	2.94 g (71.9%)
L (TEEDA)	1	1	3	5	12	2.93 g (71.7%)
M (Glyme)	1	1	3	5	24	1.47 g (36.0%)
N (Glyme)	1	0.1	3	5	24	1.27 g (31.1%)
O (Glyme)	1	0.1	3	5	72	21.3 g (50.5%)
P (Glyme)	1	0.1	3	5	72	59.7 g (53.1%)
Q (Glyme)	1	0.1	3	5	72	124.9 g (57.2%)

-Type of chelating ligand listed in parentheses.

-Yields use Ph₃BnPCl/EDIPA as the limiting reagents.

The solubility of three separate [Si₆Cl₁₄²⁻] salts were recorded in CH₂Cl₂: R2 salt, [PEDETA·H₂SiCl⁺]₂[Si₆Cl₁₄²⁻] (synthesized in lab), and [PEDETA·H₂SiCl⁺]₂[Si₆Cl₁₄²⁻] (purchased from vendor, table 3). All measurements were performed in triplicate. The R2 salt was treated with trityl chloride prior to testing to ensure the Si₆ ring was fully chlorinated. The in lab [PEDETA·H₂SiCl⁺]₂[Si₆Cl₁₄²⁻] was synthesized according to the procedure developed at NDSU. The vendor supplied [PEDETA·H₂SiCl⁺]₂[Si₆Cl₁₄²⁻] was used as is.

The vendor [PEDETA·H₂SiCl⁺]₂[Si₆Cl₁₄²⁻] had the highest solubility of 9.59 g/L whereas the in lab [PEDETA·H₂SiCl⁺]₂[Si₆Cl₁₄²⁻] had the lowest solubility of 0.830 g/L. The R2 salt had a solubility of 5.97 g/L.

Table 3. Solubility of the following $[\text{Si}_6\text{Cl}_{14}^{2-}]$ salts in CH_2Cl_2 : R2 salt, $[\text{PEDETA}\cdot\text{H}_2\text{SiCl}^+]_2[\text{Si}_6\text{Cl}_{14}^{2-}]$ (synthesized in lab), and $[\text{PEDETA}\cdot\text{H}_2\text{SiCl}^+]_2[\text{Si}_6\text{Cl}_{14}^{2-}]$ (purchased from vendor).

$[\text{Si}_6\text{Cl}_{14}^{2-}]$ Salt	Solubility (g/L)	Standard Deviation (g/L)
R2 Salt	5.97	0.30
$[\text{PEDETA}\cdot\text{H}_2\text{SiCl}^+]_2[\text{Si}_6\text{Cl}_{14}^{2-}]$ (in lab)	0.830	0.052
$[\text{PEDETA}\cdot\text{H}_2\text{SiCl}^+]_2[\text{Si}_6\text{Cl}_{14}^{2-}]$ (vendor)	9.59	0.38

2.4. Experimental Methods

2.4.1. Preparation of Starting Materials

Starting materials were reagent grade quality or higher, unless otherwise noted. The presence of O_2 or H_2O , whether in solvents or the atmosphere, is detrimental to these reactions as the trichlorosilane and products are $\text{O}_2/\text{H}_2\text{O}$ sensitive. For this reason, all experiments were performed under a dry, inert atmosphere (i.e. nitrogen or argon) either in a glove box or by using air-free Schlenk line techniques, unless otherwise noted. Glassware (including stir bars) was dried in a drying oven at 150°C for ≥ 2 h and transferred to the glove box antechamber while still hot. This reduces the effects of H_2O condensation as the glassware returned to room temperature.

Solvents were dried according to literature protocols,⁶⁸ either by passage through a neutral alumina column or purchased from the vendor anhydrous. They were subsequently deoxygenated via sparging with N_2 while stirring for ≥ 2 h. They were stored under an inert atmosphere over either 3 Å or 4 Å molecular sieves. The molecular sieves were dried at 300°C under a vacuum of ≤ 50 mTorr for ≥ 12 h and stored under an inert atmosphere. Solvents were checked for water and oxygen prior to use by adding diethyl zinc solution (pyrophoric) and checking for the formation of fumes.

Amines (TEEDA and EDIPA) were deoxygenated via sparging with N_2 while stirring for ≥ 2 h. They were subsequently stored in an inert atmosphere over NaOH or KOH for a minimum of 12 h.

Solids were dried under a vacuum of ≤ 50 mTorr for ≥ 12 h either at room temperature or elevated temperature, depending on the material's melting point. They were subsequently checked for dryness by collecting an FTIR spectrum for said materials (H_2O has a characteristic broad peak from $3200\text{-}3650\text{ cm}^{-1}$ due to its O-H bonds).⁶⁹

2.4.2. Characterization of Materials

NMR characterization used either a JEOL 400 MHz NMR Spectrometer with solid state capabilities or a Bruker 400 MHz NMR Spectrometer. FTIR spectra were recorded using either a Bruker Optics Vertex 70 Fourier Transform Infrared Spectrometer or a Thermo Scientific Nicolet 8700 FT-IR. Samples were prepared in KBr pellets. Due to the air sensitive nature of the materials being tested, samples were transferred to the FTIR under dry, N_2 conditions and quickly transferred to the FTIR, whose sample chamber was constantly being flushed with dry N_2 . XRD characterization used a Kappa Apex II Duo. Samples were immersed in mineral oil during transfer to the instrument as a way of mitigating atmospheric exposure.

2.4.3. Experimental Procedures

The small scale syntheses (A-L) followed the same procedure, while the scale up syntheses (M-N) followed a modified procedure to accommodate the increased amount of starting materials.

2.4.3.1. Small Scale Syntheses (A-N)

Reactions were conducted in pressure vessels equipped with magnetic stir bars (pressure vessels allowed for addition of liquid starting materials via syringe). The reaction vessel was charged with the necessary Ph_3BnPCl , chelating ligand, EDIPA and CH_2Cl_2 .

The Ph_3BnPCl was not fully dissolved at this point and floated to the top of the reaction mixture. The mother liquor, while initially clear colorless (with a possible light yellow

discoloration depending on the quality of the amines), became pink in some instances. The HSiCl_3 was subsequently added via syringe upon cooling the reaction mixture and $\text{HSiCl}_3 \leq 14^\circ\text{C}$. This was accompanied by the immediate disappearance of pink color (if present) along with the near total dissolution of the Ph_3BnPCl . The reaction vessel was cooled at $\leq 14^\circ\text{C}$ for ≥ 15 min to mitigate any exotherm formation.

The reaction vessel was heated at 55°C while under stirring for the duration of the reaction. The remaining undissolved Ph_3BnPCl dissolved in ≤ 1 h, forming a clear solution. Following heating, the reaction mixture was stored at -28°C to facilitate precipitation of product (note that removal of the pressure cap was necessary for the initiation of precipitation).

The precipitate was cold filtered via frit. As the precipitate was soluble in CH_2Cl_2 , it was washed once with the filtrate, which was assumed to be saturated. The solids were dried under vacuum for ≥ 30 min, and the crude yield collected based on the remaining mass of solids.

2.4.3.2. Large Scale Syntheses (O-Q)

Reactions were conducted at atmospheric pressure (a condenser was used to keep the volatiles in the reaction mixture). The reaction vessel was charged with the necessary Ph_3BnPCl , chelating ligand, EDIPA and CH_2Cl_2 . The Ph_3BnPCl was not fully dissolved at this point and floated to the top of the reaction mixture. The mother liquor was clear colorless with a possible light yellow discoloration depending on the quality of the amines. The reaction mixture was set to stir and the HSiCl_3 was added via addition funnel over ≥ 30 min. This created an exotherm that resulted in refluxing. The addition rate was controlled to keep the refluxing rate ≤ 1 drop/second. Complete addition of HSiCl_3 resulted in the full dissolution of Ph_3BnPCl .

The reaction vessel was heated at 50-60°C while under stirring for the duration of the reaction. The remaining undissolved Ph₃BnPCl dissolved in ≤1 h, forming a clear solution. Following heating, the reaction mixture was stored at -28°C to facilitate precipitation of product.

The precipitate was cold filtered via frit. As the precipitate was soluble in CH₂Cl₂, it was washed once with the filtrate, which was assumed to be saturated. The solids were dried under vacuum for ≥1 h, and the crude yield collected based on the remaining mass of solids.

2.4.3.3. Reaction Conditions

2.4.3.3.1. Reaction A (1:1:3:3 Ph₃BnPCl:TEEDA:EDIPA:HSiCl₃, 72 h)

Reaction vessel was charged with 1.858 g Ph₃BnPCl (4.778 mmol), 0.828 g TEEDA (4.81 mmol), 1.860 g EDIPA (14.39 mmol), and 12.8 mL CH₂Cl₂, forming clear colorless mother liquor. Ph₃BnPCl floated on top of reaction mixture as a hard cake. Reaction vessel and 1.5 mL HSiCl₃ (15 mmol) were cooled to -28°C. HSiCl₃ was added via syringe, resulting in near total dissolution of Ph₃BnPCl. Heating at 55°C caused remaining Ph₃BnPCl to dissolve ≤20 min, forming clear colorless solution. Cloudy sediment began forming in reaction mixture at 70 h. Heating ceased after 72 h. Storage at -28°C for 66 h resulted in precipitation of white crystals. Crystals filtered via frit and dried under vacuum for 30 min. 2.65 g crude yield (1.56 mmol, 64.8% yield).

2.4.3.3.2. Reaction B (1:1:3:5 Ph₃BnPCl:TEEDA:EDIPA:HSiCl₃, 72 h)

Reaction vessel was charged with 1.860 g Ph₃BnPCl (4.782 mmol), 0.828 g TEEDA (4.80 mmol), 1.858 g EDIPA (14.37 mmol), and 12.8 mL CH₂Cl₂, forming clear colorless mother liquor. Ph₃BnPCl floated on top of reaction mixture as a hard cake. Reaction vessel and 2.5 mL HSiCl₃ (25 mmol) were cooled to -28°C. HSiCl₃ was added via syringe, resulting in near total dissolution of Ph₃BnPCl. Heating at 55°C caused remaining Ph₃BnPCl to dissolve ≤20 min,

forming clear colorless solution. Heating ceased after 72 h. Storage at -28°C for 51 h resulted in precipitation of white crystals. Crystals filtered via frit and dried under vacuum for 30 min. 2.96 g crude yield (1.74 mmol, 72.4% yield).

2.4.3.3.3. Reaction C (1:0.1:3:5 Ph₃BnPCl:TEEDA:EDIPA:HSiCl₃, 72 h)

Reaction vessel was charged with 1.862 g Ph₃BnPCl (4.787 mmol), 0.0836 g TEEDA (0.485 mmol), 1.858 g EDIPA (14.38 mmol), and 12.8 mL CH₂Cl₂, forming clear pink mother liquor. Ph₃BnPCl floated on top of reaction mixture as a hard cake. Reaction vessel and 2.5 mL HSiCl₃ (25 mmol) were cooled to -28°C. HSiCl₃ was added via syringe, resulting in near total dissolution of Ph₃BnPCl. Heating at 55°C caused remaining Ph₃BnPCl to dissolve ≤20 min, forming clear colorless solution. Heating ceased after 72 h. Storage at -28°C for 66 h resulted in precipitation of white crystals. Crystals filtered via frit and dried under vacuum for 30 min. 2.03 g crude yield (1.19 mmol, 49.7% yield).

2.4.3.3.4. Reaction D (1:1:3:3 Ph₃BnPCl:Diglyme:EDIPA:HSiCl₃, 72 h)

Reaction vessel was charged with 1.865 g Ph₃BnPCl (4.796 mmol), 0.645 g diglyme (4.81 mmol), 1.863 g EDIPA (14.41 mmol), and 12.8 mL CH₂Cl₂, forming clear colorless mother liquor. Ph₃BnPCl floated on top of reaction mixture as a hard cake. Reaction vessel and 1.5 mL HSiCl₃ (15 mmol) were cooled to -28°C. HSiCl₃ was added via syringe, resulting in near total dissolution of Ph₃BnPCl. Heating at 55°C caused remaining Ph₃BnPCl to dissolve ≤10 min, forming clear colorless solution. Heating ceased after 72 h. Storage at -28°C for 3.5 h resulted in precipitation of white crystals. Crystals filtered via frit and dried under vacuum for 30 min. 1.19 g crude yield (0.699 mmol, 29.1% yield).

2.4.3.3.5. Reaction E (1:1:3:5 Ph₃BnPCl:Diglyme:EDIPA:HSiCl₃, 72 h)

Reaction vessel was charged with 1.870 g Ph₃BnPCl (4.809 mmol), 0.644 g diglyme (4.80 mmol), 1.859 g EDIPA (14.38 mmol), and 12.8 mL CH₂Cl₂, forming clear colorless mother liquor. Ph₃BnPCl floated on top of reaction mixture as a hard cake. Reaction vessel and 2.5 mL HSiCl₃ (25 mmol) were cooled to -28°C. HSiCl₃ was added via syringe, resulting in near total dissolution of Ph₃BnPCl. Heating at 55°C caused remaining Ph₃BnPCl to dissolve ≤10 min, forming clear colorless solution. Heating ceased after 72 h. Storage at -28°C for 69 h resulted in precipitation of white crystals. Crystals filtered via frit and dried under vacuum for 30 min. 1.35 g crude yield (0.793 mmol, 33.0% yield).

2.4.3.3.6. Reaction F (1:0.1:3:5 Ph₃BnPCl:Diglyme:EDIPA:HSiCl₃, 72 h)

Reaction vessel was charged with 1.865 g Ph₃BnPCl (4.797 mmol), 0.0641 g diglyme (0.478 mmol), 1.859 g EDIPA (14.38 mmol), and 12.8 mL CH₂Cl₂, forming clear colorless mother liquor. Ph₃BnPCl floated on top of reaction mixture as a hard cake. Reaction vessel and 2.5 mL HSiCl₃ (25 mmol) were cooled to -28°C. HSiCl₃ was added via syringe, resulting in near total dissolution of Ph₃BnPCl. Heating at 55°C caused remaining Ph₃BnPCl to dissolve ≤10 min, forming clear colorless solution. Heating ceased after 72 h. Storage at -28°C for 69 h resulted in precipitation of white crystals. Crystals filtered via frit and dried under vacuum for 30 min. 1.50 g crude yield (0.881 mmol, 36.7% yield).

2.4.3.3.7. Reaction G (1:1:3:3 Ph₃BnPCl:Glyme:EDIPA:HSiCl₃, 72 h)

Reaction vessel was charged with 1.871 g Ph₃BnPCl (4.811 mmol), 0.433 g glyme (4.81 mmol), 1.859 g EDIPA (14.38 mmol), and 12.8 mL CH₂Cl₂, forming clear colorless mother liquor. Ph₃BnPCl floated on top of reaction mixture as a hard cake. Reaction vessel and 1.45 mL HSiCl₃ (14.4 mmol) were cooled to -28°C. HSiCl₃ was added via syringe, resulting in near total

dissolution of Ph_3BnPCl . Heating at 55°C caused remaining Ph_3BnPCl to dissolve ≤ 30 min, forming clear colorless solution. White flakes began forming in reaction mixture during heating. Heating ceased after 72 h. Storage at -28°C for 64 h resulted in precipitation of white crystals. Crystals filtered via frit and dried under vacuum for 30 min. 1.80 g crude yield (1.06 mmol, 44.0% yield).

2.4.3.3.8. Reaction H (1:1:3:5 Ph_3BnPCl :Glyme:EDIPA: HSiCl_3 , 72 h)

Reaction vessel was charged with 1.870 g Ph_3BnPCl (4.810 mmol), 0.433 g glyme (4.80 mmol), 1.859 g EDIPA (14.38 mmol), and 12.8 mL CH_2Cl_2 , forming clear colorless mother liquor. Ph_3BnPCl floated on top of reaction mixture as a hard cake. Reaction vessel and 2.42 mL HSiCl_3 (24.0 mmol) were cooled to -28°C . HSiCl_3 was added via syringe, resulting in near total dissolution of Ph_3BnPCl . Heating at 55°C caused remaining Ph_3BnPCl to dissolve ≤ 30 min, forming clear colorless solution. White flakes began forming in reaction mixture during heating. Heating ceased after 72 h. Storage at -28°C for 64 h resulted in precipitation of white crystals. Crystals filtered via frit and dried under vacuum for 30 min. 1.88 g crude yield (1.10 mmol, 46.0% yield).

2.4.3.3.9. Reaction I (1:0.1:3:3 Ph_3BnPCl :Glyme:EDIPA: HSiCl_3 , 72 h)

Reaction vessel was charged with 1.869 g Ph_3BnPCl (4.807 mmol), 0.0431 g glyme (0.478 mmol), 1.860 g EDIPA (14.39 mmol), and 12.8 mL CH_2Cl_2 , forming clear colorless mother liquor. Ph_3BnPCl floated on top of reaction mixture as a hard cake. Reaction vessel and 2.42 mL HSiCl_3 (24.0 mmol) were cooled to -28°C . HSiCl_3 was added via syringe, resulting in near total dissolution of Ph_3BnPCl . Heating at 55°C caused remaining Ph_3BnPCl to dissolve ≤ 30 min, forming clear colorless solution. White flakes began forming in reaction mixture during heating. Heating ceased after 72 h. Storage at -28°C for 64 h resulted in precipitation of white

crystals. Crystals filtered via frit and dried under vacuum for 30 min. 2.09 g crude yield (1.23 mmol, 51.1% yield).

2.4.3.3.10. Reaction J (1:1:3:5 Ph₃BnPCl:TEEDA:EDIPA:HSiCl₃, 24 h)

Reaction vessel was charged with 1.866 g Ph₃BnPCl (4.799 mmol), 0.828 g TEEDA (4.81 mmol), 1.862 g EDIPA (14.41 mmol), and 12.8 mL CH₂Cl₂, forming clear colorless mother liquor. Ph₃BnPCl floated on top of reaction mixture as a hard cake. Reaction vessel and 2.42 mL HSiCl₃ (24.0 mmol) were cooled to -28°C. HSiCl₃ was added via syringe, resulting in near total dissolution of Ph₃BnPCl. Heating at 55°C caused remaining Ph₃BnPCl to dissolve ≤30 min, forming clear colorless solution. Heating ceased after 24 h. Storage at -28°C for 44.5 h resulted in precipitation of white crystals. Crystals filtered via frit and dried under vacuum for 30 min. 2.80 g crude yield (1.64 mmol, 68.5% yield).

2.4.3.3.11. Reaction K (1:1:3:5 Ph₃BnPCl:TEEDA:EDIPA:HSiCl₃, 24 h)

Reaction vessel was charged with 1.866 g Ph₃BnPCl (4.799 mmol), 0.827 g TEEDA (4.80 mmol), 1.861 g EDIPA (14.40 mmol), and 12.8 mL CH₂Cl₂, forming clear slightly yellow mother liquor. Ph₃BnPCl floated on top of reaction mixture as a hard cake. Reaction vessel and 2.42 mL HSiCl₃ (24.0 mmol) were cooled to -28°C. HSiCl₃ was added via syringe, resulting in near total dissolution of Ph₃BnPCl. Heating at 55°C caused remaining Ph₃BnPCl to dissolve ≤30 min, forming clear slightly yellow solution. Heating ceased after 24 h. Storage at -28°C for 21 h resulted in precipitation of white crystals. Crystals filtered via frit and dried under vacuum for 30 min. 2.94 g crude yield (1.73 mmol, 71.9% yield).

2.4.3.3.12. Reaction L (1:1:3:5 Ph₃BnPCl:TEEDA:EDIPA:HSiCl₃, 12 h)

Reaction vessel was charged with 1.868 g Ph₃BnPCl (4.804 mmol), 0.827 g TEEDA (9.18 mmol), 1.860 g EDIPA (14.39 mmol), and 12.8 mL CH₂Cl₂, forming clear colorless

mother liquor. Ph_3BnPCl floated on top of reaction mixture as a hard cake. Reaction vessel and 2.42 mL HSiCl_3 (24.0 mmol) were cooled to -28°C . HSiCl_3 was added via syringe, resulting in near total dissolution of Ph_3BnPCl . Heating at 55°C caused remaining Ph_3BnPCl to dissolve ≤ 30 min, forming clear colorless solution. Heating ceased after 12 h. Storage at -28°C for 66 h resulted in precipitation of white crystals. Crystals filtered via frit and dried under vacuum for 30 min. 2.93 g crude yield (1.72 mmol, 71.7% yield).

2.4.3.3.13. Reaction M (1:1:3:5 Ph_3BnPCl :Glyme:EDIPA: HSiCl_3 , 24 h)

Reaction vessel was charged with 1.866 g Ph_3BnPCl (4.799 mmol), 0.433 g (4.80 mmol), 1.859 g EDIPA (14.38 mmol), and 12.8 mL CH_2Cl_2 , forming clear colorless mother liquor. Ph_3BnPCl floated on top of reaction mixture as a hard cake. Reaction vessel and 2.42 mL HSiCl_3 (24.0 mmol) were cooled to -14°C . HSiCl_3 was added via syringe, resulting in near total dissolution of Ph_3BnPCl . Heating at 55°C caused remaining Ph_3BnPCl to dissolve ≤ 30 min, forming clear colorless solution. Heating ceased after 24 h. Storage at -28°C for 21 h resulted in precipitation of white crystals. Crystals filtered via frit and dried under vacuum for 30 min. 1.47 g crude yield (0.863 mmol, 36.0% yield).

2.4.3.3.14. Reaction N (1:0.1:3:5 Ph_3BnPCl :Glyme:EDIPA: HSiCl_3 , 24 h)

Reaction vessel was charged with 1.869 g Ph_3BnPCl (4.806 mmol), 0.0435 g glyme (0.483 mmol), 1.862 g EDIPA (14.41 mmol), and 12.8 mL CH_2Cl_2 , forming clear colorless mother liquor. Ph_3BnPCl floated on top of reaction mixture as a hard cake. Reaction vessel and 2.42 mL HSiCl_3 (24.0 mmol) were cooled to -28°C . HSiCl_3 was added via syringe, resulting in near total dissolution of Ph_3BnPCl . Heating at 55°C caused remaining Ph_3BnPCl to dissolve ≤ 30 min, forming clear colorless solution. Heating ceased after 24 h. Storage at -28°C for 4 h resulted

in precipitation of white crystals. Crystals filtered via frit and dried under vacuum for 30 min. 1.27 g crude yield (0.746 mmol, 31.1% yield).

2.4.3.3.15. Reaction O (1:0.1:3:5 Ph₃BnPCl:Glyme:EDIPA:HSiCl₃, 72 h)

Reaction vessel was charged with 19.26 g Ph₃BnPCl (49.52 mmol), 0.4469 g glyme (4.959 mmol), 19.21 g EDIPA (148.6 mmol), and 133 mL CH₂Cl₂, forming clear yellow mother liquor. The reaction vessel was fitted with a condenser set to -10°C. Ph₃BnPCl floated on top of reaction mixture as a hard cake. 25.0 mL HSiCl₃ (248 mmol) was added via addition funnel over 20 min while stirring, resulting in the total dissolution of the Ph₃BnPCl. Heat was applied and refluxing controlled at ≤1 drop/second. Heating ceased after 70 h. Storage at -28°C for 22.5 h resulted in precipitation of white crystals. Crystals filtered via frit and dried under vacuum for 1 h. 21.3 g crude yield (12.5 mmol, 50.5% yield).

2.4.3.3.16. Reaction P (1:0.1:3:5 Ph₃BnPCl:Glyme:EDIPA:HSiCl₃, 72 h)

Reaction vessel was charged with 51.19 g Ph₃BnPCl (131.6 mmol), 1.19 g glyme (13.2 mmol), 51.2 g EDIPA (396 mmol), and 150. mL CH₂Cl₂, forming clear yellow mother liquor. The reaction vessel was fitted with a condenser set to -10°C. Ph₃BnPCl floated on top of reaction mixture as a hard cake. 67.0 mL HSiCl₃ (664 mmol) was added via addition funnel over 30 min while stirring, resulting in the total dissolution of the Ph₃BnPCl. Heat was applied and refluxing controlled at ≤1 drop/second. Heating ceased after 72 h. Storage at -28°C for 21 h resulted in precipitation of white crystals. Crystals filtered via frit and dried under vacuum for 1 h. 59.72 g crude yield (35.1 mmol, 53.1% yield).

2.4.3.3.17. Reaction Q (1:0.1:3:5 Ph₃BnPCl:Glyme:EDIPA:HSiCl₃, 72 h)

Reaction vessel was charged with 100.0 g Ph₃BnPCl (257.2 mmol), 2.319 g glyme (25.73 mmol), 99.4 g EDIPA (769 mmol), and 690. mL CH₂Cl₂, forming a clear colorless mother

liquor. The reaction vessel was fitted with a condenser set to -10°C . Ph_3BnPCl floated on top of reaction mixture as a hard cake. 130. mL HSiCl_3 (1280 mmol) was added via addition funnel over 45 min while stirring, resulting in the total dissolution of the Ph_3BnPCl . Heat was applied and refluxing controlled at ≤ 1 drop/second. Heating ceased after 72 h. Storage at -28°C for 22 h resulted in precipitation of white crystals. Crystals filtered via frit and dried under vacuum for 45 min. 124.9 g crude yield (73.3 mmol, 57.2% yield).

2.4.3.4. Crude RR' + $\text{CHCl}_3 \rightarrow$ Crude R2 Salt

2.4.3.4.1. Reaction K (1:1:3:5 Ph_3BnPCl :TEEDA:EDIPA: HSiCl_3 , 24 h)

2.94 g crude RR' was added to 30.0 mL CHCl_3 , forming a clear colorless solution in < 2 min. Following this, white solids began precipitating within 5 min. The mixture was stirred for 45 min and subsequently allowed to settle for 15 min. The precipitate was filtered via frit and washed 3x with 6 mL -28°C CHCl_3 (CHCl_3 was kept cold to minimize dissolution of crude R2 salt). 1.37 g crude R2 (0.999 mmol) was collected (57.9% yield).

2.4.3.4.2. Reaction M (1:1:3:5 Ph_3BnPCl :Glyme:EDIPA: HSiCl_3 , 24 h)

1.47 g crude RR' (0.863 mmol) was added to 15 mL CHCl_3 , forming a clear colorless solution in < 2 min. Following this, white solids began precipitating within 5 min. The mixture was stirred for 45 min and subsequently allowed to settle for 15 min. The precipitate was filtered via frit and washed 3x with 6 mL -28°C CHCl_3 (CHCl_3 was kept cold to minimize dissolution of crude R2 salt). 0.57 g crude R2 (0.42 mmol) was collected (48.1% yield).

2.4.3.4.3. Reaction Q (1:0.1:3:5 Ph_3BnPCl :Glyme:EDIPA: HSiCl_3 , 72 h)

124.9 g crude RR' (73.34 mmol) was added to 625 mL CHCl_3 , forming a clear colorless solution in < 2 min. Following this, white solids began precipitating within 5 min. The mixture was stirred 1 h and subsequently allowed to settle for 15 min. The precipitate was filtered via frit

and washed 3x with 80. mL -9°C CHCl₃ (CHCl₃ was kept cold to minimize dissolution of crude R2 salt). 45.6 g crude R2 (33.2 mmol) was collected (45.3% yield).

2.4.3.5. [Ph₃BnP⁺]₂[Si₆Cl_{14-n}H_n²⁻] + 3 Trityl Chloride → [Ph₃BnP⁺]₂[Si₆Cl₁₄²⁻]

4.990 g (3.638 mmol) crude R2 salt was mixed with 140. mL CH₂Cl₂. This created a cloudy white solution with a clear colorless mother liquor as crude R2 is not fully soluble in CH₂Cl₂ at this concentration. 3.048 g trityl chloride (10.93 mmol) was mixed with 20. mL CH₂Cl₂, forming a clear yellow solution. The trityl chloride solution was added to the reaction mixture over 2 min while under stirring, changing the color of the mother liquor to clear light yellow. This addition caused a significant precipitation of white solids within 5 min. The reaction mixture was stirred for 24 h.

160. mL hexanes were added to the reaction mixture to facilitate precipitation of the R2 salt dissolved in CH₂Cl₂. It was stirred an additional 5 min and subsequently allowed to sit undisturbed for 2 h. The reaction mixture was filtered via frit and washed 3x with 20. mL CHCl₃ chilled at -28°C. 4.905 g R2 salt (3.576 mmol, 98.3% recovery) was isolated following drying under vacuum for 1.5 h. FTIR data did not show the presence of Si-H bonding.

2.4.3.6. Solubility Study of [Si₆Cl₁₄²⁻] Salt in CH₂Cl₂

The solubility was tested for three separate [Si₆Cl₁₄²⁻] salts in CH₂Cl₂: R2 salt, [PEDETA·H₂SiCl⁺]₂[Si₆Cl₁₄²⁻] (synthesized in lab), and [PEDETA·H₂SiCl⁺]₂[Si₆Cl₁₄²⁻] (purchased from vendor). The solubilities were determined by mixing 20.0 mL CH₂Cl₂ with a known amount of salt. The mixtures were stirred for >18 h to ensure that they were saturated. They were subsequently filtered via frit, producing a clear filtrate. The solvent was removed from the filtrate via vacuum, leaving behind the dissolved salt whose mass was recorded. The

solubility in CH_2Cl_2 was calculated by dividing this mass by the 20.0 mL originally used to dissolve the salt. All measurements were performed in triplicate.

3. CRUDE R2 AND R2 SALTS AS PRECURSORS TO $\text{Si}_6\text{Cl}_{12}$

3.1. Abstract

R2 salt was converted to $\text{Si}_6\text{Cl}_{12}$ upon reaction with AlCl_3 in benzene as originally described in Tillman's synthesis. Modifying the synthesis by performing a heptane extraction of the product versus a hexane extraction eliminated the need to perform the extraction in a pressure vessel without significantly affecting the yield. This advantage allowed the reaction to be successfully scaled up to produce 9.38 g product (6.84 mmol). Reacting crude R2 salt with AlCl_3 produced a partially hydrogenated $\text{Si}_6\text{Cl}_{12-n}\text{H}_n$ product. In all cases yields were high, with the lowest being 87.9%.

3.2. Background

The motivation for using R2 salt as a starting material for $\text{Si}_6\text{Cl}_{12}$ was outlined in greater detail in chapters 1 and 2, however it stems primarily from its soluble nature and the ease with which it is synthesized in comparison to the $[\text{nBu}_4\text{N}^+]_2[\text{Si}_6\text{Cl}_{14}^{2-}]$ that was used in Tillman's synthesis. The work in chapter 2 demonstrated a viable route towards producing working quantities of R2 salt.

As a proof of concept, an $\text{Si}_6\text{Cl}_{12}$ synthesis was performed analogously to Tillman's synthesis where the reaction conditions were kept the same with the exception of the starting material $[\text{nBu}_4\text{N}^+]_2[\text{Si}_6\text{Cl}_{14}^{2-}]$ being replaced with R2 salt (reaction **A**). A second analogous synthesis was performed using crude R2 salt as the starting material to test whether any of the AlCl_3 species present in the reaction mixture had the capability of chlorinating the partially hydrogenated $\text{Si}_6\text{Cl}_{12-n}\text{H}_n$ ring in crude R2 salt (reaction **B**).

A third analogous synthesis (reaction **C**) was performed using R2 salt as the starting material, with the difference being that the hexane extraction was replaced with an *n*-heptane

extraction. Though this extraction was performed in a pressure vessel, the success of this extraction could potentially eliminate the future need to use a pressure vessel as *n*-heptane has a higher boiling point than hexanes (97-98°C versus 69°C) and the extraction only occurs at 85°C. This would increase the feasibility of scaling up the reaction as a larger pressure vessel would introduce safety issues to the synthesis.

A fourth scale up synthesis was performed using 10 times the amount of R2 salt used in the previous reactions (reaction **D**). In addition, an *n*-heptane extraction was performed at atmospheric pressure in non-pressurized vessel.

3.3. Results and Discussion

Four different syntheses were performed, all of which produced near quantitative yields of Si₆Cl₁₂ (table 4). Reaction A followed the literature protocol for the reaction of [nBu₄N⁺]₂[Si₆Cl₁₄²⁻] + 2.5 AlCl₃ in benzene with the only difference being that [nBu₄N⁺]₂[Si₆Cl₁₄²⁻] was replaced with R2 salt. Reaction B used the same procedure, except crude R2 salt was used as the starting material. Reaction C used R2 salt as the starting material, but performed a heptane extraction of the product instead of the hexane extraction used in reactions A-B. Reaction D was a scale up version of reaction C.

Table 4. Summary of reactions [Ph₃BnP⁺]₂[Si₆Cl₁₄²⁻] + 2.5 AlCl₃ → Si₆Cl₁₂.

Reaction	Starting Material	Extracting Solvent	Yield
A	R2 Salt	Hexanes	1.00 g (95.2%)
B	Crude R2 Salt	Hexanes	1.05 g (101%)
C	R2 Salt	Heptane	0.923 g (87.9%)
D	R2 Salt	Heptane	9.38 g (90.2%)

Raman characterization confirmed that Si₆Cl₁₂ was the product of reaction A (figure 11). Reaction B yielded similar results, however Raman characterization shows there to be Si-H present on the Si₆ ring (figure 12). Raman characterization for reaction C showed the product to

be $\text{Si}_6\text{Cl}_{12}$ with a minor amount of Si-H (figure 13). Raman characterization for reaction D showed $\text{Si}_6\text{Cl}_{12}$ without any Si-H (figure 14).

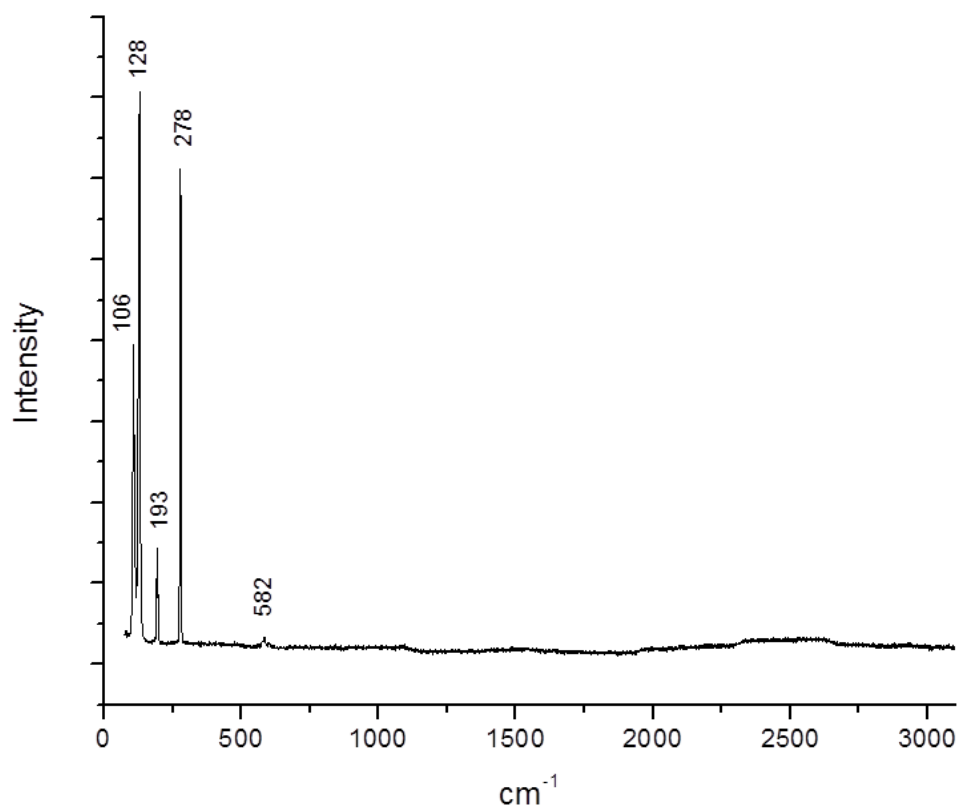


Figure 11. Raman data for product of R2 salt + 2.5 AlCl₃ (reaction A). Note the characteristic peak for the $\text{Si}_6\text{Cl}_{12}$ ring breathing mode at 278 cm⁻¹.

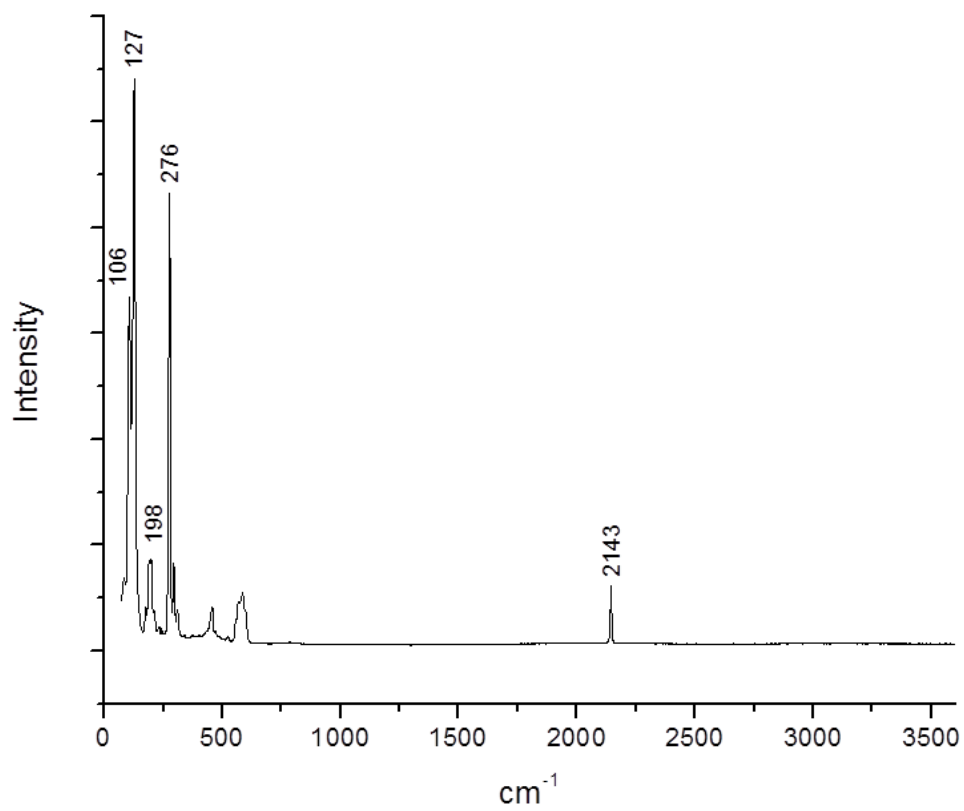


Figure 12. Raman data for product of crude R2 salt + 2.5 AlCl₃ (reaction B). Note the characteristic peak for the Si₆Cl₁₂ ring breathing mode at 276 cm⁻¹ along with Si-H bonding at 2143 cm⁻¹.

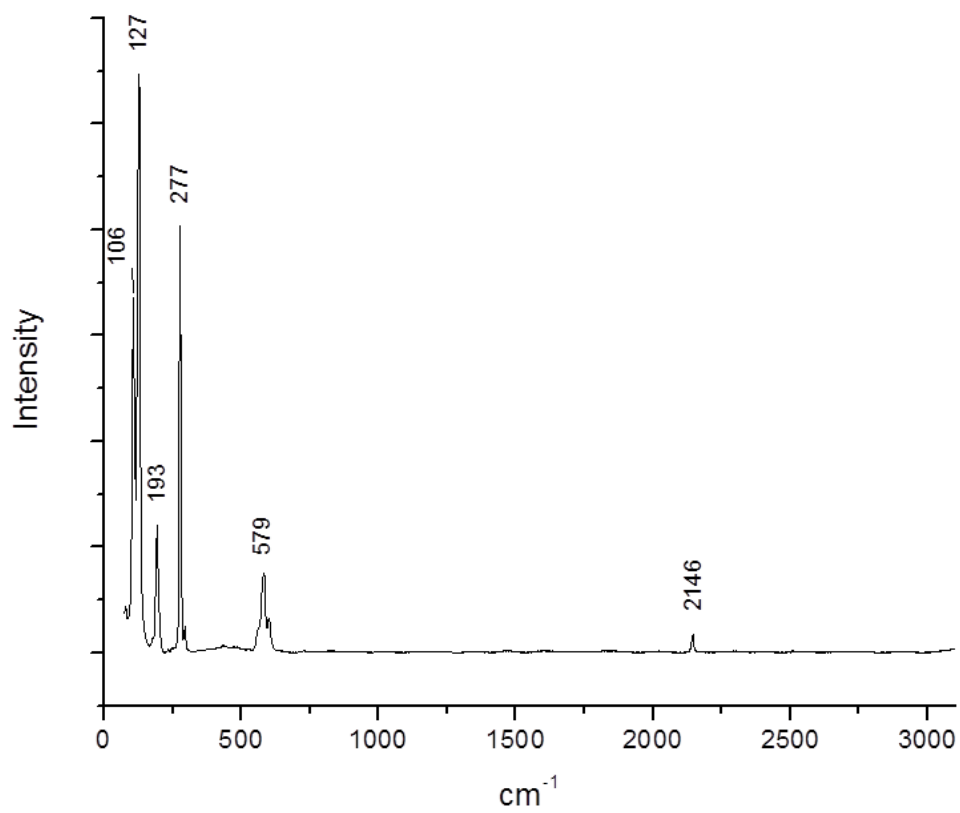


Figure 13. Raman data for product of R2 salt + 2.5 AlCl₃ with a heptane extraction of the product (reaction C). Note the characteristic peak for the Si₆Cl₁₂ ring breathing mode at 276 cm⁻¹ along with Si-H bonding at 2146 cm⁻¹.

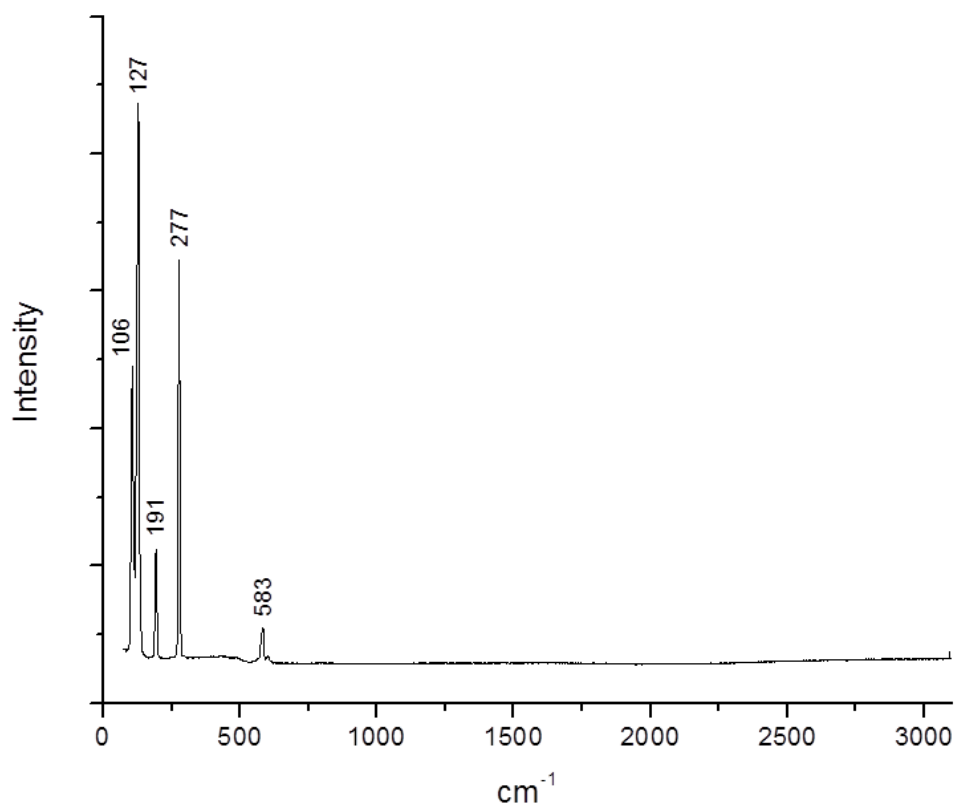


Figure 14. Raman data for product of scale up reaction R2 salt + 2.5 AlCl₃ with a heptane extraction of the product (reaction D). Note the characteristic peak for the Si₆Cl₁₂ ring breathing mode at 277 cm⁻¹.

3.4. Experimental Methods

3.4.1. Preparation of Starting Materials

Starting materials were reagent grade quality or higher, unless otherwise noted. The presence of O₂ or H₂O, whether in solvents or the atmosphere, is detrimental to these reactions as the AlCl₃ and products are O₂/H₂O sensitive. For this reason, all experiments were performed under a dry, inert atmosphere (i.e. nitrogen or argon) either in a glove box or by using air-free Schlenk line techniques, unless otherwise noted. Glassware (including stir bars) was dried in a

drying oven at 150°C for ≥ 2 h and transferred to the glove box antechamber while still hot in order to reduce H₂O condensation on the glassware as it returned to room temperature.

Solvents were dried according to literature protocols,⁶⁸ either by passage through a neutral alumina column or purchased from the vendor anhydrous. They were subsequently deoxygenated via sparging with N₂ while stirring for ≥ 2 h. They were stored under an inert atmosphere over either 3 Å or 4 Å molecular sieves. The molecular sieves were dried at 300°C under a vacuum of ≤ 50 mTorr for ≥ 12 h and stored under an inert atmosphere. Solvents were checked for water and oxygen prior to use by adding diethyl zinc solution (pyrophoric) and checking for the formation of fumes.

AlCl₃ was sublimed twice and immediately stored in a sealed container.

3.4.2. Characterization of Materials

FTIR spectra were recorded using either a Bruker Optics Vertex 70 Fourier Transform Infrared Spectrometer or a Thermo Scientific Nicolet 8700 FT-IR. Samples were prepared in KBr pellets. Due to the air sensitive nature of the materials being tested, samples were transferred to the FTIR under dry, N₂ conditions and quickly transferred to the FTIR, whose sample chamber was constantly being flushed with dry N₂. Raman spectra were recorded using a Horiba Jobin Yvon Aramis Confocal Raman Imaging System which was equipped with 532 and 785 nm lasers. To prevent air exposure, samples were placed in between two quartz slides sealed on the sides with vacuum grease. This preparation occurred in a dry, inert atmosphere (i.e. nitrogen or argon).

3.4.3. [Ph₃BnP⁺]₂[Si₆Cl₁₄²⁻] + 2.5 AlCl₃ → Si₆Cl₁₂ with Hexane Extraction

Reaction vessel was charged with 0.588 g AlCl₃ (4.41 mmol) and 20.0 mL benzene. No significant amount of AlCl₃ went into solution, even upon stirring. 2.42 g R2 salt (1.76 mmol)

was added to the reaction mixture in quarter increments every 30 min. Each addition resulted in one quarter of the AlCl_3 going into solution along with all of the R2 salt. Each addition was accompanied by the formation of ~1 mL of clear yellow liquid that settled out upon cessation of stirring, creating three layers: undissolved AlCl_3 (bottom), clear yellow liquid layer (middle) and clear colorless mother liquor (top). The reaction mixture stirred for 1 h following the final addition.

Solvent was removed from the reaction mixture via a vacuum, revealing yellow solids. Vacuum was applied an additional 30 min following complete solvent removal, resulting in the solids changing from yellow to yellow-green.

The $\text{Si}_6\text{Cl}_{12}$ was extracted from the solids by adding 20.0 mL hexanes to the reaction vessel. The reaction vessel was sealed with a pressure cap and the reaction mixture heated while under stirring. The insoluble solids became an immiscible liquid upon reaching 85°C . The reaction mixture was stirred for 30. min at this temperature, during which time the solids changed from yellow-green to yellow.

The mother liquor was decanted and filtered via a $0.2\ \mu\text{m}$ PTFE filter upon returning to room temperature, revealing a clear colorless filtrate. Solvent was removed from the filtrate via vacuum, revealing 1.00 g white solids (1.68 mmol, 95.4% yield). Characterization via Raman spectroscopy showed an intact $\text{Si}_6\text{Cl}_{12}$ ring with no Si-H.

3.4.4. $[\text{Ph}_3\text{BnP}^+]_2[\text{Si}_6\text{H}_n\text{Cl}_{14-n}^{2-}] + 2.5\ \text{AlCl}_3 \rightarrow \text{Si}_6\text{H}_n\text{Cl}_{12-n}$ with Hexane Extraction

Reaction vessel was charged with 0.585 g AlCl_3 (4.39 mmol) and 20.0 mL benzene. No significant amount of AlCl_3 went into solution, even upon stirring. 2.41 g crude R2 (1.76 mmol, non-trityl chloride treated) was added to the reaction mixture in quarter increments every 30 min. Each addition resulted in one quarter of the AlCl_3 going into solution along with all of the R2

salt. Each addition was accompanied by the formation of ~1 mL of clear yellow liquid that settled upon cessation of stirring, creating three layers: undissolved AlCl₃ (bottom), clear yellow liquid layer (middle) and clear colorless mother liquor (top). The reaction mixture stirred for 1 h following the final addition.

Solvent was removed from the reaction mixture via a vacuum, revealing white-yellow solids. Vacuum was applied an additional 30 min following complete solvent removal.

The Si₆Cl₁₂ was extracted from the solids by adding 20.0 mL hexanes to the reaction vessel. The reaction vessel was sealed with a pressure cap and the reaction mixture heated while under stirring. The insoluble solids became an immiscible liquid upon reaching 88°C. The reaction mixture was stirred for 30. min at this temperature.

The mother liquor was decanted and filtered via a 0.2 μm PTFE filter upon returning to room temperature, revealing a clear colorless filtrate. Solvent was removed from the filtrate via vacuum, revealing 1.05 g white solids (1.77 mmol, 101% yield). Characterization via Raman spectroscopy and FTIR revealed an intact Si₆Cl₁₂ ring along with Si-H.

3.4.5. [Ph₃BnP⁺]₂[Si₆Cl₁₄²⁻] + 2.5 AlCl₃ → Si₆Cl₁₂ with n-Heptane Extraction

Reaction vessel was charged with 0.588 g AlCl₃ (4.41 mmol) and 20.0 mL benzene. No significant amount of AlCl₃ went into solution, even upon stirring. 2.41 g R2 salt (1.76 mmol) was added to the reaction mixture in quarter increments every 30 min. Each addition resulted in one quarter of the AlCl₃ going into solution along with all of the R2 salt. Each addition was accompanied by the formation of ~1 mL of clear yellow liquid that settled out upon cessation of stirring, creating three layers: undissolved AlCl₃ (bottom), clear yellow liquid layer (middle) and clear colorless mother liquor (top). The reaction mixture stirred for 1 h following the final addition.

Solvent was removed from the reaction mixture via a vacuum, revealing yellow solids. Vacuum was applied an additional 30 min following complete solvent removal.

The $\text{Si}_6\text{Cl}_{12}$ was extracted from the solids by adding 20.0 mL n-heptane to the reaction vessel. The reaction vessel was sealed with a pressure cap and the reaction mixture heated while under stirring. The insoluble solids became an immiscible liquid upon reaching 88°C. The reaction mixture was stirred for 30. min at this temperature, during which time the solids changed from yellow to white.

The mother liquor was decanted and filtered via 1.0 μm PTFE filter upon returning to room temperature, revealing a clear colorless filtrate. Solvent was removed from the filtrate via vacuum, revealing 0.923 g white solids (1.55 mmol, 88.4% yield). Characterization via Raman spectroscopy showed an intact $\text{Si}_6\text{Cl}_{12}$ ring.

3.4.6. Scale Up $[\text{Ph}_3\text{BnP}^+]_2[\text{Si}_6\text{Cl}_{14}^{2-}] + 2.5 \text{ AlCl}_3 \rightarrow \text{Si}_6\text{Cl}_{12}$ with n-Heptane Extraction

Reaction vessel was charged with 5.86 g AlCl_3 (43.9 mmol) and 200.0 mL benzene. No significant amount of AlCl_3 went into solution, even upon stirring. 24.1 g R2 salt (17.6 mmol) was added to the reaction mixture in quarter increments every 15 min. Each addition resulted in one quarter of the AlCl_3 going into solution along with all of the R2 salt. Each addition was accompanied by the formation of ~10 mL of clear yellow liquid that settled out upon cessation of stirring, creating three layers: undissolved AlCl_3 (bottom), clear yellow liquid layer (middle) and clear colorless mother liquor (top). The reaction mixture stirred for 1 h following the final addition.

Solvent was removed from the reaction mixture via a vacuum, revealing green/yellow solids. Vacuum was applied an additional 30 min following complete solvent removal.

The $\text{Si}_6\text{Cl}_{12}$ was extracted from the solids by adding 200.0 mL *n*-heptane to the reaction vessel. The reaction mixture was heated for 30 min at 95°C while under stirring. The solids became softer at elevated temperature, but never turned into a liquid. The solids lost their color in the process, turning white.

The mother liquor was decanted and filtered via 0.2 μm PTFE filter upon returning to room temperature, revealing a clear colorless filtrate. Solvent was removed from the filtrate via vacuum, revealing 9.38 g white solids (15.8 mmol, 89.9% yield). Characterization via Raman spectroscopy showed an intact $\text{Si}_6\text{Cl}_{12}$ ring.

4. GENERATING NOVEL MATERIALS FROM Si_6X_{12}

4.1. Abstract

Attempts were made to finish characterizing the series of Si_6X_{12} ($\text{X} = \text{Cl}, \text{Br}$) adducts that were previously reported in literature. Si_6X_{12} was reacted with $n\text{Bu}_4\text{NX}'$ ($\text{X}' = \text{Cl}, \text{Br}$) to produce the corresponding mixed halide $[\text{Si}_6\text{X}_{12}\text{X}'_2]^{2-}$ dianion salts. XRD spectra were recorded for both products after successfully isolating crystals, however only the spectrum for $[n\text{Bu}_4\text{N}^+]_2[\text{Si}_6\text{Cl}_{12}\text{Br}_2]^{2-}$ showed the intended product; the product of $\text{Si}_6\text{Br}_{12}$ and $n\text{Bu}_4\text{NCl}$ showed $[n\text{Bu}_4\text{N}^+]_2[\text{Si}_6\text{Br}_{14}]^{2-}$.

Trityl· X' was reacted with Si_6X_{12} to produce the dianion salts $[\text{Tr}^+]_2[\text{Si}_6\text{Cl}_{14}]^{2-}$, $[\text{Tr}^+]_2[\text{Si}_6\text{Br}_{12}\text{Cl}_2]^{2-}$ and $[\text{Tr}^+]_2[\text{Si}_6\text{Br}_{14}]^{2-}$ in good yield ($\text{Tr}^+ = \text{trityl}^+$ cation). FTIR data confirms the presence of Tr^+ cations in these products by showing the characteristic Tr^+ peaks with scale factors of 0.98-1.02. Raman data confirms the presence of the $[\text{Si}_6\text{X}_{12}\text{X}'_2]^{2-}$ dianion as evidenced by the presence of the characteristic totally symmetric Si-Si stretching frequency mode. The elemental analysis results conform to the theoretical values, particularly the C and H values which have scale factors of 0.94-0.97.

4.2. Background

The Lewis acid sites on Si_6X_{12} ($\text{X} = \text{Cl}, \text{Br}$) give it the demonstrated ability to form diadducts with Lewis bases such as halogen anions and lone electron pairs on nitrile functional groups. This property was exploited in previous work to produce a variety of diadducts from Si_6X_{12} (table 5).

Table 5. Summary of characterization methods used on Si₆X₁₂ diadducts.

Si ₆ X ₁₂ Species	XRD	Elemental Analysis	²⁹ Si-NMR Shift (CD ₂ Cl ₂)	UV-Vis	Reference
Si ₆ Cl ₁₂	✓	✗	-0.54	✓	36
[PEDETA·H ₂ SiCl ⁺] ₂ [Si ₆ Cl ₁₄ ²⁻]	✓	✓	-21.52	✓	36,41
[<i>n</i> Bu ₄ N ⁺] ₂ [Si ₆ Cl ₁₂ Br ₂ ²⁻]	✗	✓	-22.23	✓	36
[<i>n</i> Bu ₄ N ⁺] ₂ [Si ₆ Cl ₁₂ I ₂ ²⁻]	✓	✓	-21.88	✓	36
(<i>p</i> -CH ₃ C ₆ H ₄ CN) ₂ ·Si ₆ Cl ₁₂	✗	✓	✗	✓	35
Si ₆ Br ₁₂	✓	✓	-25.92	✓	35-36
[<i>n</i> Bu ₄ N ⁺] ₂ [Si ₆ Br ₁₂ Cl ₂ ²⁻]	✗	✓	.37.44	✓	36
[<i>n</i> Bu ₄ N ⁺] ₂ [Si ₆ Br ₁₄ ²⁻]	✓	✓	-37.40	✓	36
[<i>n</i> Bu ₄ N ⁺] ₂ [Si ₆ Br ₁₂ I ₂ ²⁻]	✓	✓	-37.92	✓	36
(<i>p</i> -CH ₃ C ₆ H ₄ CN) ₂ ·Si ₆ Br ₁₂	✓	✓	-25.80	✓	35

The Si₆X₁₂ diadducts summarized in table 5 were characterized using XRD, ²⁹Si-NMR and UV-Vis, with the exception of [*n*Bu₄N⁺]₂[Si₆Cl₁₂Br₂²⁻], [*n*Bu₄N⁺]₂[Si₆Br₁₂Cl₂²⁻] and (*p*-CH₃C₆H₄CN)₂·Si₆Cl₁₂, for which there were no XRD spectra. Attempts were made in this work to collect the XRD spectra for these dianions (offset with Ph₄P⁺ cations), with only that of [Ph₄P⁺]₂[Si₆Cl₁₂Br₂²⁻] being successfully collected.

Si₆X₁₂ was tested for its ability to form diadducts with trityl·X' (X' = Cl, Br) creating [Tr⁺]₂[Si₆X₁₂X'₂²⁻]. Such diadducts would constitute novel materials as no prior Si₆X₁₂ adducts have been offset by carbenium ions.

4.3. Results and Discussion

4.3.1. Diadducts of Si₆X₁₂ (X = Cl, Br) and Ph₄PX' (X' = Cl, Br)/*p*-Tolunitrile

The XRD spectrum for the diadduct of Si₆Cl₁₂ and Ph₄PBr showed the intended mixed halogen dianion salt [Ph₄P⁺]₂[Si₆Cl₁₂Br₂²⁻] whereas the diadduct of Si₆Br₁₂ and Ph₄PBr showed [Ph₄P⁺]₂[Si₆Br₁₄²⁻]. It is unknown why there are no chlorine atoms in the diadduct of Si₆Br₁₂ and Ph₄PBr as the chemical equation for said reaction is stoichiometrically unbalanced. In both cases the spectra conformed to previously characterized inverse sandwich complexes wherein halogen anions were located in the Lewis acid wells of the Si₆X₁₂ (X = Cl, Br) ring, forming an

$[\text{Si}_6\text{X}_{12}\text{X}'_2]^{2-}$ dianion offset by two tetraphenylphosphonium cations (figures 15-16). Thermal ellipsoid plots with corresponding crystallographic information provided in the appendix (table A1, figures A1-A2).³⁶

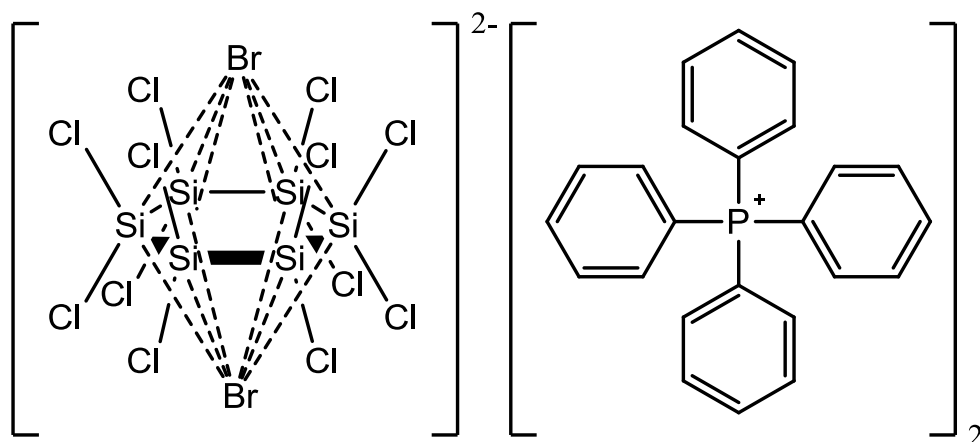


Figure 15. Chemical structure of $[\text{Ph}_4\text{P}^+]_2[\text{Si}_6\text{Cl}_{12}\text{Br}_2]^{2-}$.

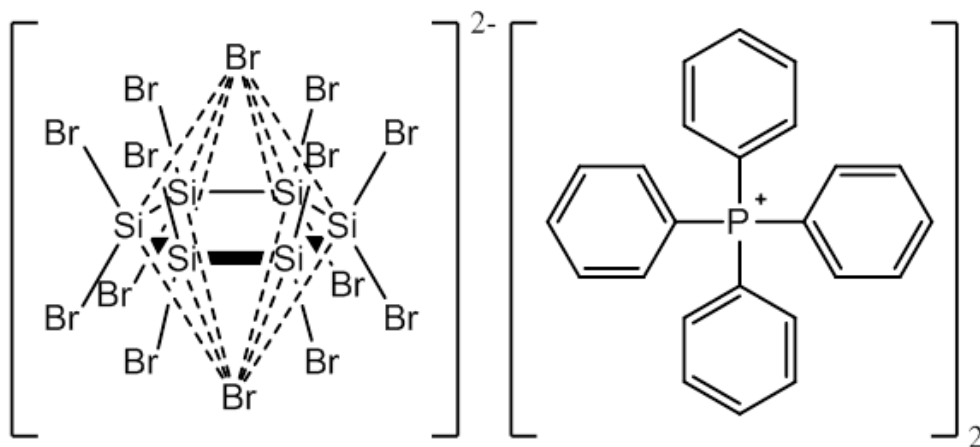


Figure 16. Chemical structure of $[\text{Ph}_4\text{P}^+]_2[\text{Si}_6\text{Br}_{14}]^{2-}$.

4.3.2. Synthesis and Characterization of $[\text{Tr}^+]_2[\text{Si}_6\text{X}_{12}\text{X}'_2]^{2-}$ ($\text{X} = \text{X}' = \text{Cl}, \text{Br}$)

Reactions between Si_6X_{12} and trityl· X' in a 1:2 mole ratio resulted in the rapid precipitation of colored solids in high yields (table 6).

Table 6. Summary of reactions between Si_6X_{12} and trityl·X'.

Substrate	Reagent	Reaction Time	Product Color	Yield
$\text{Si}_6\text{Cl}_{12}$	Trityl chloride	5 min	Yellow	118 mg (90.3%)*
$\text{Si}_6\text{Br}_{12}$	Trityl chloride	<1 min	Orange	85 mg (76%)
$\text{Si}_6\text{Br}_{12}$	Trityl bromide	<3 min	Orange	26.31 mg (87.14%)
$\text{Si}_6\text{Cl}_{12}$	4-MeTrCl	4 min	Yellow/orange	17.2 mg (45.6%)

*Highest yield of three different reaction conditions which varied solvent and reaction time.

Raman data confirmed the presence of the $[\text{Si}_6\text{X}_{12}\text{X}'_2]^{2-}$ dianion in the aforementioned products. Quantum chemical calculations predict that there should be a relaxation of the totally symmetric Si-Si stretching frequency mode for Si_6X_{12} upon complexing to $[\text{Si}_6\text{X}_{12}\text{X}'_2]^{2-}$ (table 7). This relaxation is attributed to the suppression of the pseudo-Jahn-Teller (PJT) effect, which results in the puckered chair structure of free $\text{Si}_6\text{Cl}_{12}$ flattening to a planar structure upon complexation. Literature quantum chemical calculations were performed using the hybrid density functional theory (DFT) method B3LYP with the 6-311+G(3df) basis set.^{2,70} Experimental Raman data for Si_6X_{12} and $[\text{Tr}^+]_2[\text{Si}_6\text{X}_{12}\text{X}'_2]^{2-}$ show this predicted relaxation, confirming the presence of the dianion in the product (table 7, figures 17-19).

Table 7. Theoretical/experimental Raman shifts for totally symmetric Si-Si stretching frequency mode in $[\text{Si}_6\text{X}_{12}\text{X}'_2]^{2-}$.

Product	Theoretical Raman Shift (cm^{-1})	Experimental Raman Shift (cm^{-1})*
$\text{Si}_6\text{Cl}_{12}$	267 ²	278
$[\text{Si}_6\text{Cl}_{14}]^{2-}$	242 ²	257
$\text{Si}_6\text{Br}_{12}$	194 ⁷⁰	185
$[\text{Si}_6\text{Br}_{12}\text{Cl}_2]^{2-}$	181 ⁷⁰	172
$[\text{Si}_6\text{Br}_{14}]^{2-}$	176 ⁷⁰	173

*Experimental values for $[\text{Si}_6\text{X}_{12}\text{X}'_2]^{2-}$ products are offset by $[\text{Tr}^+]_2$ cations.

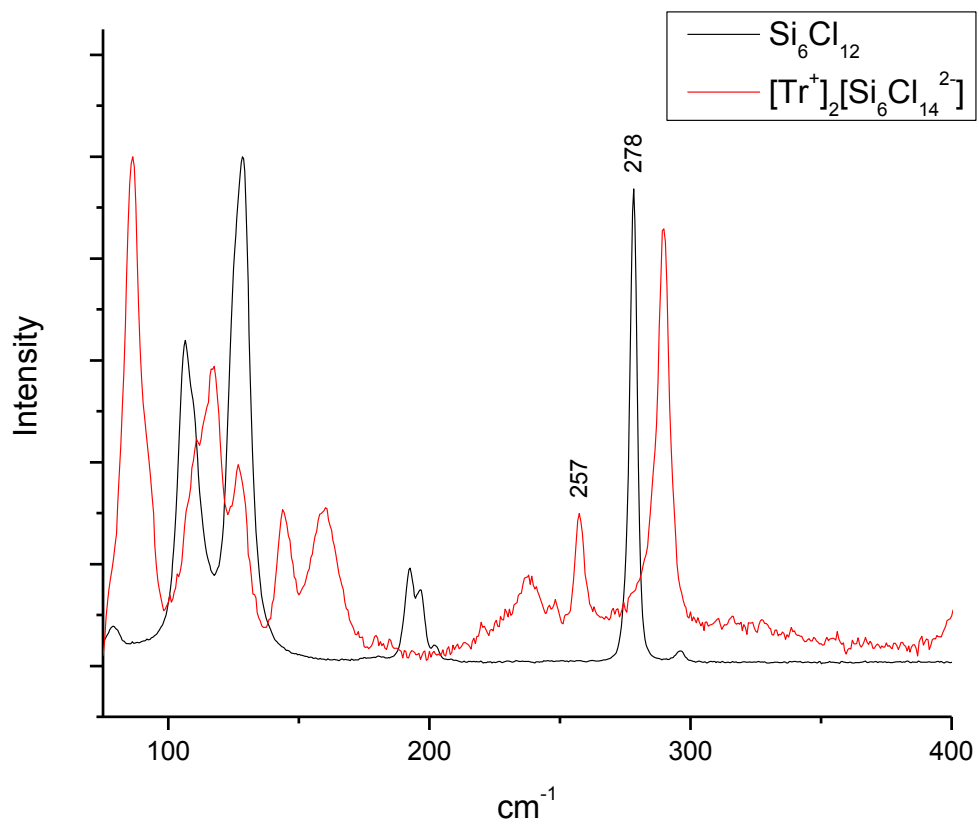


Figure 17. Comparison Raman spectra for $\text{Si}_6\text{Cl}_{12}$ (black) and $[\text{Tr}^+]_2[\text{Si}_6\text{Cl}_{14}^{2-}]$ (red) with the totally symmetric Si-Si stretching frequency mode relaxing from 278 to 257 cm^{-1} upon complexation of $\text{Si}_6\text{Cl}_{12}$ with trityl chloride.

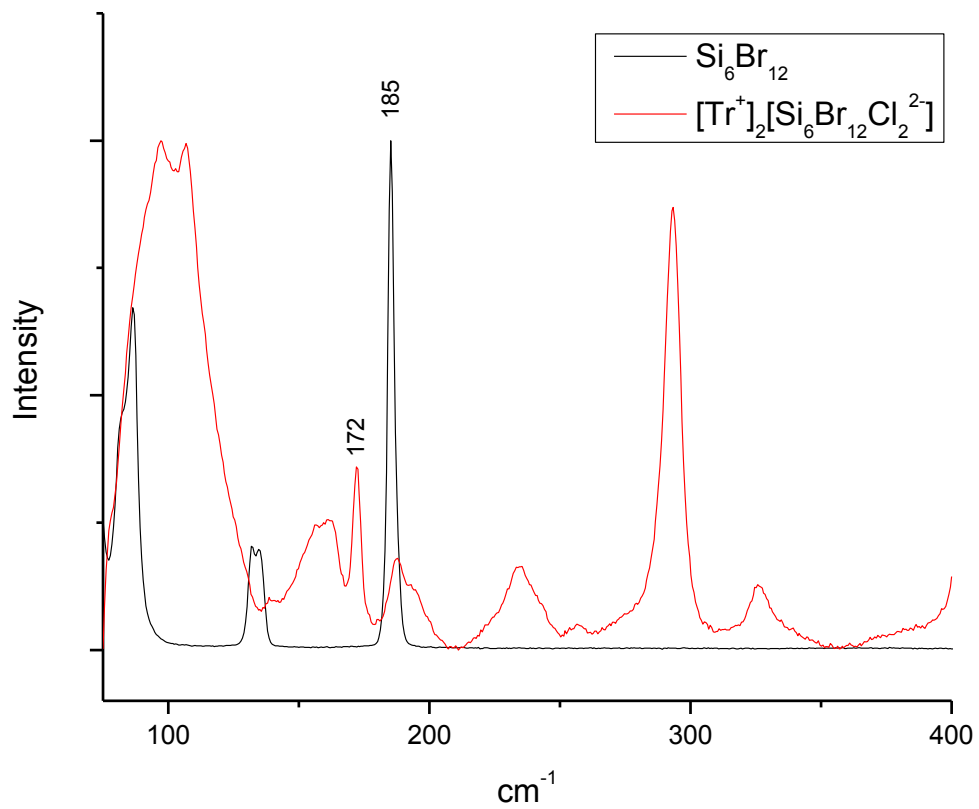


Figure 18. Comparison Raman spectra for $\text{Si}_6\text{Br}_{12}$ (black) and $[\text{Tr}^+]_2[\text{Si}_6\text{Br}_{12}\text{Cl}_2^{2-}]$ (red) with the totally symmetric Si-Si stretching frequency mode relaxing from 185 to 172 cm^{-1} upon complexation of $\text{Si}_6\text{Br}_{12}$ with trityl chloride.

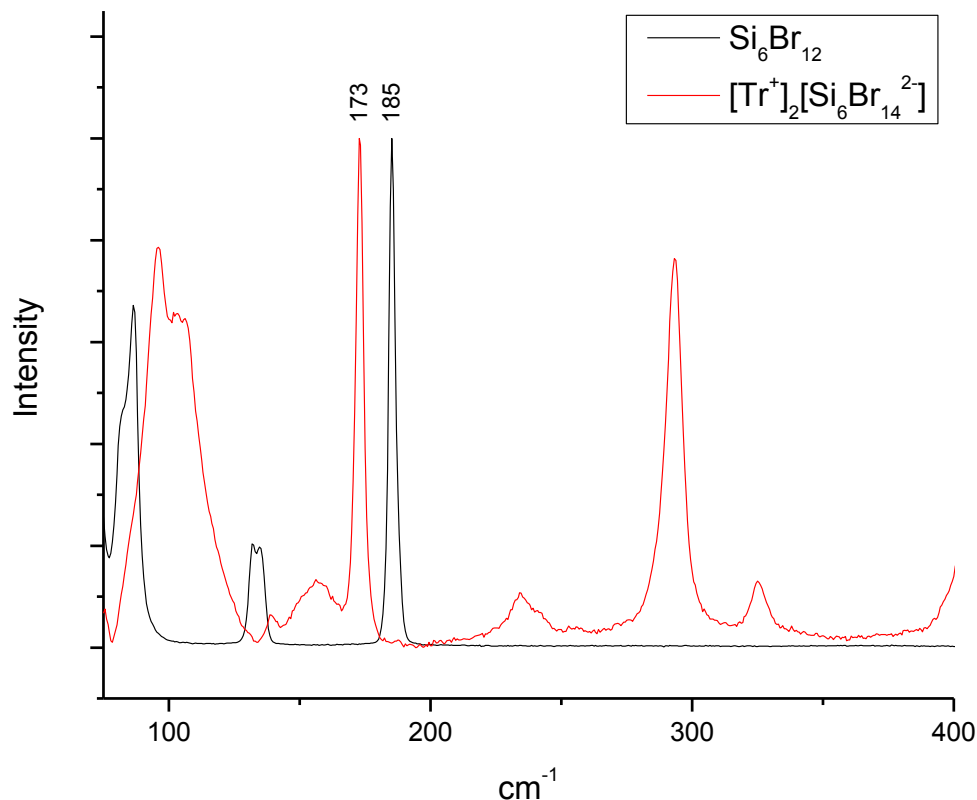


Figure 19. Comparison Raman spectra for Si₆Br₁₂ (black) and [Tr⁺]₂[Si₆Br₁₄²⁻] (red) with the totally symmetric Si-Si stretching frequency mode relaxing from 185 to 173 cm⁻¹ upon complexation of Si₆Br₁₂ with trityl bromide.

FTIR data was recorded for trityl chloride and the aforementioned products. This data was compared to theoretical and experimental values for trityl chloride and [Tr⁺][AlCl₄⁻] seen in literature (table 8). Literature theoretical values were calculated using DFT method B3LYP with the 6-31+G(d,p) basis set.⁷¹⁻⁷²

The ratio between this work's experimental values and the literature values (known as the scale factor) was consistently in the range of 0.98-1.02. The only exceptions were the weaker peaks which inconsistently appeared. In the occasions that they did appear, the scaling factor was

still within the range of 0.98-1.02. This tight scaling confirms the presence of trityl cations in the $[\text{Tr}^+]_2[\text{Si}_6\text{X}_{12}\text{X}'_2{}^{2-}]$ products.

Table 8. Observed and calculated FTIR frequencies with corresponding assignments for trityl chloride, $[\text{Tr}^+][\text{AlCl}_4^-]$, and $[\text{Tr}^+]_2[\text{Si}_6\text{X}_{12}\text{X}'_2{}^{2-}]$.

Assignment	Trityl Chloride			$[\text{Tr}^+][\text{AlCl}_4^-]$		$[\text{Tr}^+]_2[\text{Si}_6\text{Cl}_{14}{}^{2-}]$	$[\text{Tr}^+]_2[\text{Si}_6\text{Br}_{12}\text{Cl}_2{}^{2-}]$	$[\text{Tr}^+]_2[\text{Si}_6\text{Br}_{14}{}^{2-}]$
	Calc (lit)	Exp (lit)	Exp	Calc (lit)	Exp (lit)	Exp	Exp	Exp
C-C stretch	1616	1597 m	1595 w	1599	1583 s	1579 s	1579 s	1579 s
C-C stretch	1596	1582 m	1581 w	1569	1562 w	----	1559 w	1558 w
C-C stretch	1499	1488 s	1489 m	1488	1483 m	1483 m	1481 m	1481 m
Asym. Me. Def. C-C stretch	1449	1445 s	1444 m	1450	----	1450 m	1450 s	1448 s
Sym. Me def. C-H bend (\parallel)	1338	1336 sh	----	----	----	----	----	----
C-C stretch	1314	1318 m	1317 w	----	----	1309 w	----	----
C-H bend (\parallel)	----	----	----	1327	1295 s	1296 m	1296 s	1296 m
Asym. C- Φ stretch	1196	1215 m	1215 w	1357	1358 s	1356 s	1356 s	1358 s
C-H bend (\parallel)	1190	1182 m	1182 w	1189	1186 s	1188 m	1186 m	1184 m
C-H bend (\parallel)	1163	1158 m	1157 w	1172	1166 m	1167 m	1167 w	1167 w
Sym. C- Φ stretch	1142	1147 m	1147 w	1182	----	----	----	----
C-H bend (\parallel)	1090	1082 m	1082 w	1098	1089 vw	1088 vw	----	----
C-H bend (\parallel)	1036	1033 m	1034 w	1028	1030 m	1026 vw	----	1028 w
C-H bend (\perp)	----	----	----	1009	----	----	----	----
Me def. ring breathe	996	1001 m	1001 w	989	996 m	997 m	994 m	995 m
C-H bend (\perp)	986	988 vw	----	985	980 w	984 m	983 w	982 w

Table 8. Observed and calculated FTIR frequencies with corresponding assignments for trityl chloride, $[\text{Tr}^+][\text{AlCl}_4^-]$, and $[\text{Tr}^+]_2[\text{Si}_6\text{X}_{12}\text{X}'_2{}^{2-}]$ (continued).

Assignment	Trityl Chloride			$[\text{Tr}^+][\text{AlCl}_4^-]$		$[\text{Tr}^+]_2[\text{Si}_6\text{Cl}_{14}{}^{2-}]$	$[\text{Tr}^+]_2[\text{Si}_6\text{Br}_{12}\text{Cl}_2{}^{2-}]$	$[\text{Tr}^+]_2[\text{Si}_6\text{Br}_{14}{}^{2-}]$
	Calc (lit)	Exp (lit)	Exp	Calc (lit)	Exp (lit)	Exp	Exp	Exp
C-H bend (\perp)	972	975 vw	----	----	----	----	----	----
C-H bend (\perp)	932	931 m	931 w	956	952 vw	951 w	----	----
C-H bend (\perp)	926	924 w	----	952	949 vw	----	----	949 w
C- Φ def.	891	895 m	893 w	910	916 w	916 w	----	914 w
C-H bend (\perp)	845	848 m	849 w	843	842 w	847 w	845 w	843 w
C-H bend (\perp)	841	843 sh	----	----	----	----	----	----
C-H bend (\perp)/C-Cl stretch	805	821 m	822 w	----	----	----	----	----
C-H bend (\perp)	----	----	810 w	808	806 m	806 m	807 m	806 w
C-H bend (\perp)	758	758 s	758 m	770	768 sh	771 m	766 m	768 m
C-H bend (\perp)	----	762 sh	----	----	----	----	----	----
C-Cl stretch	728	747 s	746 m	----	----	----	----	----
C-Cl stretch	----	736 s	737 m	----	----	----	736 w	735 w
C-C-C bend (\perp)	697	698 s	698 s	705	----	704 m	703 m	702 m

Table 8. Observed and calculated FTIR frequencies with corresponding assignments for trityl chloride, $[\text{Tr}^+][\text{AlCl}_4^-]$, and $[\text{Tr}^+]_2[\text{Si}_6\text{X}_{12}\text{X}'_2{}^{2-}]$ (continued).

Assignment	Trityl Chloride			$[\text{Tr}^+][\text{AlCl}_4^-]$		$[\text{Tr}^+]_2[\text{Si}_6\text{Cl}_{14}{}^{2-}]$	$[\text{Tr}^+]_2[\text{Si}_6\text{Br}_{12}\text{Cl}_2{}^{2-}]$	$[\text{Tr}^+]_2[\text{Si}_6\text{Br}_{14}{}^{2-}]$
	Calc (lit)	Exp (lit)	Exp	Calc (lit)	Exp (lit)	Exp	Exp	Exp
C-C-C bend ()/C-Cl stretch	660	667 s	667 m	----	----	----	----	----
C-C-C bend (⊥)	----	----	660 m	659	660 w	----	----	660 w
C-C-C bend ()	627	627 s	627 m	622	623 m	623 m	622 m	623 m
C-C-C bend ()	618	918 m	617 m	609	609 m	607 m	608 m	607 m
C-C-C bend (⊥)/Me def.	509	508 m	507 w	----	----	----	----	----

Literature values and peak assignments come from work reported by Eide et al.⁷¹ Values marked with “----“ mean no peak was present at that location.

$[\text{Tr}^+]_2[\text{Si}_6\text{Cl}_{14}^{2-}]$ was synthesized using three different reaction conditions which varied the reaction time, reaction solvent, and solvent used to wash the crude product (wash solvent). Altering the reaction conditions was shown to have a significant impact on the reaction yield (table 9).

Table 9. Summary of $[\text{Tr}^+]_2[\text{Si}_6\text{Cl}_{14}^{2-}]$ syntheses.

Reaction	Reaction Time (min)	Reaction Solvent	Wash Solvent	Yield
1	90	CH_2Cl_2	CH_2Cl_2	44.42%
2	10	CH_2Cl_2	hexanes	86.76%
3	5	hexanes	hexanes	90.28%

EA (C, H, Cl and Si) was recorded for the products from all three reactions (table 10). In all cases the carbon and hydrogen values matched the theoretical values for $[\text{Tr}^+]_2[\text{Si}_6\text{Cl}_{14}^{2-}]$, both with scale factors of 0.94-0.97. To a lesser extent the silicon values matched the theoretical values with scale factors of 0.98-1.12. The chlorine values had scale factors of 0.87-1.15 that did not closely match theoretical values.

Table 10. Theoretical/experimental elemental analysis results for synthesis of $[\text{Tr}^+]_2[\text{Si}_6\text{Cl}_{14}^{2-}]$.

	Carbon	Hydrogen	Chlorine	Silicon
Theoretical	39.64	2.63	43.10	14.6
Reaction 1	37.44 (0.07)	2.57 (0.01)	49.54 (----)	14.3 (----)
Reaction 2	38.28 (1.00)	2.59 (0.38)	37.43 (3.41)	16.3 (1.7)
Reaction 3	37.49 (----)	2.69 (----)	40.23 (----)	15.4 (----)

Theoretical values based on $[\text{Tr}^+]_2[\text{Si}_6\text{Cl}_{14}^{2-}]$. Standard deviation provided in parentheses for analyses performed in duplicate. Samples marked “----“ were performed in singlicate.

EA was collected for a dichloromethylphenylsilane standard to test the accuracy of the instrument (table 11). The analysis was performed in triplicate. Dichloromethylphenylsilane was selected as a standard due to the fact that its theoretical values are similar to those of $[\text{Tr}^+]_2[\text{Si}_6\text{Cl}_{14}^{2-}]$ (table 12). In addition, it was chemically similar to $[\text{Tr}^+]_2[\text{Si}_6\text{Cl}_{14}^{2-}]$ in that it contained phenyl groups and Si-Cl bonds.

Table 11. Theoretical/experimental elemental analysis results for dichloromethylphenylsilane.

	Carbon	Hydrogen	Chlorine	Silicon
Theoretical	43.99	4.22	37.10	14.7
Experimental	42.29 (0.45)	4.17 (0.05)	33.80 (0.15)	14.3 (0.6)

Analyses were performed in triplicate. Standard deviations shown in parentheses.

Table 12. Comparison of elemental compositions for pure dichloromethylphenylsilane and $[\text{Tr}^+]_2[\text{Si}_6\text{Cl}_{14}^{2-}]$.

	Carbon	Hydrogen	Chlorine	Silicon
Dichloromethylphenylsilane	43.99	4.22	37.10	14.69
$[\text{Tr}^+]_2[\text{Si}_6\text{Cl}_{14}^{2-}]$	39.64	2.63	43.10	14.63

Characterization of the standard via gas chromatography-mass spectroscopy (GC-MS) revealed it to have a purity of 99.5%. Despite this high purity, the scale factors were similar to those seen for $[\text{Tr}^+]_2[\text{Si}_6\text{Cl}_{14}^{2-}]$. Carbon, hydrogen and silicon matched their theoretical values with respective scale factors of 0.96, 0.99 and 0.97. Chlorine was not accurate with a scale factor of 0.91. This similarity in results indicates that the discrepancies in scale factors seen for $[\text{Tr}^+]_2[\text{Si}_6\text{Cl}_{14}^{2-}]$ could potentially have been due to instrument error, as opposed to sample impurities.

4.4. Experimental Methods

4.4.1. Preparation of Starting Materials

Starting materials were reagent grade quality or higher, unless otherwise noted. The presence of O_2 or H_2O , whether in solvents or the atmosphere, is detrimental to these reactions as the trichlorosilane and products are $\text{O}_2/\text{H}_2\text{O}$ sensitive. For this reason, all experiments were performed under a dry, inert atmosphere (i.e. nitrogen or argon) either in a glove box or by using air-free Schlenk line techniques, unless otherwise noted. Glassware (including stir bars) was dried in a drying oven at 150°C for ≥ 2 h and transferred to the glove box antechamber while still hot. This would reduce the effects of H_2O condensation as the glassware returned to room temperature.

Solvents were dried according to literature protocols,⁶⁸ either by passage through a neutral alumina column or purchased from the vendor anhydrous. They were subsequently deoxygenated via sparging with N₂ while stirring for ≥ 2 h. They were stored under an inert atmosphere over either 3 Å or 4 Å molecular sieves. The molecular sieves were dried at 300°C under a vacuum of ≤ 50 mTorr for ≥ 12 h and stored under an inert atmosphere. Solvents were checked for water and oxygen prior to use by adding diethyl zinc solution (pyrophoric) and checking for the formation of fumes.

Solids were dried under a vacuum of ≤ 50 mTorr for ≥ 12 h either at room temperature or elevated temperature, depending on the material's melting point. They were subsequently checked for dryness by collecting an FTIR spectrum for said materials as the O-H bonds in H₂O have a characteristic broad peak from 3200-3650 cm⁻¹.⁶⁹

4.4.2. Characterization of Materials

NMR characterization used either a JEOL 400 MHz NMR Spectrometer with solid state capabilities or a Bruker 400 MHz NMR Spectrometer. FTIR spectra were recorded using either a Bruker Optics Vertex 70 Fourier Transform Infrared Spectrometer or a Thermo Scientific Nicolet 8700 FT-IR. Samples were prepared in KBr pellets. Due to the air sensitive nature of the materials being tested, samples were transferred to the FTIR under dry, N₂ conditions and quickly transferred to the FTIR, whose sample chamber was constantly being flushed with dry N₂. XRD characterization used a Kappa Apex II Duo. Samples were immersed in mineral oil during transfer to the instrument as a way of mitigating atmospheric exposure. UV-Vis characterization used a Cary 5000 UV-vis-near-IR spectrometer. GC-MS characterization used a Hewlett Packard Series 6890-5973 Gas Chromatograph-Mass Spectrometer. Raman spectra were recorded using a Horiba Jobin Yvon Aramis Confocal Raman Imaging System which was

equipped with 532 and 785 nm lasers. To prevent air exposure, samples were placed in between two quartz slides sealed on the sides with vacuum grease. This preparation occurred in a dry, inert atmosphere (i.e. nitrogen or argon).

EA was collected by shipping samples to Galbraith Laboratories (located in Knoxville, Tennessee). Due to the air sensitive nature of the materials being characterized, samples were shipped in 4 mL vials which were contained within 20 mL vials. Both vials were prepared under a dry, N₂ atmosphere. They were contained within sealable plastic bags containing absorbent materials such as vermiculite or carbon impregnated cloth. The sealable bags were flushed with dry N₂.

4.4.3. Experimental Procedures

4.4.3.1. Synthesis and Recrystallization of [Ph₄P⁺]₂[Si₆Cl₁₂Br₂²⁻]

49.4 mg Si₆Cl₁₂ (0.0832 mmol) was dissolved in 2.000 mL CH₂Cl₂, forming a clear colorless solution with a small amount of undissolved white particulate. The mixture was filtered, removing the particulate. Separately, 70.5 mg Ph₄PBr (0.168 mmol) was dissolved in 2.000 mL CH₂Cl₂, forming a clear colorless solution. The Ph₄PBr solution was added to the Si₆Cl₁₂ solution over 10 min while stirring. The first 2 mL addition created a clear colorless solution. Following that, every addition resulted in the immediate precipitation of white solids, which gradually became light yellow as the addition neared completion.

Solids were washed 2x with 4 mL CH₂Cl₂ and dried via a vacuum. They were recrystallized by dissolving in DMF to the point of saturation. The DMF solution was contained in a 4 mL vial, which was placed uncapped in a 20 mL vial. The 20 mL vial contained toluene and was capped. The toluene was allowed to diffuse into the DMF solution at room temperature

over 6 days, causing colorless crystals to precipitate (figure 20). The crystals were isolated, immersed in oil and characterized via XRD.

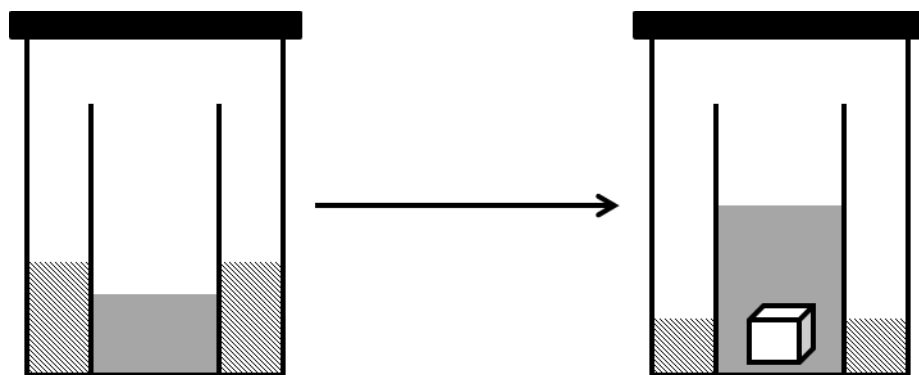


Figure 20. Diffusion crystallization method used for $\text{Si}_6\text{X}_{12}/\text{Ph}_4\text{PX}'$ product. Inner vial contains saturated solution of product in DMF while outer vial contains toluene. Diffusion of toluene over several days causes toluene to accumulate in inner vial, resulting in precipitation.

4.4.3.2. Attempted Synthesis and Recrystallization of $[\text{Ph}_4\text{P}^+]_2[\text{Si}_6\text{Br}_{12}\text{Cl}_2^{2-}]$

49.9 mg $\text{Si}_6\text{Br}_{12}$ (0.0443 mmol) was dissolved in 15.000 mL CH_2Cl_2 , forming a clear colorless solution with a small amount of undissolved white particulate. The mixture was filtered, removing the particulate. Separately, an excess of 33.4 mg Ph_4PCl (0.0891 mmol) was dissolved in 3.000 mL CH_2Cl_2 , forming a clear colorless solution. The Ph_4PCl solution was added to the $\text{Si}_6\text{Br}_{12}$ solution over 10 min while stirring. Every addition caused instant precipitation of white solids.

Solids were washed 2x with 4 mL CH_2Cl_2 and dried via a vacuum. They were recrystallized by dissolving in DMF to the point of saturation. The DMF solution was contained in a 4 mL vial, which was placed uncapped in a 20 mL vial. The 20 mL vial contained toluene and was capped. The toluene was allowed to diffuse into the DMF solution at room temperature

over 6 days, causing the precipitation of what appeared to be a mixture of crystals and powder (figure 20). The crystals were isolated, immersed in oil and characterized via XRD.

4.4.3.3. Elemental Analysis of Standard Material

The dichloromethylphenylsilane standard characterized via elemental analysis was purchased from Sigma-Aldrich (product number 440116, lot number SHBD9771V). The certificate of analysis showed a purity of 99.6% according to GC-MS. An independent GC-MS analysis for this material showed the purity to be 99.5%.

4.4.3.4. Synthesis of $[\text{Tr}^+]_2[\text{Si}_6\text{Cl}_{14}^{2-}]$

$[\text{Tr}^+]_2[\text{Si}_6\text{Cl}_{14}^{2-}]$ was synthesized under three different reaction conditions, all of which produced the same product in different yields. Reaction time and solvent varied between reactions.

4.4.3.4.1. Reaction 1

150.8 mg $\text{Si}_6\text{Cl}_{12}$ (0.2540 mmol) was dissolved in 0.9 mL CH_2Cl_2 , forming a clear yellow solution. A separate solution was created containing 154.9 mg trityl chloride (0.5556 mmol) in 0.9 mL CH_2Cl_2 , forming a clear light yellow solution. Addition of the trityl chloride solution to the $\text{Si}_6\text{Cl}_{12}$ solution while stirring instantly created a clear orange solution, however the solution changed to clear yellow ≤ 1 min. Instant addition of the remaining trityl chloride solution resulted in the rapid precipitation of yellow solids with a clear orange mother liquor. Mixture was stirred an additional 1.5 h, filtered via frit, washed 3x with ~ 4 mL CH_2Cl_2 and dried under vacuum for >1 h, leaving 129.9 mg of yellow powder (0.1128 mmol, 44.43% yield). Theoretical elemental analysis for $\text{C}_{38}\text{H}_{30}\text{Cl}_{14}\text{Si}_6$: C, 39.64; H, 2.63; Cl, 43.10; Si, 14.63. Experimental: C, 37.44; H, 2.57; Cl, 49.54; Si, 14.3.

4.4.3.4.2. Reaction 2

Conditions and observations were the same as in reaction 1, except solution was only allowed to stir for 10 min as opposed to 1.5 h. 150.1 mg $\text{Si}_6\text{Cl}_{12}$ (0.2527 mmol) was dissolved in 1 mL CH_2Cl_2 . A separate solution was created containing 178.5 mg trityl chloride (0.6404 mmol) in 1 mL CH_2Cl_2 . 252.5 mg of yellow powder was isolated (0.2193 mmol, 86.77% yield).

A sample of product was taken and washed 4x with ~2 mL hexanes (95% n-hexane), and characterized via elemental analysis. Theoretical elemental analysis for $\text{C}_{38}\text{H}_{30}\text{Cl}_{14}\text{Si}_6$: C, 39.64; H, 2.63; Cl, 43.10; Si, 14.63. Experimental: C, 38.28; H, 2.59; Cl, 37.43; Si, 16.3.

4.4.3.4.3. Reaction 3

67.21 mg $\text{Si}_6\text{Cl}_{12}$ (0.1132 mmol) was dissolved in 0.500 mL hexanes (95% n-hexane), forming a clear colorless solution. 66.44 mg trityl chloride (0.2383 mmol) was dissolved in 2.500 mL hexanes. Dropwise addition of the trityl chloride solution to the $\text{Si}_6\text{Cl}_{12}$ solution resulted in the immediate precipitation of yellow solids. Instant addition of the remaining trityl chloride solution resulted in the rapid precipitation of yellow solids with clear orange mother liquor. Mixture was stirred an additional 5 min, filtered via frit, washed 8 times with ~2 mL hexanes and dried under vacuum for 15 min, leaving 117.6 mg yellow powder (0.1021 mmol, 90.25% yield). Theoretical elemental analysis for $\text{C}_{38}\text{H}_{30}\text{Cl}_{14}\text{Si}_6$: C, 39.64; H, 2.63; Cl, 43.10; Si, 14.63. Experimental: C, 37.49; H, 2.69; Cl, 40.23; Si, 15.4.

4.4.3.5. Synthesis of $[\text{Tr}^+]_2[\text{Si}_6\text{Br}_{12}\text{Cl}_2^{2-}]$

75 mg $\text{Si}_6\text{Br}_{12}$ (0.067 mmol) was dissolved in 2.3 mL CH_2Cl_2 , forming a cloudy yellow mixture. A separate solution was created containing 49.93 mg trityl chloride (0.1791 mmol) in 0.500 mL CH_2Cl_2 , forming a clear light yellow solution. Addition of the trityl solution to the $\text{Si}_6\text{Br}_{12}$ mixture while stirring instantly created a clear orange solution. Instant addition of the

remaining trityl chloride solution resulted in the rapid precipitation of orange solids with a clear orange mother liquor. Mixture was filtered via frit, washed 2x with ~3mL CH₂Cl₂ and dried under vacuum for 50 min, leaving 85.30 mg orange powder (0.051 mmol, 76% yield).

4.4.3.6. Synthesis of [Tr⁺]₂[Si₆Br₁₄²⁻]

20.20 mg Si₆Br₁₂ (0.01792 mmol) was dissolved in 1.000 mL CH₂Cl₂. 11.86 mg trityl bromide (0.03669 mmol) was dissolved in 0.500 mL CH₂Cl₂. Dropwise addition of the trityl bromide solution to the Si₆Br₁₂ solution initially resulted in the immediate formation of a clear yellow solution. Further addition changed the mother liquor to orange which was accompanied by the precipitation of orange solids. The mixture was filtered after <3 min stirring, washed 4x with 1.5 mL CH₂Cl₂ and dried under vacuum for 30 min, leaving 26.31 mg orange powder (0.01483 mmol, 82.78% yield).

4.4.3.7. Attempted Synthesis of [4-MeTr⁺]₂[Si₆Cl₁₄²⁻]

18.13 mg Si₆Cl₁₂ (0.03052 mmol) was dissolved in 0.2 mL CD₂Cl₂. 20.62 mg 4,4',4''-(chloromethanetriyl)tris(methylbenzene) (4-MeTrCl, 0.06426 mmol) was dissolved in 0.6 mL CD₂Cl₂, forming a clear yellow solution. Dropwise addition of the 4-MeTrCl solution to the Si₆Cl₁₂ solution initially resulted in the immediate formation of an orange solution. Instant addition of the remaining solution resulted in the immediate formation of a clear brown/red solution which changed to a cloudy yellow/orange mixture over 4 min. Mixture was filtered via frit, and dried via vacuum, leaving 17.2 mg yellow/orange solids in frit (0.0139 mmol, 45.6% yield) with red/brown filtrate.

5. FUTURE WORK

- Perform a LAH reduction of crude RR' or crude R2 salt to produce Si_6H_{12} . Collect the yield for each reaction and perform comparative analysis with Hengge's, Tillman's and Boudjouk's syntheses.
- Complete the table for characterization of Si_6X_{12} and corresponding adducts. Includes synthesizing/characterizing Si_6I_{12} and its nitrile/mixed halide adducts. Collect EA results for $\text{Si}_6\text{Cl}_{12}$ and XRD spectrum for $[\text{Si}_6\text{Br}_{12}\text{Cl}_2]^{2-}$ dianion salt.
- Collect an XRD spectrum for a $[\text{Tr}^+]_2[\text{Si}_6\text{X}_{12}\text{X}'_2]^{2-}$ dianion salt.
- Synthesize $\text{Si}_6\text{Cl}_{12}$ from $[\text{PEDETA}\cdot\text{H}_2\text{SiCl}^+]_2[\text{Si}_6\text{Cl}_{14}]^{2-}$ and AlCl_3 . Collect the yield and perform a comparative analysis with Hengge's, Tillman's and Frohlich's syntheses.

REFERENCES

- (1) Guruvenket, S.; Hoey, J.; Anderson, K. J.; Frohlich, M. T.; Sailer, R. A.; Boudjouk, P. Aerosol assisted atmospheric pressure chemical vapor deposition of silicon thin films using liquid cyclic hydrosilanes *Thin Solid Films* **2015**, *589*, 465-471.
- (2) Pokhodnya, K.; Olson, C.; Dai, X. L.; Schulz, D. L.; Boudjouk, P.; Sergeeva, A. P.; Boldyrev, A. I. Flattening a puckered cyclohexasilane ring by suppression of the pseudo-Jahn-Teller effect *J. Chem. Phys.* **2011**, *134*.
- (3) Guruvenket, S.; Hoey, J. M.; Anderson, K. J.; Frohlich, M. T.; Krishnan, R.; Sivaguru, J.; Sibi, M. P.; Boudjouk, P. Synthesis of silicon quantum dots using cyclohexasilane (Si₆H₁₂) *J. Mater. Chem. C* **2016**, *4*, 8206-8213.
- (4) Srinivasan, G.; Anderson, K.; Hoey, J.; Sailer, R. A. U.S. Patent 20,160,251,227 A1, 2016.
- (5) Lu, X.; Anderson, K. J.; Boudjouk, P.; Korgel, B. A. Low temperature colloidal synthesis of silicon nanorods from isotetrasilane, neopentasilane, and cyclohexasilane *Chem. Mater.* **2015**, *27*, 6053-6058.
- (6) Schulz, D. L.; Hoey, J.; Smith, J.; Elangovan, A.; Wu, X.; Akhatov, I.; Payne, S.; Moore, J.; Boudjouk, P.; Pederson, L.; Xiao, J.; Zhang, J. G. Si₆H₁₂/Polymer Inks for Electrospinning a-Si Nanowire Lithium Ion Battery Anodes *Electrochem. Solid-State Lett.* **2010**, *13*, A143-A145.
- (7) Dohnalová, K.; Gregorkiewicz, T.; Kůsová, K. Silicon quantum dots: surface matters *J. Phys.: Condens. Matter* **2014**, *26*, 173201.
- (8) Cheng, X.; Lowe, S. B.; Reece, P. J.; Gooding, J. J. Colloidal silicon quantum dots: from preparation to the modification of self-assembled monolayers (SAMs) for bio-applications *Chem. Soc. Rev.* **2014**, *43*, 2680-2700.
- (9) Orii, T.; Hirasawa, M.; Seto, T. Tunable, narrow-band light emission from size-selected Si nanoparticles produced by pulsed-laser ablation *Appl. Phys. Lett.* **2003**, *83*, 3395-3397.
- (10) Wei, S.; Yamamura, T.; Kajiya, D.; Saitow, K.-i. White-light-emitting silicon nanocrystal generated by pulsed laser ablation in supercritical fluid: investigation of spectral components as a function of excitation wavelengths and aging time *J. Phys. Chem. C* **2012**, *116*, 3928-3934.
- (11) Nakamura, T.; Yuan, Z.; Adachi, S. High-yield preparation of blue-emitting colloidal Si nanocrystals by selective laser ablation of porous silicon in liquid *Nanotechnology* **2014**, *25*, 275602.
- (12) Bley, R. A.; Kauzlarich, S. M.; Davis, J. E.; Lee, H. W. Characterization of silicon nanoparticles prepared from porous silicon *Chem. Mater.* **1996**, *8*, 1881-1888.
- (13) Murthy, T.; Miyamoto, N.; Shimbo, M.; Nishizawa, J. Gas-phase nucleation during the thermal decomposition of silane in hydrogen *J. Cryst. Growth* **1976**, *33*, 1-7.
- (14) Alam, M.; Flagan, R. Controlled nucleation aerosol reactors: production of bulk silicon *Aerosol Sci. Technol.* **1986**, *5*, 237-248.
- (15) Li, X.; He, Y.; Swihart, M. T. Surface functionalization of silicon nanoparticles produced by laser-driven pyrolysis of silane followed by HF–HNO₃ etching *Langmuir* **2004**, *20*, 4720-4727.

- (16) Ostraat, M. L.; De Blauwe, J. W.; Green, M. L.; Bell, L. D.; Atwater, H. A.; Flagan, R. C. Ultraclean two-stage aerosol reactor for production of oxide-passivated silicon nanoparticles for novel memory devices *J. Electrochem. Soc.* **2001**, *148*, G265-G270.
- (17) Holunga, D. M.; Flagan, R. C.; Atwater, H. A. A scalable turbulent mixing aerosol reactor for oxide-coated silicon nanoparticles *Ind. Eng. Chem. Res.* **2005**, *44*, 6332-6341.
- (18) Mangolini, L.; Jurbergs, D.; Rogojina, E.; Kortshagen, U. Plasma synthesis and liquid-phase surface passivation of brightly luminescent Si nanocrystals *J. Lumin.* **2006**, *121*, 327-334.
- (19) Pell, L. E.; Schricker, A. D.; Mikulec, F. V.; Korgel, B. A. Synthesis of amorphous silicon colloids by trisilane thermolysis in high temperature supercritical solvents *Langmuir* **2004**, *20*, 6546-6548.
- (20) Schmidt, V.; Wittemann, J. V.; Senz, S.; Gösele, U. Silicon nanowires: a review on aspects of their growth and their electrical properties *Adv. Mater.* **2009**, *21*, 2681-2702.
- (21) Heitsch, A. T.; Fanfair, D. D.; Tuan, H.-Y.; Korgel, B. A. solution- liquid- solid (SLS) growth of silicon nanowires *J. Am. Chem. Soc.* **2008**, *130*, 5436-5437.
- (22) Heitsch, A. T.; Hessel, C. M.; Akhavan, V. A.; Korgel, B. A. Colloidal silicon nanorod synthesis *Nano Lett.* **2009**, *9*, 3042-3047.
- (23) Lu, X.; Hessel, C. M.; Yu, Y.; Bogart, T. D.; Korgel, B. A. Colloidal luminescent silicon nanorods *Nano Lett.* **2013**, *13*, 3101-3105.
- (24) Hessel, C. M.; Heitsch, A. T.; Korgel, B. A. Gold seed removal from the tips of silicon nanorods *Nano Lett.* **2009**, *10*, 176-180.
- (25) Lu, X.; Korgel, B. A. A Single-Step Reaction for Silicon and Germanium Nanorods *Chem.-Eur. J.* **2014**, *20*, 5874-5879.
- (26) Wagner, R.; Ellis, W. Vapor-liquid-solid mechanism of single crystal growth *Appl. Phys. Lett.* **1964**, *4*, 89-90.
- (27) Givargizov, E. Fundamental aspects of VLS growth *J. Cryst. Growth* **1975**, *31*, 20-30.
- (28) Eversteyn, F. Chemical-reaction engineering in the semiconductor industry *Philips Research Rep.* **1974**, *29*, 45-66.
- (29) Chu, T. L.; Chu, S. S.; Ang, S. T.; Lo, D. H.; Duong, A.; Hwang, C. G. Deposition and Photoconductivity of Hydrogenated Amorphous-Silicon Films by the Pyrolysis of Disilane *J. Appl. Phys.* **1986**, *59*, 1319-1322.
- (30) Chu, T. L.; Chu, S. S.; Ang, S. T.; Duong, A.; Han, Y. X.; Liu, Y. H. Hydrogenated Amorphous-Silicon Films Deposited in a Helium Atmosphere *J. Appl. Phys.* **1986**, *60*, 4268-4272.
- (31) Kanoh, H.; Sugiura, O.; Breddels, P. A.; Matsumura, M. Optimization of chemical vapor deposition conditions of amorphous-silicon films for thin-film transistor application *Jpn. J. Appl. Phys.* **1990**, *29*, 2358.
- (32) Kanoh, H.; Sugiura, O.; Matsumura, M. Chemical vapor deposition of amorphous silicon using tetrasilane *Jpn. J. Appl. Phys.* **1993**, *32*, 2613.
- (33) Briend, P.; Alban, B.; Chevrel, H.; Jahan, D. U.S. Patent 20,110,011,129 A1, 2009.
- (34) Kreiger, M.; Shonnard, D.; Pearce, J. M. Life cycle analysis of silane recycling in amorphous silicon-based solar photovoltaic manufacturing *Resour., Conserv. Recycl.* **2013**, *70*, 44-49.
- (35) Dai, X. L.; Schulz, D. L.; Braun, C. W.; Ugrinov, A.; Boudjouk, P. "Inverse Sandwich" Complexes of Perhalogenated Cyclohexasilane *Organometallics* **2010**, *29*, 2203-2205.

- (36) Dai, X.; Choi, S.-B.; Braun, C. W.; Vaidya, P.; Kilina, S.; Ugrinov, A.; Schulz, D. L.; Boudjouk, P. Halide Coordination of Perhalocyclohexasilane Si₆X₁₂ (X = Cl or Br) *Inorg. Chem.* **2011**, *50*, 4047-4053.
- (37) Tillmann, J.; Moxter, M.; Bolte, M.; Lerner, H.-W.; Wagner, M. Lewis Acidity of Si₆Cl₁₂ and Its Role as Convenient SiCl₂ Source *Inorg. Chem.* **2015**, *54*, 9611-9618.
- (38) Abe, T.; Imoto, S.-y. Japanese Patent JP2016020301A, 2015.
- (39) Abe, T.; Imoto, S.-y.; Kitamura, M.; Takahashi, H. U.S. Patent US 2014/0012029 A1, 2014.
- (40) Boudjouk, P.; Kim, B.-K.; Remington, M. P.; Chauhan, B. U.S. Patent 5,942,637, 1999.
- (41) Choi, S. B.; Kim, B. K.; Boudjouk, P.; Grier, D. G. Amine-promoted disproportionation and redistribution of trichlorosilane: Formation of tetradecachlorocyclohexasilane dianion *J. Am. Chem. Soc.* **2001**, *123*, 8117-8118.
- (42) Gilman, H.; Tomasi, R. A. The preparation of dodecamethylcyclohexasilane *J. Org. Chem.* **1963**, *28*, 1651-1653.
- (43) zu Stolberg, U. G. Dodecamethylcyclohexasilane *Angew. Chem., Int. Ed. Engl.* **1963**, *2*, 150-151.
- (44) West, R.; Brough, L.; Wojnowski, W.; Van Beek, D. A.; Allred, A. L. Dodecamethylcyclohexasilane *Inorg. Synth., Vol. 19* **1979**, 265-268.
- (45) Kipping, F. S.; Sands, J. E. XCIII.—Organic derivatives of silicon. Part XXV. Saturated and unsaturated silicohydrocarbons, Si 4 Ph 8 *J. Chem. Soc., Trans.* **1921**, *119*, 830-847.
- (46) Gilman, H.; Peterson, D.; Jarvie, A.; Winkler, H. The formation of dodecaphenylcyclohexasilane from the reaction of dichlorodiphenylsilane with sodium and with lithium *Tetrahedron Lett.* **1960**, *1*, 5-7.
- (47) Hengge, E.; Kovar, D. Reaction of Silicon-Phenyl Bond with Hcl *J. Organomet. Chem.* **1977**, *125*, C29-C32.
- (48) Hengge, E.; Kovar, D. Preparation of Cyclohexasilane Si₆H₁₂ *Angew. Chem. Int. Ed.* **1977**, *16*, 403-403.
- (49) Jarvie, A.; Winkler, H.; Peterson, D.; Gilman, H. Preparation and Characterization of Octaphenylcyclotetrasilane *J. Am. Chem. Soc.* **1961**, *83*, 1921-1924.
- (50) Winkler, H.; Jarvie, A.; Peterson, D.; Gilman, H. Preparation and Characterization of Dodecaphenylcyclohexasilane *J. Am. Chem. Soc.* **1961**, *83*, 4089-4093.
- (51) Gilman, H.; Schwebke, G. L. Reactions and Structure of Decaphenylcyclopentasilane *J. Am. Chem. Soc.* **1964**, *86*, 2693-2699.
- (52) Campbell-Ferguson, H.; Ebsworth, E. Adducts of the halogenosilanes. Part II. Physical properties and structures *J. Chem. Soc. A* **1967**, 705-712.
- (53) Boudjouk, P.; Kloos, S. D.; Kim, B. K.; Page, M.; Thweatt, D. An unexpected redistribution of trichlorosilane. Synthesis, structure and bonding of (N,N,N',N'-tetraethylethylenediamine)dichlorosilane *J. Chem. Soc., Dalton Trans.* **1998**, 877-879.
- (54) Kim, B. K.; Choi, S. B.; Kloos, S. D.; Boudjouk, P. Synthesis and characterization of new cationic hexacoordinate silanes *Inorg. Chem.* **2000**, *39*, 728-731.
- (55) Kim, B.-K. *New cationic hexacoordinate complexes of silanes*, 1998.
- (56) Elangovan, A.; Anderson, K.; Boudjouk, P. R.; Schulz, D. L. U.S. Patent 8,975,429 B2, 2015.
- (57) Elangovan, A.; Anderson, K.; Frohlich, M., Unpublished Results, 2014.
- (58) Anderson, K., Unpublished Results, 2014.

- (59) Tillmann, J.; Meyer-Wegner, F.; Nadj, A.; Becker-Baldus, J.; Sinke, T.; Bolte, M.; Holthausen, M. C.; Wagner, M.; Lerner, H.-W. Unexpected Disproportionation of Tetramethylethylenediamine-Supported Perchlorodisilane $\text{Cl}_3\text{SiSiCl}_3$ *Inorg. Chem.* **2012**, *51*, 8599-8606.
- (60) Tillmann, J.; Meyer, L.; Schweizer, J. I.; Bolte, M.; Lerner, H.-W.; Wagner, M.; Holthausen, M. C. Chloride-Induced Aufbau of Perchlorinated Cyclohexasilanes from Si_2Cl_6 : A Mechanistic Scenario *Chem.-Eur. J.* **2014**, *20*, 9234-9239.
- (61) Anderson, K.; Frohlich, M., Unpublished Results, 2016.
- (62) Donoghue, N.; Gallagher, M. J. Mono- and dihydrophosphoranes and dihydrophosphoranates as intermediates in the reaction of phosphonium salts with LiAlH_4 *Phosphorus, Sulfur Silicon Relat. Elem.* **1997**, *123*, 169-173.
- (63) Dai, X. L.; Choi, S. B.; Braun, C. W.; Vaidya, P.; Kilina, S.; Ugrinov, A.; Schulz, D. L.; Boudjouk, P. Halide Coordination of Perhalocyclohexasilane Si_6X_{12} (X = Cl or Br) *Inorg. Chem.* **2011**, *50*, 4047-4053.
- (64) Abe, T.; Imoto, S.-y.; Kitamura, M.; Takahashi, H. U.S. Patent 9,290,525 B2, 2013.
- (65) Brodsky, M.; Cardona, M.; Cuomo, J. J. Infrared and Raman spectra of the silicon-hydrogen bonds in amorphous silicon prepared by glow discharge and sputtering *Phys. Rev. B* **1977**, *16*, 3556.
- (66) Chabal, Y.; Higashi, G.; Christman, S. Hydrogen chemisorption on Si (111)-(7×7) and-(1×1) surfaces. A comparative infrared study *Phys. Rev. B* **1983**, *28*, 4472.
- (67) Boonekamp, E.; Kelly, J.; Van de Ven, J.; Sondag, A. The chemical oxidation of hydrogen-terminated silicon (111) surfaces in water studied in situ with Fourier transform infrared spectroscopy *J. Appl. Phys.* **1994**, *75*, 8121-8127.
- (68) Williams, D. B. G.; Lawton, M. Drying of organic solvents: quantitative evaluation of the efficiency of several desiccants *J. Org. Chem.* **2010**, *75*, 8351-8354.
- (69) Brown, B.; Foote, C.; Iverson, B. *Organic Chemistry*; Fourth ed.; Thomson Brooks/Cole: Belmont, CA, 2005.
- (70) Pokhodnya, K., Unpublished Results, 2016.
- (71) Eide, O.; Ystenes, M.; Støvneng, J.; Eilertsen, J. Investigation of ion pair formation in the triphenylmethyl chloride-trimethyl aluminium system, as a model for the activation of olefin polymerization catalyst *Vib. Spectrosc.* **2007**, *43*, 210-216.
- (72) Weston, R.; Tsukamoto, A.; Lichtin, N. Infrared spectra and vibrational frequency assignment of triphenylcarbinol, triphenylmethyl chloride, triphenylmethyl fluoborate, and their 1-¹³C and ϕ -d 5 analogs *Spectrochim. Acta* **1966**, *22*, 433-453.

APPENDIX: CRYSTALLOGRAPHIC INFORMATION

Table A1. Crystallographic data for $[\text{Ph}_4\text{P}^+]_2[\text{Si}_6\text{Cl}_{12}\text{Br}_2^{2-}]$ and $[\text{Ph}_4\text{P}^+]_2[\text{Si}_6\text{Br}_{14}^{2-}]$.

Compound	$[\text{Ph}_4\text{P}^+]_2[\text{Si}_6\text{Cl}_{12}\text{Br}_2^{2-}]$	$[\text{Ph}_4\text{P}^+]_2[\text{Si}_6\text{Br}_{14}^{2-}]$
Formula	$\text{C}_{48}\text{H}_{40}\text{Cl}_{12}\text{Br}_2\text{P}_2\text{Si}_6$	$\text{C}_{48}\text{H}_{40}\text{Br}_{14}\text{P}_2\text{Si}_6$
Formula Weight, $\text{g}\cdot\text{mol}^{-1}$	1432.54	1965.95
Space Group	P-1	P1 21/n 1
a, Å	11.3347 (6)	13.1237 (16)
b, Å	12.0928 (7)	14.0918 (16)
c, Å	12.6559 (7)	16.7460 (19)
α , deg	69.039 (1)	90
β , deg	64.263 (1)	103.376 (2)
γ , deg	75.045 (1)	90
Volume	1448.30 (14)	3012.9 (6)
ρ , $\text{g}\cdot\text{mL}^{-1}$	1.642	2.167
μ , mm^{-1}	2.168	9.509
F(000)	716.0	1864.0
Reflns collected	6450	6692

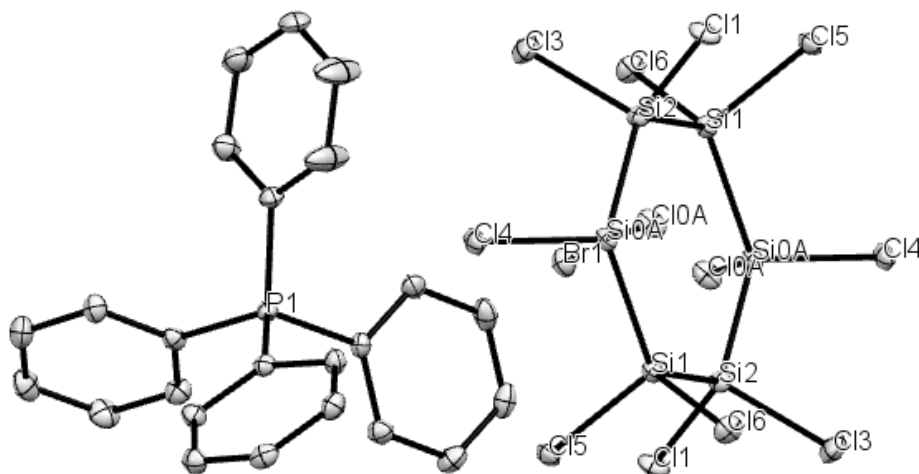


Figure A1. Thermal ellipsoid plot of $[\text{Ph}_4\text{P}^+]_2[\text{Si}_6\text{Cl}_{12}\text{Br}_2^{2-}]$. Thermal ellipsoids set at 50% probability. Hydrogen atoms omitted for clarity.

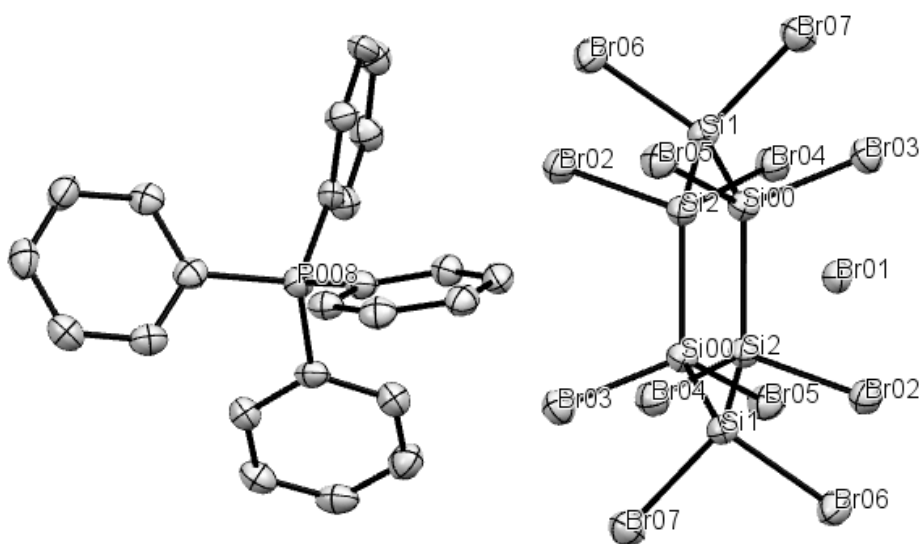


Figure A2. Thermal ellipsoid plot of $[\text{Ph}_4\text{P}^+]_2[\text{Si}_6\text{Br}_{14}]^{2-}$. Thermal ellipsoids set at 50% probability. Hydrogen atoms omitted for clarity.